CHARACTERIZATION OF THE FUNCTION OF TIGHT JUNCTION PROTEINS IN TRANSGENIC MICE

Xu Jianliang

INSTITUTE OF MOLECULAR AND CELL BIOLOGY
NATIONAL UNIVERSITY OF SINGAPORE

2008

ACKNOWLEGMENTS

I would like to express my special thanks to my supervisor, A/P Walter Hunziker, for his patient guidance and encouragement throughout my study. I also wish to thank my supervisory committee members, Prof. Ito Yoshiaki and Asst. Prof. Li Baojie, for their invaluable advice and the time spent on my postgraduate committee meetings every year. I thank Dr. Zakir Hossain for his help during the initial stages of my project, Dr. Ke Guo for her help on the histological analysis, and Mr. Chee Peng Ng for his support with the EM work. I thank past and present members of WH lab and other IMCB members.

TABLE OF CONTENTS

LIST OF FIGURES

LIST OF TABLES

LIST OF VIDEOS

Abbreviation

a.a.: amino acid
AJ: adherens junction
AMP: adenosine monophosphate
ATP: adenosine triphosphate
BBB: blood-brain barrier
BrdU: bromodeoxyuridine
CIS: carcinoma in situ
CRC: primary colorectal cancer
CX: Connexin
EB: embryoid body
EGFR: epidermal growth factor receptor
EMT: epithelial-mesenchymal transition
ES: embryonic stem
FHC: familial hypercholanemia
GUK: guanylate-like
GMP: guanosine monophosphate
JAM: junctional adhesion molecule
kDa: kiloDalton
MAGUK: membrane-associated guanylate kinase homolog
MDCK: Madin-Darby Canine Kidney
NES: nuclear export signal
NLS: nuclear localization signal
PATJ: PALS1-associated TJ protein
PKC: protein kinase C
PDZ: PSD-95, Dlg, ZO-1
SAF-B: scaffold attachment factor-B
SH3: Src homology 3
TER: transepithelial electrical resistance
TM: transmembrane
TJ: tight junction
ZO: Zonula Occludens
ZO-1: Zonula Occludens-1
ZO-2: Zonula Occludens-2
ZO-3: Zonula Occludens-3
ZONAB: ZO-1 associated nuclei acid binding

Abstract

ZO-1, *ZO-2* and *ZO-3* are closely related scaffolding proteins that link tight junction (TJ) transmembrane proteins such as occludin, claudins and junctional adhesion molecules to the actin cytoskeleton. Despite being among the first TJ proteins to have been identified and having undergone extensive biochemical analysis, little is know about the physiological roles of individual ZO proteins in different tissues or during vertebrate development. Here, we show that *ZO-3-/-* mice lack an obvious phenotype. In contrast, embryos deficient for *ZO-2* die shortly after implantation due to an arrest in early gastrulation. *ZO-2-/-* embryos show decreased proliferation at E6.5, increased apoptosis at E7.5 and altered architecture of the apical junctional complex as compared to wild-type. *ZO-1-/-* mice are currently unavailable, while chimeric mice derived from *ZO-1-/-* embryonic stem (ES) cells are embryonic lethal. Because of the embryonic lethality of the ZO-1-/- and ZO-2-/- mice, we also generated knockout ES cell lines. We have obtained *ZO-1-/-, ZO-2-/-, ZO-3-/-, ZO-1-/-ZO-2-/-,* and *ZO-2-/-ZO-3-/-* ES cells. These cell lines have shown various defects in their ability to differentiate into epithelial cells, cardiomyocytes or skeletal muscle cells.

Chapter 1 Introduction

Multicellular organisms are separated from the external environment by a layer of epithelial cells, which also line the internal cavities and ducts of tissues and organs. Epithelial tissues can be grouped into three basic types: squamous (such as skin, the linings of the peritoneum and the epidermis), cuboidal (such as the the epithelium forming the collecting duct of the kidney), and columnar (such as that lining the small intestine) (Figure 1). Two pathways are available for the transepithelial transport of molecules. The first one is the transcellular pathway that requires the solutes to be internalized to cross the epithelial cells. The second one is the paracellular pathway, where solutes pass the paracellular barrier. Establishment of a paracellular barrier with controlled permeability between the epithelial cells is important for the maintenance of a specific internal environment that is crucial for the development and survival of multicellular organisms. The epithelial cell layer is closely joined by membrane structures named tight junctions (TJs), which play a role in allowing different tissue or organ compartments to maintain different solute composition without, however, completely obstructing the exchange of solutes between bordering compartments. The permeability of TJ barrier is controlled by both internal (for example, cyclic AMP and RhoA) and external signals (for example, zonulin antagonists and agonists), and thus can be modulated under certain circumstances (for example, in the process EMT during differentiation). Modulation of the TJ barrier is also of clinical interest for drug delivery.

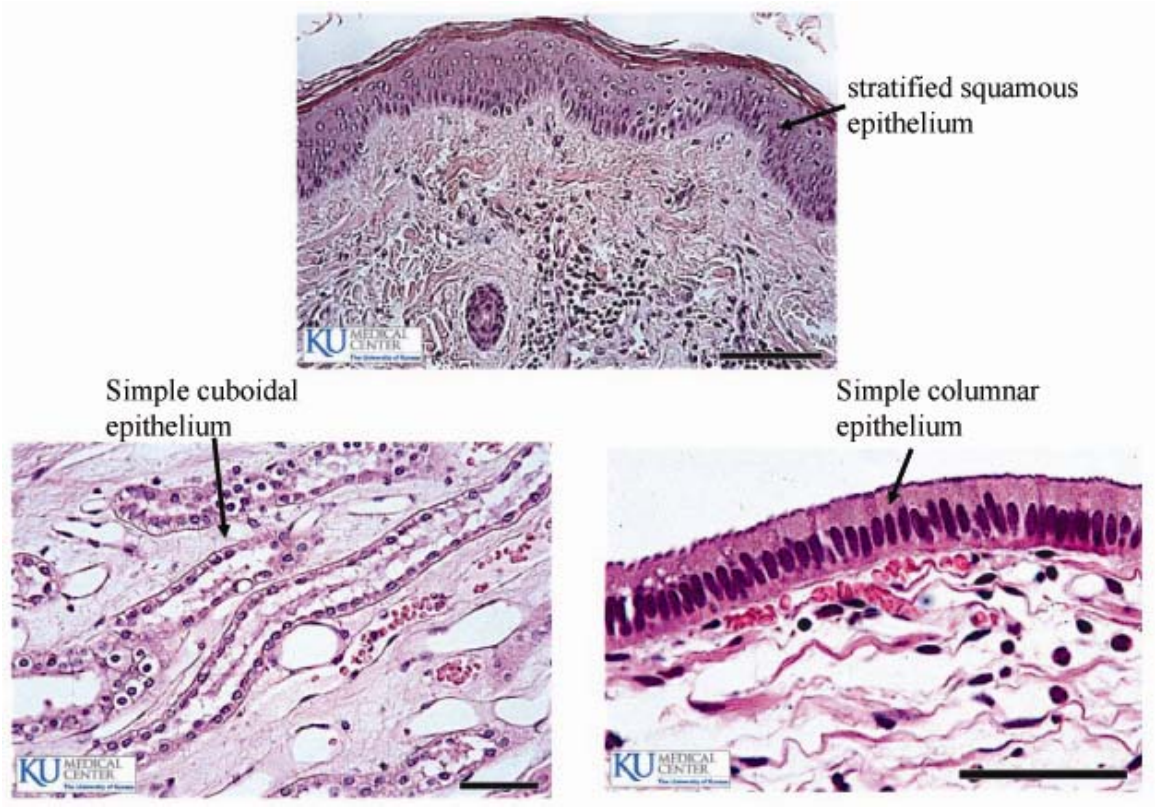

Figure 1 Three types of basic epithelial tissues in different organs.
Stratified squamous epithelia form the skin; simple cuboidal epithelia line the collecting ducts of the kidney; simple columnar cells consist of the gall bladder. (http://www.kumc.edu/instruction/medicine/anatomy/histoweb/epithel/epithel.htm)

1.1 Tight junctions

1.1.1 Structure and function of TJs

TJs locate at the most apical side of two adjacent epithelial or endothelial cells (Figure 2A). In a freeze-fracture, TJs appear as strands (Figure 2B). These strands, derived from the two adjacent cells, form a series of fusion points, which surround each cell on the most apical side and thus obliterate the intercellular space (Figure 2 C, D). The major function of TJs is to seal the paracellular pathway and block the diffusion of solutes between the external (luminal) and the internal (serosal) space. Claudins, a protein family with over 20 members in mammals, are thought to form the charge-selective pores in the TJ barriers. If the net charge of the pores is negative, the cations are allowed to pass the TJ barriers (Sasaki et al., 2003). Since non-charged solutes are not affected by the net charge in the claudins pores, they are thought to cross the TJ barriers via a different mechanism. TJ strands are able to dynamically break and reseal and non-charged solutes can cross TJs through the temporal gaps during this dynamic process (Sasaki et al., 2003). The permeability of TJs varies in different tissues depending on the functions they performed, and this is thought to reflect different claudin repertoires. For example, the urinary bladder and the stomach duct can have a transepithelial electrical resistance (TER) up to a few thousand Ω cm2, while the small intestine has a TER of a few Ω cm2. The TJ permeability is not always the same even in the same organ. For example, paracellular transport across renal tubular epithelial TJs varies in different segments of the nephron.

TJs also function as a fence between apical and basolateral membrane domains to block protein and lipid diffusion within the plasma membrane and maintain cell polarity.

In addition to being a permeability barrier and a fence, TJs also act as a multifunctional complex that regulates various cellular functions such as membrane trafficking (exocyst, rab13), signal transduction (cell density, ZO-1), tumor suppression (suppression of Ad9 E4-ORF1-induced focus formation, ZO-2), cell proliferation (ZONAB). In addtion, TJs often serve as entry points for the infection by different pathogens (adenovirus, ZO-2).

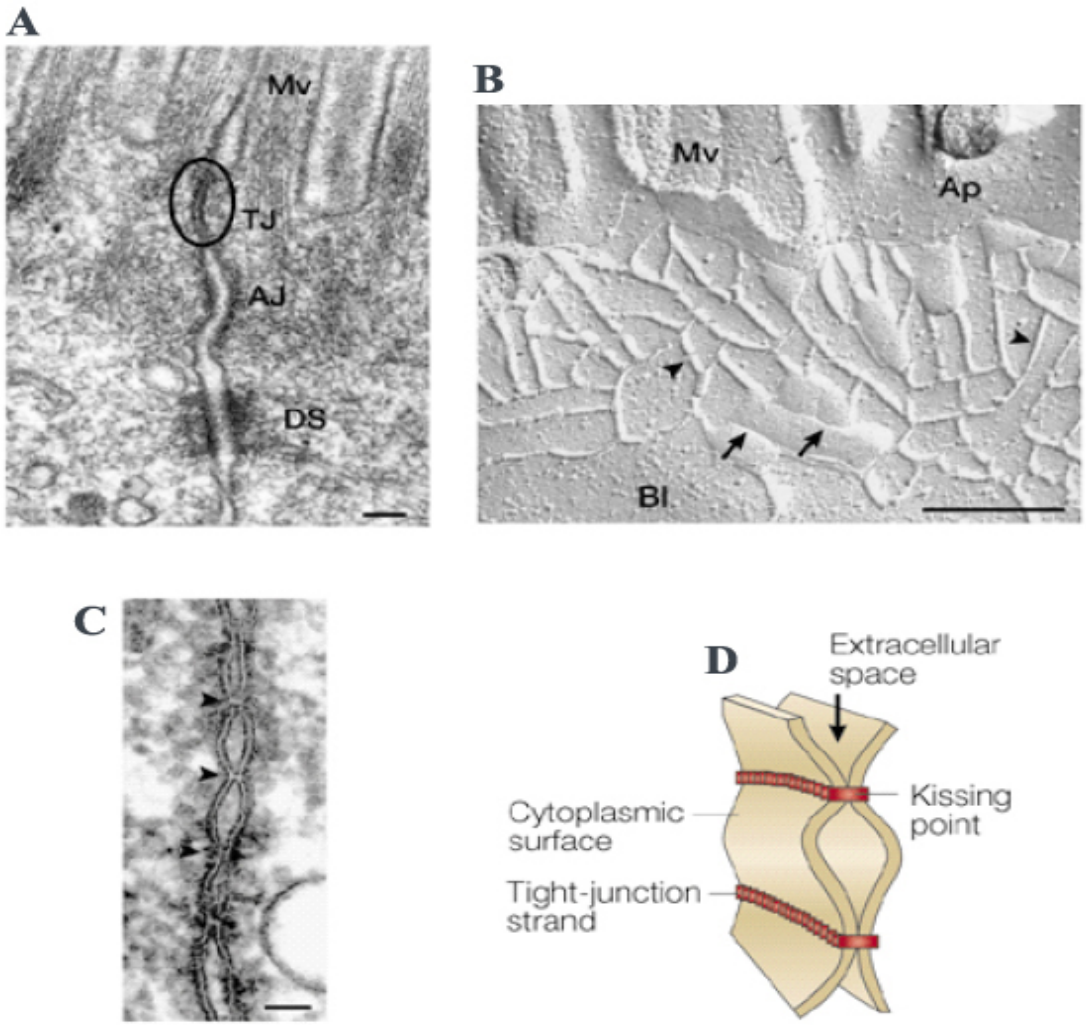

Figure 2 Location and structure of TJs. *(A) The TJ (circled) is located at the most apical region of lateral membranes. (B) Freeze-fracture image shows the the strands (arrowheads) and grooves (arrows) of TJs. (C) Ultrathin sectional view demonstrates that kissiong points (arrowheads) obliterate the intercellular space in TJs. (D) Schematic drawing of the TJs. (Tsukita et al., 2001) Mv, microvilli; TJ, tight junction; AJ, adherens junction; DS, desmosome; AP, apical membrane; Bl, basalateral membrane*

1.1.2 TJ proteins

In TJs, transmembrane (TM) proteins that interact with corresponding proteins on the adjacent membranes are tethered to the actin cytoskeleton via scaffolding proteins (Figure 3). The TM proteins are integrated in the plasma membrane and may be able to transduce extracellular signals, for example in response to cell-cell contact, into the cells. The scaffolding or plaque proteins locate on the cytoplasmic surface of the plasma membrane (Figure 3). They link the integral proteins with the actin cytoskeleton. Some plaque proteins are also involved in vesicular trafficking, nuclear shuttling, control of gene expression and infection of viruses and bacteria. The structure and function of selected integral and plaque proteins of TJs are discussed in more detail below.

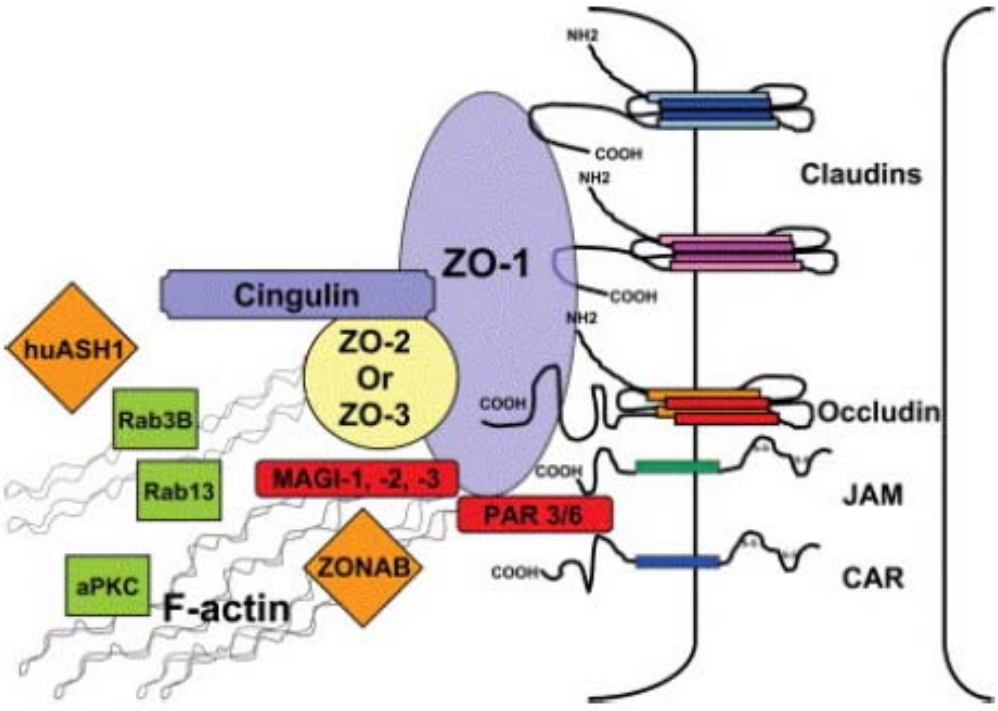

Figure 3 Schematic drawing of the TJ proteins. *TJ proteins consist of TM proteins and plaque proteins that link TM proteins to the cytoskeleton. (Johnson LG. 2005)*

TM proteins of TJ

The three most common TM proteins of TJs are occludin, claudins, and junctional adhesion molecules (JAMs) (Figure 3). Both occludin and claudins have four TM regions and two extracellular domains. Their C- and N-terminal ends reside in the cytoplasm. Occludin is encoded by a single gene, while claudins form a large gene family of more than twenty members in mammals. Occludin and claudins form the backbone of the TJ strands. The combination of occludin and different members of claudins is thought to determine the tightness of the TJs. In contrast to occludin and claudins, JAMs have only one TM domain, with the C-terminal end locating outside the cell and the short N-terminal tail residing inside the cytosplasm. JAMs mainly function in immune response, involving trafficking of T-lymphocytes, neutrophiles and dentritic cells.

Plaque proteins of TJs

Plaque proteins locate under the plasma membrane and function as scaffolds to link the TM proteins to the actin cytoskeleton (Figure 3). Plaque proteins can be grouped into two types based on the presence (for example the ZO proteins) or absence (for example cingulin) of one or multiple PDZ domains (González-Mariscal et al., 2007; Guillemot et al., 2008). The PDZ domain is a short module of 80-90 amino acids, capable of binding small C-terminal peptide motifs or other PDZ domains. Thus, PDZ domain proteins can function as scaffolds to bring together integral, signaling and cytoskeleton proteins. Some scaffolding TJ proteins lacking PDZ domains such as cingulin can also link integral proteins to the actin cytoskeleton, whereas other function in vesicular trafficking and other cellular processes.

1.1.3 TJ modulation

The structure and function of TJs is dynamically regulated and this regulation is fundamental to many physiological processes in multicellular organisms. Many cytokines have been shown to modulate TJ function through their effects on TJ proteins and the associated actin cytoskeleton (Walsh et al., 2000). Small GTPases form a large family of signal transduction molecules. They control cell-cell contact and regulate parecellular permeability through G protein-coupled events (Hopkins et al., 2000). In addition to cytokines and small GTPases, protein kinase C (PKC) also plays a role in the regulation of TJs. PKC activation dramatically increases TJ permeability and the increased leakiness correlates with tumor promotion in epithelial cancers (Mullin et al., 2000). Specific TJ modulation is also of interest for therapeutic drug delivery. Drugs can cross membranes by transcellular or paracellular pathway and the paracellular pathway is controlled by TJs. Temporal opening of the TJs may be a promising approach for delivering therapeutic agents (for example across the intestinal barrier) to the systemic circulation and finally to the site of action (for example across the BBB to target the brain) (Salama et al., 2006).

1.2 MAGUK proteins

ZO-1, ZO-2 and ZO-3 are TJ associated scaffold proteins belonging to the MAGUK (membrane-associated guanylate kinase homologs) protein family. The MAGUK proteins are a family of proteins that locate to various junctional complexes, including TJs in the epithelial and endothelial cells, as well as synaptic and neuromuscular junctions. They are required for the formation of various cell junctions since loss of particular MAGUK members may result in disruption of specific junctional complexes. For example,

combined ZO-1 knockout and ZO-2 knockdown completely blocks TJ formation in epithelial cells (Umeda et al., 2006)

All MAGUK proteins have three PDZ domains, one Src homology 3 (SH3) and one guanylatekinase-like (GUK) domain (Figure 4). As discribed above, PDZ domains bind short C-terminal peptides or other PDZ domains. SH3 domains usually consist of 50-70 amino acids and bind ligands containing PXXP sequences or, in the case of MAGUKs, the GUK domain. The GUK domain is homologous to the enzyme guanylate kinase, which can catalyze the GMP at the expense of ATP. However, the GUK domain in MAGUKs can bind neither GMP nor ATP and is thus most likely enzymatically inactive.

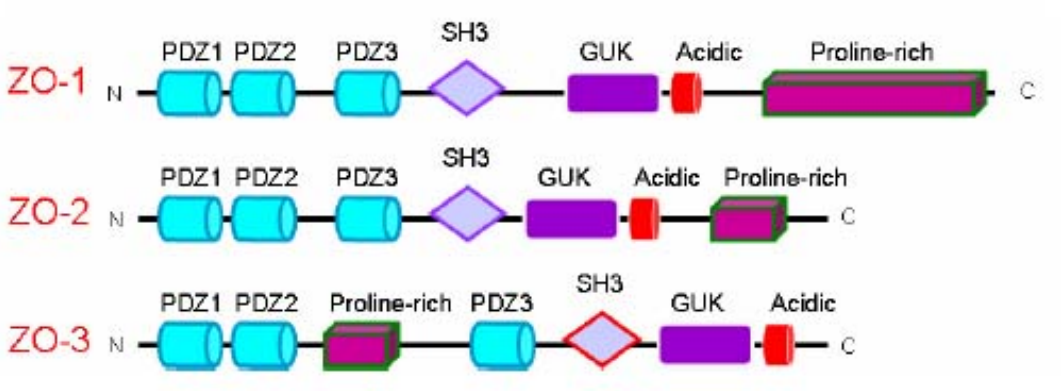

Figure 4 Schematic structures of the MAGUK proteins, ZO-1, ZO-2 and ZO-3. *All three members have three PDZ domains, one SH3 and one GUK domain, one C-terminal acidic region. ZO-1 and ZO-2 have a Proline-rich region in the C-terminus, while the Proline-rich region of ZO-3 is located between the second and third PDZ domain (Kausalya PJ 2005).*

MAGUK proteins bind directly to the C-terminal portion of the TM proteins as well as other signal transduction proteins and, in some cases, to actin. They function as molecular platforms to assemble and regulate signaling pathways at the plasma membrane and couple various extracellular signals with intracellular signal transduction

pathways. They also work as molecular scaffolds to maintain the structural specialization of plasma membrane domains.

MAGUK proteins regulate the polarity of epithelial cells. Multi-domain scaffolding proteins of the MAGUK family are widely expressed at the plasma membrane of the polarized epithelial cells, where they participate in junction assembly, recruitment of proteins to specific plasma membrane domains, the organization of polarized signaling complexes and the maintenance of asymmetric proteins distributions, thus controlling important features of cell polarity (Caruana et al., 2002).

Some MAGUK proteins can also shuttle between TJs and nucleus, where they might be involved in the regulation of gene expression (González-Mariscal et al., 2000).

1.3 ZO proteins

1.3.1 ZO-1

1.3.1.1 Molecular structure of ZO-1

ZO-1 was the first protein shown to associate with TJs (Stevenson et al., 1986). It has a molecular weight of 225 kDa in mouse tissues and 210 kDa in MDCK cells (Anderson et al., 1988). The human ZO-1 is predicted to have 1763 amino acids, with the N-terminal 793 amino acids homologous to the Drosophila discs-large tumor suppressor protein of septate junctions and to PSD95, a postsynaptic density protein of 95 kDa (Willott et al., 1993). Typical for a MAGUK family member, ZO-1 has three PDZ domains, followed by one SH3 domain and one GUK domain. In addition, ZO-1 carries one proline-rich domain at its C-terminus (Figure 4). ZO-1 has two nuclear localization signals (NLS), one located in the first PDZ domain and the other in the GUK domain

(González-Mariscal et al., 1999). ZO-1 localizes to TJs but in some cases has been reported to be present in the nucleus in sparse cell cultures (Gottardi et al. 1996). In the proline-rich domain, ZO-1 contains splicing variants, namely alpha, beta and gamma (Willott et al. 1992; González-Mariscal et al. 1999). ZO-1 has two variable regions, U5 and U6. U5 locates between the SH3 and GUK domain and U6 is immediately after the C-terminal of the GUK domain. In cultured cells, ZO-1 protein lacking U5 can not localize to TJs, while the lack of U6 will localize ZO-1 protein to the lateral membrane, followed by subsequent recruitment of occludin and claudins. These data indicate that the SH3-U5-GUK-U6 region is important for protein interactions, and also for signaling (Fanning et al. 2007).

1.3.1.2 Expression pattern of ZO-1

ZO-1 is expressed as early as in the 8-cell stage of the mouse embryo and initially emerges as a series of punctate sites between apposed cells that subsequently punctate and merge to form a linear belt around blastocyst trophectoderm cells. ZO-1 expression is delayed after inhibition of cell adhesion at the 8-cell stage and its localization is disturbed after microfilament disruption, suggesting that ZO-1 expression is dependent on cell adhesion and cytoskeleton activity (Fleming et al., 1989, 1991).

In adult tissues, ZO-1 is expressed in various epithelia and its expression level varies depending on the particular tissue. For example, in kidney epithelium ZO-1 expression is highest in glomerular epithelium and lowest in the proximal tubule (Schnabel et al., 1990). In addition to epithelia, ZO-1 is also expressed in endothelial cells and its expression level correlates with the cell confluence. ZO-1 expression is low in sparse cell culture and its expression level is increased when the culture becomes confluent (Li et al.,

1990). Beides epithelial and endothelial cells, ZO-1 is also expressed in several non-epithelial cell types that may or may not have typical TJs. For example, in astrocytes, ZO-1 localizes to the cell-cell contact sites, while in S-180 cells ZO-1 is expressed at the cell periphery and within the cytoplasm (Howarth et al., 1992). ZO-1 also distributes to the intercalated disc of cardiomyocytes and the apposed membranes of myelinating Schwann cells (Toyofuku et al. 1998; Poliak et al., 2002). Furthermore, ZO-1 is a major component of the blood-testis barrier. In the testis of newborn mice, ZO-1 locates over the apicolateral Sertoli cell membrane. After establishment of TJs, ZO-1 expression is restricted to tight junctional regions (Byers et al., 1991). ZO-1 is also detected in human and rat BBB. Immunostaining indicates that ZO-1 forms a banded pattern outlining individual endothelial cells in blood vessels (Watson et al., 1991).

1.3.1.3 Expression pattern of ZO-1 isoforms

In the ZO-1 cDNA, 240-bp region is subject to alternative splicing. This exon encodes an in-frame insertion of 80 amino acids, known as alpha motif. The skipping of the corresponding alpha exon depends on two antagonistic exonic elements located in the constitutive flanking exons. Depending on the presence or absence of the alpha motif, two ZO-1 splice varients, known as ZO-1 alpha+ and ZO-1 alpha- are expressed. Both variants are expressed in epithelial cells and localize to the TJs, while their relative expression levels vary greatly in different cell lines. These two isoforms form hermetic TJs but TJs become leakier when the ZO-1 alpha- is predominantly expessed (Willott et al.,1992; Martínez-Contreras et al., 2003).

The expression pattern of ZO-1 alpha- and alpha+ is different during early embryo development. ZO-1 alpha- mRNA is expressed during all pre-implantation stages, while

the ZO-1 alpha+ mRNA only appears at the morula stage. These two isoforms also function differently in membrane assembly. ZO-1 alpha- initially forms punctuate sites at the cell-cell contacts during the 8-cell stage; while ZO-1 alpha+ initially forms perinuclear foci during the late morulae stages and joins the membrane assembly only around the 32-cell stage. Importantly, ZO-1 alpha+ co-localizes with occludin at the perinuclear sites in late morulae stages and at the newly assembled cell junctions. The expression of ZO-1 alpha+ and its interaction with occludin might act as a time-limiting step in the assembly of TJs and blastocoel formation (Sheth et al., 1997).

In animal tissues, ZO-1 alpha- is expressed in structurally dynamic junctions such as endothelial cells, renal glomeruli and seminiferous tubules. ZO-1 alpha+ is expressed in all other epithelial cells that are structurally less dynamic (Balda et al., 1993). Both ZO-1 alpha+ and ZO-1 alpha- are expressed in typical epithelial TJs of the kidney, while only ZO-1 alpha- is expressed in the extremely dynamic structures such as the slit diaphragms, where the intercellular spaces are loose, or endothelial junctions that open in response to physiologic signals (Kurihara et al., 1992). Both ZO-1 alpha+ and alpha- are also expressed in the testis, but their distribution varies in different locations. ZO-1 alpha+ localizes to certain TJs that join the Sertoli cells to specific classes of germ cells (spermatogonia, preleptotene, and leptotene spermatocytes), while ZO-1 alpha- is found in TJs joining Sertoli cells to all classes of germ cells, suggesting that the expression of ZO-1 isoforms might be regulated by specific Sertoli cell-germ cell contacts (Pelletier et al., 1997).

1.3.1.4 Interaction partners

Interaction partners of TJs

The first interaction partner discovered for ZO-1 was ZO-2, which was co-immunoprecipitated with ZO-1 from MDCK cell lysates (Gumbiner et al., 1991). ZO-1 also directly interacts with ZO-3 and co-localizes with it at the TJs in MDCK cells (Haskins et al., 1998). Immunoprecipitation analysis indicates that the three members of the ZO protein family form independent ZO-1/ZO-2 and ZO-1/ZO-3 complexs rather than a ZO-1/ZO-2/ZO-3 trimeric complex (Wittchen et al., 1999). In addition to forming heterodimers with ZO-2 and ZO-3, ZO-1 can also form homodimers via its second PDZ domain. Immunoprecipitation experiments indicate that a substantial fraction of ZO-1 is present as homodimers in MDCK cells. ZO-1 homodimers and ZO-1/ZO-2 and ZO-1/ZO-3 heterodimers might form distinct scaffolds for differnt protein networks (Utepbergenov et al., 2006).

ZO-1 interacts with most types of TM proteins of TJs. Its association with occludin is important for membrane localization of occludin (Furuse et al., 1994). The C-terminal coil-coil domain of occludin dimerizes and forms a four-helix bundle that interacts with ZO-1. The helix bundle of occludin (a.a. 406-521) interacts with the hinge region of ZO-1 (a.a. 591-632) and ZO-1 (a.a. 726-754) in the GUK domain (Müller et al., 2005). ZO-1 interacts with claudin-1 to –8. The interaction of claudins with ZO-1 is mediated by the C-terminal YV sequence of claudins. When claudin-1 and claudin-2 were transfected into L fibroblasts, which only express ZO-1, all the three proteins co-localize to cell-cell borders (Itoh et al., 1999). ZO-1 also interacts with the C-terminal TRV sequence of Cldn16 (also known as paracellin-1/PCLN-1). Mutation of the TRV motif in Cldn16 that

abolishes its interaction with ZO-1, result in a predominantly lysosomal localization (Ikari et al., 2004; Muller et al., 2003; Kausalya et al., 2006). ZO-1 can be co-immunoprecipitated with JAM and the second and third PDZ domains of ZO-1 are crucial for the interaction with the C-terminal PDZ-binding motif of JAM. Deletion of the PDZ binding domain of JAM not only abolishes its interaction with ZO-1, but also disrupts its junctional localization, indicating that ZO-1 plays a role in recruiting or retaining JAM to intercellular junctions (Bazzoni et al., 2000; Ebnet et al., 2000).

ZO-1 also binds to cytosolic TJ plaque proteins. ZO-1 binds to the Ras-binding domain of the Ras target AF-6 and this interaction is inhibited by activated Ras. ZO-1 and AF-6 co-localize at TJs in epithelial cells and at cell-cell adhesion sites in non-epithelial cells. ZO-1 can be immunoprecipitated by AF-6 from Rat1 cells, indicating that ZO-1 interacts with AF-6 in vivo (Yamamoto et al., 1999). Overexpression of activated Ras in Rat1 cells interrupts cell-cell contacts and reduces the cell surface accumulation of ZO-1 and AF-6, suggesting that ZO-1 may serve as an adapter protein for AF-6 to regulate cell-cell contact formation (Yamamoto et al., 1997).

Another cytosolic TJ protein that ZO-1 interacts with is cingulin (Cordenonsi et al., 1999). Pull-down analysis shows that the N-terminal ZIM motif of cingulin (1-378) is crucial for this interaction. ZO-1 can be immunoprecipitated by cingulin. However, cingulin lacking the ZIM motif is still recruited to TJs, indicating that ZO-1 is not the only protein that can recruit cingulin. Endogenous ZO-1 localization is disrupted in Xenopus A6 cells overexpressing cingulin, suggesting that ZO-1 functionally interacts with cingulin in vivo (D'Atri et al., 2002).

Interaction partners of adherens junctions (AJs)

ZO-1 localizes to the cell-cell adhesion sites in non-epithelial cells. The N-terminal half of ZO-1 interacts with the E-cadherin/alpha, β-catenin complex, while the C-terminal half of ZO-1 binds to actin. Therefore, ZO-1 might serve as a linker between the cadherin/catenin complex and the actin cytoskeleton (Itoh et al., 1997). ZO-1 directly interacts with alpha-catenin, which binds to ZO-1 in a similar way as occludin. The helix bundle of alpha-catenin (a.a. 509-906) interacts with the hinge region of ZO-1 (a.a. 591-622) and ZO-1 (a.a. 756-781) in the GUK domain (Müller et al., 2005). ZO-1 can bind to the C-terminal PDZ-binding motif of ARVCF, which is an armadillo-repeat protein of the p120 family. P120 family members interact with E-cadherin and localize to AJs. The interaction with ZO-1 may provide an alternative for the recruitment of ARVCF to the plasma membrane (Kausalya et al., 2004).

Interaction partners of gap junctions

ZO-1 co-localizes with Connexin 43 (Cx43), which plays a critical role in the synchronized contraction of cardiomyocytes. The interaction between ZO-1 and Cx43 occurs via the first PDZ domain of ZO-1 and the C-terminus of Cx43. Overexpression of the N-terminal domain of ZO-1 in Cx43-expression cells disrupts the localization of Cx43 to the cell-cell interface, concomitant with a loss of electrical coupling. These data suggest that ZO-1 may help to recruit Cx43 to the intercalated disc to generate functional gap junctions between cardiomyocytes (Toyofuku et al., 1998; Giepmans et al., 2001). Both ZO-1 and Cx43 localize to the intercalated discs, but only display moderate co-localization. However, the degree of co-localization increases significantly after enzymatic dissociation of cardiomyocytes from intact ventricles. Co-immunoprecipitation

using ZO-1 and Cx43-specific antibodies confirm and increased interaction between ZO-1 and Cx43 in dissociated as compared to intact ventricles. These data suggest that ZO-1 might play an important role in gap junction turnover during heart development and disease processes (Barker et al., 2002). ZO-1 regulates the function of Cx43 not only in cardiomyocytes, but also in other cell types. When Sertoli cells were treated with gamma-hexachlorocyclohexane (HCH), which induces gap junction endocytosis, ZO-1/Cx43 association was increased in the cytoplasm, suggesting that ZO-1 might play a role in the turnover of Cx43 during the endocytosis of gap junction plaques (Segretain et al., 2004). Overexpression of the connexin-interacting fragment of ZO-1 in ROS osteoblastic cells disrupted the Cx43/ZO-1 interaction reduced gap junction permeability. On the contrary, gap junction permeability and membrane staining for Cx43 were increased in ROS cells transfected with full-length ZO-1. These data indicate that Cx43 membrane localization and Cx43-mediated gap junction function in ROS osteoblastic cells is regulated by ZO-1 (Laing et al., 2005). Knockdown of ZO-1 in lens epithelial cells results in accumulation of Cx43 aggregates inside the cells. These aggregates are not disassembled by PKC-gamma activation and Cx43 phosphorylation. In these ZO-1 knockdown cells, the large Cx43 plaques are lost and consequently no functional dye transfer is observed. These data confrim a critical role for ZO-1 in the regulation of Cx43 function (Akoyev et al., 2007). Furthermore, ZO-1 also co-localizes with Cx43 in glial gap junctions of astrocytes and can be co-immunoprecipitated by Cx43 (Penes et al., 2005). The interaction between ZO-1 and Cx43 can be regulated by c-Src. Active c-Src phosphorylates Tyr265 of Cx43 and inhibits the interaction between ZO-1 and Cx43 via binding to Cx43 through its SH2 domain. The interaction between ZO-1 and mutant Cx43 lacking the c-Src

phosphorylation site, in contrast, is not affected by activated c-Src (Toyofuku et al., 2001).

In addition to Cx43, ZO-1 also interacts with other connexins. ZO-1 can be co-immunoprecipitated with Cx45 due to its interaction with the C-terminal PDZ binding motif of Cx45. Endogenous ZO-1 co-localizes with wild type Cx45, but not a mutant in which the C-terminal PDZ-binding motif was inactivated, in tranfected MDCK cells (Kausalya et al., 2001). ZO-1 also co-localizes with alpha3 Cx46 and alpha8 Cx50 throughout the lens. This interaction is via the second PDZ domain of ZO-1 and the C-terminus of the two connexins (Nielsen et al., 2003). Co-localization of ZO-1 and Cx36 is widespread in the central nervous system. ZO-1 can pull down Cx36 via its first PDZ domain, while the four C-terminal amino acids of Cx36 are crucial for this interaction. Further studies demonstrated that ZO-1 and Cx36 co-localize at individual gap junction plaques (Li et al., 2004; Rash et al., 2004). ZO-1 co-localizes with Cx47 in oligodendrocytes and can pull it down through its second PDZ domain (Li et al., 2004). In glial gap junctions of astrocytes, also Cx30 co-localizes and co-precipitates with ZO-1. The second PDZ domain of ZO-1 is sufficient for its binding with Cx30 (Penes et al., 2005). These data indicate that ZO-1 may play a crucial role in organizing gap junctions and recruiting signaling molecules that regulate intercellular communication.

Other interaction partners

ZO-1 also interacts with several other proteins, some of which are discussed below. ZO-1 binds actin via its C-terminal portion and can be immunoprecipitated with actin filaments in vitro. When the C-terminal portion of ZO-1 was transfected into mouse L fibroblasts, it localized to actin stress fibers (Itoh et al., 1997). Similarly, the

overexpressed C-terminal portion of ZO-1 locates along the lateral plasma membrane and other actin-rich structures in MDCK cells (Fanning et al., 1998). In addition, ZO-1 interacts with the actin binding protein 4.1 (Mattagajasingh et al., 2000). These data suggest that ZO-1 might function as a linker between TM proteins and the actin cytoskeleton.

ZO-1 furthermore interacts via its SH3 domain with a Y-box transcription factor, ZONAB (ZO-1-associated nucleic acid-binding protein) and negatively regulates ErbB-2 promoter activity through ZONAB in a cell density-dependent manner. Stable overexpression of ZO-1 and ZONAB controls endogenous ErbB-2 expression. These data indicate that ZO-1 participates in the control of gene expression and might play a role in the regulation of epithelial cell differentiation (Balda et al., 2000). ZO-1 also interacts via its SH3 domain with the heat shock protein Apg-2. Apg-2 thus competes with ZONAB for binding to the SH3 domain of ZO-1, leading to the release of ZONAB and increased cell proliferation (Tsapara et al., 2006).

The first PDZ domain of ZO-1 interacts with the TRL motif of TRPC4, which is a member of the mammalian transient receptor potential (TRP) protein family. TRPC4 forms cation-permeable channels in the plasma membrane and membrane localization of TRPC4 depends on the C-terminal TRL motif that interacts with the ZO-1 PDZ domains (Song et al., 2005).

The first PDZ domain of ZO-1 furthermore interacts with the cortical membrane scaffolding protein alpha-actinin-4 in both cultured cells and tissues, including brain and heart (Chen et al., 2006).

1.3.1.5 ZO-1 functions, regulation and associated diseases

ZO-1 functions

ZO-1 is thought to be involved in TJ formation. At the initiation of cell-cell contact formation, ZO-1 localizes at the primordial cell-cell contact sites together with E-cadherin to form spot-like junctions at the tips of cellular processes. As cellular polarization continues, occludin is recruited to the ZO-1-positive spot-like junctions and gradually forms belt-like TJs, while E-cadherin leaves the ZO-1-positive spot-like junctions to form belt-like adherens junctions (Ando-Akatsuka et al., 1999). However, knockout of the ZO-1 gene in Eph4 cells does not affect the formation of TJs and the establishment of cell polarity. In ZO-1 deficient Eph4 cells, occludin and claudins are normally recruited to the TJ region, while ZO-2 is up regulated and cingulin is down regulated. Ca^{2+} switch experiments indicate that ZO-1 deficiency does not affect adherens junction initiation, but delays the subsequent TJ formation (Umeda et al., 2004). However, if ZO-2 is silenced in ZO-1 deficient Eph4 cells, TJs are completely disrupted. Exogenous expression of either ZO-1 or ZO-2 can rescue the formation of TJs, suggesting that both ZO-1 and ZO-2 can independently determine the formation of TJs (Umeda et al., 2006). In ZO-1 knockout / ZO-2 knockdown cells, adherens junction formation is delayed, suggesting that ZO proteins are not only involved in TJ formation, but also play a role for AJ assembly. Mutational analysis indicated that ZO-1 might be directly involved in the formation of TJs and adherens junctions, but that its role in these two processes differs (Ikenouchi et al., 2007).

ZO-1 is expressed in the blood-testis barrier. In carcinoma in situ (CIS) of seminiferous tubules, ZO-1 and ZO-2 mislocalize from the blood-testis barrier region of adjacent Sertoli cells to the Sertoli cell cytoplasm. Lanthanum tracer permeability studies

demonstrated that the integrity of the blood-testis barrier is disrupted; suggesting that ZO-1 might play a crucial role in the blood-testis barrier (Fink et al., 2006).

ZO-1 also participates in the regulation of gene expression. It interacts with the Y-box transcription factor ZONAB to regulate the ErbB-2 promoter in a cell density-dependent manner. Stable overexpression of ZO-1 and ZONAB controls the expression of endogenous ErbB-2 (Balda et al., 2000). ZO-1 may also play a role in regulating cell differentiation. Stable expression of the N-terminus of ZO-1 in corneal epithelial cells leads to a dramatic change in cell shape and gene expression. The cobblestone morphology of epithelial cells is lost in the transfected cells which show an elongated fibroblast-like appearence. Concomitantly, occludin is down regulated and the localization of endogenous ZO-1 and ZO-2 is disrupted (Ryeom et al., 2000). A similar EMT and an activation of Wnt signaling is observed in MDCK cells overexpressing the N-terminus of ZO-1 (Reichert et al., 2000) or in breast cancer cell lines where, due to the lack of occludin, ZO-1 is present in the cytosol (Polette et al., 2005).

Regulation of ZO-1

The localization of ZO-1 can be regulated by its phosphorylation of tyrosine. ZO-1 is phosphorylated during the rearrangement of TJs in glomeruli when there are rapid changes in epithelial cell shape, suggesting that ZO-1 phosphorylation might be required for the re-organization of TJs (Kurihara et al., 1995). The phosphorylation status of ZO-1 can be regulated by epidermal growth factor (EGF) in A431 human epidermal carcinoma cells. Addition of EGF to A431 cells results in phosphorylation of ZO-1 on tyrosine residues. Concomitantly, ZO-1 is redistributed from the lateral membranes to apical sites of cell-cell contact, indicating that the transient tyrosine phosphorylation of ZO-1 might

be involved in the rearrangement of the intercellular junctions. EGF also causes actin re-organization, which is required for EGF-induced rearrangement of ZO-1 (Van Itallie et al., 1995). ZO-1 localization furthermore depends on rab3B. Stable expression of rab3B in PC12 neuroendocrine cells leads to redistribution of ZO-1, while a mutant rab3B (N135I) has no effect (Sunshine et al., 2000). ZO-1 expression levels are directly affected by PKC in T84 cell line. Activation or inhibition of PKC induces or decreases ZO-1 transcription, respectively (Weiler et al., 2005).

ZO-1 and associated diseases

ZO-1 in celiac disease and kidney diseases

ZO-1 is downregulated in duodenal mucosa of active celiac disease patients (Montalto et al., 2002). ZO-1 is also lost in dextran sulfate sodium (DSS) induced colitis. Further analysis showed that loss of ZO-1 and increased permeability start before the development of significant intestinal inflammation, suggesting that DDS induced colitis is a consequence of the alterations in the TJ complex (Poritz et al., 2007). In addition to celiac disease, ZO-1 is also involved in kidney diseases. ZO-1 can recruit claudin 16 to the TJs in kidney epithelium cells. In human patients carrying a muation in claudin 16 that inactivates the PDZ binding motif, claudin 16 no longer localizes to the TJs but accumulates in lysosomes. This mislocalization of claudin 16 leads to familial hypomagnesemia with hypercalciuria and nephrocalcinosis (Müller et al., 2003). ZO-1 is also down regulated or mislocalized in the kidney of diabetic animals, where it is no longer found on the podocyte membrane and instead shows a diffuse cytoplasmic distribution, suggesting that ZO-1 might be involved in pathogenesis of proteinuria in diabetes (Rincon-Choles et al., 2006). Consistent with these observations, high glucose

medium reduces ZO-1 expression levels and disturbs the membrane localization of ZO-1 in glomerular epithelial cells in vitro.

ZO-1 and tumorigenesis

The role of ZO-1 in tumorigenesis remains ambiguous. ZO-1 expression is significantly downregulated in breast cancers and this correlates with tumor differentiation. The lower the ZO-1 expression levels, the less differentiated the tumor. Concomitantly, reduced ZO-1 expression strongly correlates with lower E-cadherin expression levels (Hoover et al., 1998). In squamous cell carcinoma (SCC), ZO-1 expression levels and patterns are also changed. While overall reduced, ZO-1 is strongly expressed in the keratinized tumor cells. In contrast, in normal epidermis, it is mainly expressed at the cell-cell borders of the granular layer (Morita et al., 2004). Furthermore, ZO-1 expression has been implicated in metastasis formation. ZO-1 is downregulated in primary colorectal cancer (CRC) with liver metastasis but re-expressed in liver metastasized cancers. Further studies indicated that ZO-1 interacts with epidermal growth factor receptor (EGFR) in CRC with liver metastasis and the bound ZO-1 protein is highly phosphorylated on tyrosine residues, while ZO-1 expressed in liver metastasized cancer is dephosphorylated. These data suggest a critical role for ZO-1 in CRC metastasis (Kaihara et al., 2003). In pancreatic adenocarcinoma, however, ZO-1 is upregulated and displays a variety of staining patterns in metastatic pancreatic cancer cells within lymph nodes. Some cells show apical and apical-lateral staining while others display a diffused membranous staining. Overexpression of ZO-1 in pancreatic adenocarcinoma might facilitate the metastasis of pancreatic cancer cells (Kleeff et al., 2001). Disruption of ZO-1 localization to the sites of cell-cell contact induces ERK2 and p-ERK1/2 expression and

results in dissociation of cell clones from pancreatic tumors, suggesting that ZO-1 might regulate cell adhesion of pancreatic cancer cells via activation of ERK2 (Tan et al., 2005). Furthermore, ZO-1 is expressed in most synovial sarcoma, indicating a partial epithelial differentiation of the sarcoma (Billings et al., 2004).

1.3.2 ZO-2

1.3.2.1 Molecular structure of ZO-2

The TJ protein ZO-2 has a molecular weight of 160 kDa and, as a member of the MAGUK protein family, contains three PDZ domains, one SH3 domain, and one GUK domain. Like ZO-1, ZO-2 has a proline-rich C-terminal region that is not conserved in other MAGUK family members (Figure 4). ZO-2 shares high amino acid identity with ZO-1 except in the C-terminus, which might contribute to the different functions of these two proteins (Beatch et al., 1996). ZO-2 contains several nuclear localization signals (NLS) in the N-terminal region (González-Mariscal et al., 2006). It also has four putative nuclear export signals (NES), two of which are found in the second PDZ domain, the other two in the GUK region (Jaramillo et al., 2004). In confluent MDCK cell cultures ZO-2 localizes to the plasma membrane, but it is found in the nucleus in sparse cultures (Islas et al., 2002). The change of its subcellular localization depending on cell confluency suggests a role for ZO-2 in regulating gene expression in response the cell-cell adhesion status.

1.3.2.2 Interaction partners of ZO-2

ZO-2 interacts with a large and growing number of interaction partners. Immunoprecipitation experiments show that ZO-2 binds to ZO-1 via the second PDZ

domains. When the N-terminal portion of ZO-2 was expressed in cultured cells, it co-localized with endogenous ZO-1/ZO-2. ZO-2 also binds through its GUK domain to occludin to form a complex with ZO-1/occludin that is important for the establishment of TJ domains (Itoh et al., 1999). Through the first PDZ domain, ZO-2 binds to the C-terminal YV sequence of claudin-1 to -8 **(**Itoh et al., 1999) but not to the TRV motif of Cldn16 (Müller et al., 2003). Like ZO-1, ZO-2 can independently determine the site of polymerization of claudins (Umeda et al., 2006). ZO-2 binds to the N-terminal fragment of cingulin, which links the sub-membranous plaque domain of TJs to the actin cytoskeleton (Cordenonsi et al., 1999). Similar to ZO-1, ZO-2 is present in adherens junctions in non-epithelial cells such as fibroblasts and cardiac muscle cells. In adherens junctions, ZO-2 interacts with α -catenin to form a complex with ZO-1/ α -catenin involved in the establishment of adherens junction domains (Itoh et al., 1999). ZO-2 directly binds to F-actin and the C-terminal portion of ZO-2 expressed in cultured cells co-localizes with actin filaments (Wittchen et al., 1999). ZO-2 can also be co-precipitated by the actin binding protein 4.1 and the interaction occurs via the amino acids encoded by exons 19-21 of 4.1R and residues 1054-1118 of ZO-2. By immunofluorescence microscopy, ZO-2 co-localizes with the actin binding protein 4.1R at TJs in MDCK cells (Mattagajasingh et al., 2000). ZO-2 also interacts with ARVCF, an armadillo-repeat protein of the $p120^{Ctn}$ family found in AJs and may play a role in the recruitment of ARVCF to the plasma membrane (Kausalya et al., 2004). Interestingly, ZO-2 also binds via its C-terminal motif to two PDZ domains of hScribble (Métais et al., 2005), a component of the Scrib polarity complex, highly conserved in evolution from worms to

mammals (Assémat et al., 2007). A functional significance of this interaction, however, has not been established.

In addition to integral membrane and cytosolic components of TJs and AJs, ZO-2 also associates with nuclear proteins. In sparse cell cultures, ZO-2 concentrates in the nucleus and co-localizes with splicing factor SC35 (Islas et al., 2002). ZO-2 has also been shown to directly interact with the DNA-binding protein scaffold attachment factor-B (SAF-B), an interaction mediated by the first PDZ domain of ZO-2 and the C-terminus of SAF-B (Traweger et al., 2003). Interestingly, ZO-2 directly associates with several transcription factors, in particular Jun, Fos and C/EBP, in epithelial cells (Betanzos et al., 2004). These findings suggests that ZO-2 not only functions at the level of TJs but that it may be involved regulating gene expression linked to cell proliferation and/or differentiation.

1.3.2.3 ZO-2 and associated diseases

There is evidence to support a role for ZO-2 as a tumor suppressor gene. In humans, two ZO-2 isoforms, namely ZO-2A and ZO-2C, the latter lacking the first 23 amino acids present in ZO-2A, are differentially expressed in normal and neoplastic cells. ZO-2C is expressed in both normal and neoplastic tissues, while ZO-2A is absent from pancreatic adenocarcinomas (Chlenski et al., 1999a). The loss of ZO-2A expression in neoplastic cells is due to the inactivation of the downstream promoter P(A) (Chlenski et al., 1999b). Methylation analysis also showed that ZO-2 is aberrantly methylated in 64% of 42 pancreatic cancers analyzed as compared to 10 normal pancreatic ductal epithelial samples (Sato et al., 2003). In addition to pancreatic adenocarcinoma, ZO-2 is also lost or significantly decreased in a majority of breast adenocarcinomas. (Chlenski et al., 2000).

ZO-2 is a cellular target of the tumorigenic Ad9 E4-ORF1 protein, which interacts with the first PDZ domain of ZO-2 via its C-terminal PDZ-binding motif. Over-expression of ZO-2 can repress the neoplastic growth of cells activated by Ad9 E4-ORF1 protein (Glaunsinger et al., 2001).

ZO-2 has also been implicated in human diseases other than cancer. Point mutations in first PDZ domain of ZO-2 have been linked to familial hypercholanemia (FHC), a condition characterized by elevated serum bile acid concentrations, itching, and fat mal-absorption (Carlton et al., 2003). ZO-2 is involved in maintaining the integrity of the blood-testis barrier. In CIS of seminiferous tubules, ZO-2, together with ZO-1, is mislocalized from the blood-testis barrier region to the cytosol of Sertoli cells and this change in localization correlates with a functional disruption of the TJ barrier (Fink et al., 2006).

1.3.3 ZO-3

1.3.3.1 Molecular structure of ZO-3

ZO-3 is a 130-kDa protein with, similar to ZO-1 and ZO-2, three PDZ domains, one SH3 domain, one GUK domain and a C-terminal acidic domain and a basic region between the first and second PDZ domains. The main differences compared to ZO-1 and ZO-2 are the location of the proline rich region between the second and third PDZ domain of ZO-3 (Figure 4) and to the lack of alternative splicing (Haskins et al., 1998). ZO-3 has two putative bipartite nuclear localization signals (NLS) (González-Mariscal et al., 1999) and one nuclear export signals (NES) (Islas et al., 2002), however, there is no evidence for a nuclear localization of ZO-3 so far. Unlike ZO-1 and ZO-2, ZO-3 is only

expressed in different epithelia and not in endothelia. ZO-3 is also not found at sites of E-cadherin-based cell-cell adhesion (Inoko et al., 2003).

1.3.3.2 Interaction partners of ZO-3

ZO-3 can be co-precipitated with ZO-1 and based on immunofluorescence experiments, it co-localizes with ZO-1 at TJs. In vitro binding analysis demonstrated that ZO-3 directly interacts with ZO-1 and the cytoplasmic domain of occludin, but not with ZO-2 (Haskins et al., 1998). Further studies indicated that ZO-1, ZO-2, and ZO-3 do not exist in situ as a trimeric complex but as independent ZO-1/ZO-2 and ZO-1/ZO-3 complexes (Wittchen et al., 1999). Like ZO-2, ZO-3 binds to the C-terminal YV sequence of claudin-1 to -8 through its first PDZ domain in vitro (Itoh et al., 1999) and not to the TRV motif in Cldn16 (Müller et al., 2003). Pull-down analysis indicated that ZO-3 interacts with both the N-terminal and C-terminal parts of cingulin, while ZO-1 and ZO-2 only interact with the N-terminal part of cingulin (Cordenonsi et al., 1999). ZO-3 (and ZO-1 but not ZO-2) binds via PDZ domains to Cx45 (Kausalya et al., 2001). These observations indicate that despite their high similarity, the PDZ domains of ZO proteins interact with specific ligands. This notion has been confirmed by analyzing the specificity of individual PDZ domains using small peptides displayed on phage (Sidhu et al., 2003). ZO-3 interacts directly with F-actin in vitro and immunofluorescence analysis shows that ZO-3 co-localizes with F-actin aggregates at cell borders in cytochalasin D-treated MDCK cells (Wittchen et al., 1999). While ZO-2 associates with the Scrib polarity complex, ZO-3 interacts via its C-terminus with one of the PDZ domains of PATJ (Roh et al., 2002). PATJ is a component of Crumbs, a polarity complex conserved during evolution from worms to mammals (Assémat et al., 2007). ZO-3 also interacts with p120

catenin and AF-6 (Wittchen et al., 2003), suggesting a possible role of ZO-3 in signal transduction.

1.3.3.3 Functions of ZO-3

Expression of the N-terminal region of ZO-3 (NZO-3) in MDCK cells delays the assembly of both TJs and AJs, consistent with a role in junction formation. Immunofluorescence analysis indicated that ZO-1, ZO-2, endogenous ZO-3, and occludin are mislocalized during initial steps of TJ assembly and that recruitment of E-cadherin and β-catenin to the cell membrane is delayed. A larger fraction of β-catenin is Triton X-100-soluble during the early stages of TJ assembly in the cells expressing NZO-3 protein (Wittchen et al., 2000), suggesting that NZO-3 might exert a dominant negative role on junction assembly via β-catenin. Further studies demonstrated that NZO-3 expression in MDCK cells decreases the number of stress fibers and focal adhesions and increases cell migration rate in a wound-healing assays. Expression of NZO-3 alters the interactions between endogenous ZO-3 and $p120^{Ctn}$, which may affect RhoA activity and RhoA-related signaling events (Wittchen et al., 2003). Since PATJ lacking the PDZ domain required for interaction with ZO-3 is not present in cell-cell contacts, ZO-3 could function in establishing cell polarity by recruiting PATJ and its associated proteins to TJs (Roh et al., 2002). However, recent analysis in Zebrafish indicates that depletion of ZO-3 does not affect PATJ localization (Kiener et al., in press). Furthermore, in the course of my studies, a ZO-3 KO mouse was published which was viable and fertile and did not show any phenotype. F9 teratocarcinoma cell lines deficient in ZO-3 can be differentiated to form normal visceral endoderm epithelium-like cells, which have a normal TJ structure. These data suggest that ZO-3 is dispensable for both TJ formation and viability in the

mouse (Adachi et al., 2006). Interestingly, however, depletion on ZO-3 in zebrafish leads to a permeability defect of the enveloping cell layer of embryos (Kiener et al., in press).

1.4 Rationale and aim of research

Since the discovery of ZO-1 two decades ago, the ZO proteins have been widely studied. Their structures have been unveiled, their expression patterns determined, many interaction partners discovered and putative roles in TJ structure and function explored. However, despite being the best studied TJ proteins, their precise physiological role remains unclear and many questions are still unanswered. For example, ZO proteins are expressed in the early stage of embryo development, but their function during the different stages of development is not clear. Furthermore, ZO proteins are widely expressed in the tissues of adult animals, but their precise physiological functions remain to be determined. In particular, it is not clear if the three ZO-proteins exert redundant or unique functions and, if unique, how these functions differ. ZO proteins not only localize to TJs, but also to adherens and gap junction and their function in those structures are poorly characterized. Similarly, their roles in non-epithelial or endothelial cells, such as Schwann cells or cardiac myocytes, remain largely unknown. ZO proteins can shuttle between plasma membrane and the nucleus, but their role in the nucleus has only recently been started to be unraveled. Similarly, their possible importance in human diseases, in particular as possible tumor suppressors, remains ambiguous.

The aim of this thesis was to study the function of ZO proteins in a physiological context using gene knockout strategies. In order to explore the physiological role of different ZO proteins during development and in various tissues, ZO knockout mice were generated by homozygous recombinanation. Due to the possible compensation between

individual ZO proteins, double knockout mice were also generated by crossing different single knockout strains. As a complementary approach, ZO knockout ES cells were produced by multiple gene targeting. These ZO deficient ES cells can not only be differentiated into embryloid bodies (EBs) to study the role of ZO proteins during early stages in development, but they can also be differentiated into different cell types (i.e. neurons or cardiomyocytes) to explore a possible role of ZO proteins in ES cell differentiation. Furthermore, ES cells can be used to generate chimeric mice to circumvent possible embryonic lethality. Finally, ES cells lacking ZOs can form teratoma in nude mice, allowing to explore the role of ZO proteins in tumorigenesis.

Chapter 2 Materials and Methods

2.1 Generation of ZO-1-/+ ES cells

Genomic fragments containing the ZO-1 locus were isolated from a mouse 129Sv genomic library (Stratagene) and subcloned into pBluescript II KS+ (Stratagene). A targeting vector with a LacZ neo cassette flanked by short and long arms of 3.6 kb and 6.7 kb for ZO-1 was designed to replace the exon containing the first transcriptional ATG. The targeting vector was linearized and electroporated into W4 embryonic stem cells (Taconic Transgenics), which were then selected with 250 μg/ml G418. After 7-9 days selection, the remaining colonies were picked and screened by long-range PCR.

2.2 Generation of ZO-2-/+ ES cells

Genomic fragments containing the ZO-2 locus were isolated from a mouse 129Sv genomic library (Stratagene) and subcloned into pBluescript II KS+ (Stratagene). A targeting vector with a LacZ neo cassette flanked by short and long arms of 1.8 kb and 5.9 kb for ZO-2 was designed to replace the exon containing the first transcriptional ATG. The targeting vector was linearized and electroporated into W4 embryonic stem cells, which was then selected with 250μg/ml G418. After 7-9 days selection, the remaining colonies were picked, screened by long-range PCR and confirmed by Southern blot later.

2.3 Generation of ZO-3-/+ ES cells

Genomic fragments containing the ZO-3 locus was isolated from a mouse 129Sv genomic library (Stratagene) and subcloned into pBluescript II KS+ (Stratagene). A targeting vector with a LacZ neo cassette flanked by short and long arms of 2.2 kb and

4.8 kb for ZO-3 was designed to replace the exon containing the first transcriptional ATG. The targeting vector was linearized and electroporated into W4 embryonic stem cells, which were then selected with 250μg/ml G418. After 7-9 days selection, the remaining colonies were picked, screened by long-range PCR and confirmed by Southern blot later.

2.4 Generation of ZO-1-/- ES cells

ZO-1-/+ ES cells were seeded in a 6-well plate. After two days, these cells were trypsinized and replated onto a 10 cm dish and selected with 20 mg/ml G418 (CALBIOCHEM). After 7-9 days of selection, drug-resistant colonies were picked. Half of the cells from each clone were screened with PCR and the other half were expanded on feeder cells. The targeting ES cell clones were amplified and confirmed by Western blot. Six independent ZO-1-/- ES cell clones were obtained from the screening.

2.5 Generation of ZO-2-/- ES cells

Independent ZO-2-/+ ES cells were seeded in a 6-well plate. After two days, these cells were trypsinized and replated onto a 10 cm dish and selected with 20 mg/ml G418 (Calbiochem). After 7-9 days of selection, drug-resistant colonies were picked. Half of the cells from each clone were screened with PCR and the other half were expanded on feeder cells. The targeting ES cell clones were amplified and confirmed by Western blot. Eight independent ZO-2-/- ES cell clones were obtained from two independent ZO-2-/+ mother ES cell lines.

2.6 Isolation of ZO-3 -/- ES cells

Six to eight-week-old 129SvJ ZO-3-/- female mice were mated with ZO-3-/- 129Sv males. On E3.5 (Plug=0.5 day), females were sacrificed to collect uteri, and balstocysts

were flushed out from the uteri with M2 media (Sigma). The blastocysts were then transferred into the wells of 96-well U-shape plates and cultured with ES cell medium. After four days, individual cell colonies were picked, trypsinized and mechanically dissociated. Inner cell mass cells were picked and transferred to 48-well plates with feeder cells. Around 8 days, colonies with ES cell-like morphology were observed. They were trypsinized, dissociated, and replated onto another 48-well plate with fresh feeder cells. Around 5 days later, ES cell colonies could be clearly observed. These cells were amplified and used for analysis. Two independent ZO-3-/- ES cell clones were isolated from the inner cell mass.

2.7 Generation of ZO-1-/- ZO-2-/-ES cells

The Neo gene in ZO-1 mutant allele was flanked with two loxp sites. ZO-1-/- ES cells were transfected with cre-pac plasmid (Taniguchi et al. 1998), which expresses the cre protein to specifically delete the neo sequence from the chromosome. After transfection, cells were cultured in ES cell culture media for 16 to 24 hours and then selected with puromycin for 48 hours. The surviving colonies were picked, trypsinized and dissociated. Half of the cells from each clone were cultured with normal ES cell culture media and the other half was selected with 500μg/ml G418. The neo sequence was deleted by cre in the clones that did not survive the G418 selection. The targeted clones were amplified and transfected with the ZO-2 targeting vector. ZO-2 knockout in the ZO-1 -/- ES cell line was achieved in analogy to the approach described for the generation of ZO-2-/- ES cells. ZO-1 and ZO-2 double knockout was confirmed by Western blot analysis. Seven independent ZO-1-/-ZO-2-/- ES cell clones were obtained from the screening.

2.8 Generation of ZO-2-/-ZO-3-/- ES cells

The Neo gene in ZO-3 mutant allele was flanked with two loxp sites. ZO-3-/- ES cells were transfected with cre-pac plasmid (Taniguchi et al. 1998), which expresses the cre protein to specifically delete the neo sequence from the chromosome. After transfection, cells were cultured in ES cell culture media for 16 to 24 hours and then selected with puromycin for 48 hours. The surviving colonies were picked, trypsinized and dissociated. Half of the cells from each clone were cultured with normal ES cell culture media and the other half was selected with 500μg G418. The neo sequence was deleted in the clones that did not survive the G418 selection. The clones were amplified and transfected with the ZO-2 targeting vector. ZO-2 and ZO-3 double knockout was confirmed by Western blot analysis. Five independent ZO-2-/-ZO-3-/- ES cell clones were obtained from the screening.

2.9 Generation of ZO-1 chimeric mice and embryos

ZO-1-/+ and ZO-1-/- ES clones were injected into blastocysts derived from C57BL/6 mice to generate chimeric mice and embryos.

2.10 Generation of ZO-2 chimeric and knockout mice

ZO-2-/+ and ZO-2-/- ES clones were injected into blastocysts derived from C57BL/6 mice to generate chimeras. ZO-2 -/+; +/+ chimeras with germ line transmission were used to generate ZO-2 knockout mice.

2.11 Generation of ZO-3 knockout mice

ZO-3-/+ ES clones were injected into blastocysts derived from C57BL/6 mice to

generate chimeras. The chimeras with germ line transmission were used to generate ZO-3 knockout mice.

2.12 Southern blot analysis

Genomic DNA was extracted from G418-resistant ES cell clones and completely digested with Scal I. For ZO-2, a 566-bp fragment, corresponding to the 5' end of the right arm of the target vector, was labeled with [^{32}P] dCTP by random priming (Roche) and used as a probe. For ZO-3, a 679-bp fragment, corresponding to the 3' end of the left arm of the target vector, and a 668-bp fragment, corresponding to the neo sequence, were labeled with [^{32}P] dCTP and used as probes.

2.13 PCR genotyping

For genotyping, genomic DNA isolated from tail clippings or embryo tissue and suitable primers were used in a PCR reaction. Primer 1 (5'-atg gag gag gtg ata tgg gag cag-3') and primer 2 (5'-tgt gtc att ggt gtg tgg aag gag-3') were used amplify a fragment of 367 bp for the WT allele, whereas primer 3 (5'-gag ctg tgt gga agc ata cct agt-3') and primer 4 (5'-atg gga tag gtt acg ttg gtg tag-3') yielded a 580 bp product for the mutant allele of ZO-2. For ZO-3, primer 5 (5'-gag gta tag tgg gta agc cag aca-3') and primer 6 (5'-aag gcg tta ctt ctc aga ccc ag-3') amplified a 297 bp fragment for the WT allele, whereas primer 7(5'-gag gta tag tgg gta agc cag aca-3') and primer 8 (5'-atg gga tag gtt acg ttg gtg tag-3') resulted in a 679bp product for the mutant allele.

2.14 Histological analysis

E5.5-E8.5 embryos within deciduas and mouse organs were fixed in 4% paraformaldehyde overnight, embedded in paraffin, sectioned and stained with

hematoxylin and eosin. The slides were viewed with a Leica DM4000 B microscope and photos were taken with a DFC300 FX camera. For genotyping embryos, tissue was micro-dissected from paraffin sections and digested in 20µl water containing 10µg proteinase K (Roche) at 56°C for 2 hours. Proteinase K was then inactivated at 80°C for 10 minutes and 2µl of the digest used for PCR analysis.

2.15 Immunostaining

Embryos dissected from deciduas, EBs, and mouse organs were embeded in OCT and sectioned at a thickness of 5µm. Immunostaing was carried out with rabbit polyclonal antibodies against ZO-1, ZO-2, ZO-3, occludin, cingulin, claudin 1-8 (Zymed), Brachyury (Abcam and Saint Cruz), and rat polyclonal antibodies against E-cadherin (Zymed) and prominin (eBioscience)

2.16 Isolation and culture of blastocysts in vitro

8 to 10 weeks old males and females were crossed and the blastocysts collected at 3.5 dpc by flushing the uterus of plugged females with M2 medium (Sigma). Flushed blastocysts were then cultured individually in Dulbecco's modified Eagle's medium (DMEM) supplemented with 20% fetal bovine serum (FBS) in 96-well plates at 37°C in 5% CO_2.

2.17 Transmission electron microscopy

E6.5-E7.5 embryos and EBs were fixed in 2.5% glutaraldehyde. After rinsing with 0.1 M PBS, the samples were postfixed in 1% osmium tetroxide for 1 hour, rinsed in phosphate buffer, dehydrated in ethanol and embedded in resin. Ultrathin sections were cut with a diamond knife, stained with uranyl acetate and lead citrate, and then viewed

with a transmission electron microscope (JEM-1010)

2.18 Lanthanum Nitrate Tracer Study

E7.5 embryos and Day 5 EBs were immediately fixed in 2.5% freshly made glutaraldehyde for 1-3 hours. In some experiments, WT EBs were incubated with 10 mM EGTA for 30 min on ice before fixation in 2.5% glutaraldehyde. After rinsing with 0.1 M PBS, the samples were postfixed in 1% osmium tetroxide containing 1% lanthanum nitrate for 1 hour, rinsed in phosphate buffer, dehydrated in ethanol and embedded in resin. Ultrathin sections were cut with a diamond knife, stained with uranyl acetate and lead citrate, and then viewed with a transmission electron microscope (JEM-1010)

2.19 Permeability analysis

The barrier function of epithelial cells of cystic EBs was analyzed using a surface biotinylation technique (Chen et al., 1997) with modifications (Saitou et al., 1998). Briefly, WT and ZO protein deficient cystic EBs were incubated in freshly made 1 mg/ml NHS-LC-biotin (Pierce Chemical Co.) in PBS for 30 min on ice. In control experiments, WT cystic EBs were incubated with NHS-LC-biotin in the presence of 10 mM EDTA. After washing with PBS, the EBs were fixed, embedded in OCT, and sectioned at a thickness of 1 μ m. The sections were rinsed with PBS, blocked in 1% BSA-PBS for 1 hour and then stained with phalloidin (1:200; Pierce Chemical Co.) or avidin (1:200; Pierce Chemical Co.) for 1 hour. The slides were viewed by fluorescence microscopy.

2.20 In situ cell death assay

Tunnel (terminal deoxynucleotidyltransferase-mediated dUTP-biotin nick end labeling) assays were done on cryo-sections of mouse embryos from E6.5 to 8.5, EBs, and testis with the TMR red In Situ Cell Death Detection Kit (Roche) according to the manufacturer's protocol.

2.21 BrdU labeling

For embryos, 2 hour before sacrificing the mice, 100 μg of bromodeoxyuridine (BrdU; Sigma) per gram of body weight was injected peritoneally into the pregnant females. Deciduae were removed and processed as described above. The sections were stained with the In Situ Cell Proliferation Kit, FLUOS (Roche) according to the manufacturer's protocol.

EBs were cultured in the medium containing 10mM BrdU at 37°C for 1 hour and then embedded in OCT, sectioned and stained with the In Situ Cell Proliferation Kit, FLUOS (Roche).

2.22 EB differentiation

ES cell were seeded on gelatin-coated plates without feeder cells. After 2 days culture, cells were trypsinized and dissociated. To allow for differentiation, ES cells were cultured with ES cell culture media without leukemia inhibitory factor (ESGRO; Chemicon) in bacterial dishes. Media was changed every two days. Around Day 10, cystic EBs were formed.

2.23 Preparation of lysates

ES cells or EBs were washed twice with PBS and lysed for 45 minutes with RIPA buffer (1% deoxycholate, 1% Triton, 0.5% SDS, 50mM Na2HPO4, 150mM NaCl, 2mM EDTA) on ice. For mouse tissue lysates, the organs were homogenized, sonicated, and then lysed for 45 minutes with RIPA buffer on ice. Lysates were centrifuged at 13,000 g for 15 minutes at 4^{o}C and the supernatants were collected and analyzed.

Chapter 3 Generation and phenotypic analysis of ZO-1 chimeric mice and embryos

3.1 Generation of ZO-1-/+ and ZO-1-/- ES cells

Genomic fragments containing the ZO-1 locus were isolated from a mouse 129Sv genomic library and subcloned into pBluescript II KS+. A targeting vector with a LacZ neo cassette flanked by short and long arms of 3.6 kb and 6.7 kb ZO-1 genomic DNA framgemts was designed to replace the exon containing the first ATG translational initiation codon (Figure 5A). This insertion leads to a null mutation of the corresponding gene and in principle allows the expression of the β-gal marker under the control of the endogenous transcriptional regulatory elements of the ZO-1 gene.

The targeting vector was linearized with Sal I restriction enzyme and electroporated into W4 ES cells, which were selected with 250 μg/ml G418. After 7-9 days under selection, the surviving colonies were picked and screened by long-range PCR (Figure 5B). Of the 96 G418-resistant clones examined, 3 had undergone a single homologous recombination.

To generate ZO-1-/- ES cells, independent ZO-1-/+ ES cells were selected in 20 mg/ml G418. After 7-9 days of selection, drug-resistant clones were picked and screened by PCR (Figure 5C). The targeting clones were amplified and the loss of ZO-1 protein was confirmed by Western blot (Figure 6A). Six independent ZO-1-/- clones were generated. Since these 6 clones showed the same phenotype in terms of TJ structure, cell proliferation and cell death, the data obtained from one clone, clone 23, was taken as

representative of the 6 clones. ZO-1-/- ES cells did not show any morphological differences compared to ZO-1+/+ ES cells (Figure 6B).

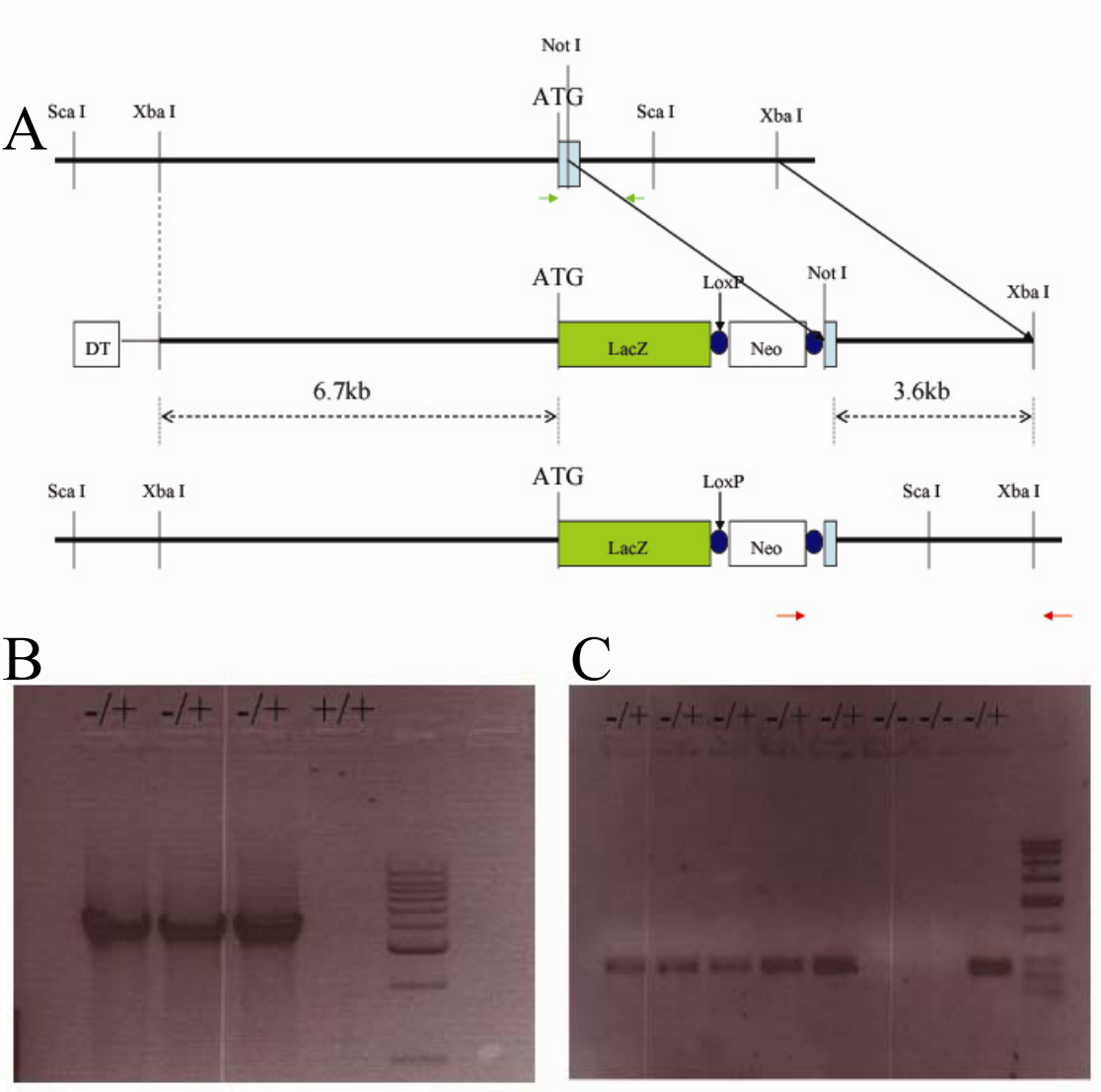

Figure 5 Targeting of ZO-1 locus and PCR screening. *(A) Schematic representation of the genomic locus of ZO-1 shows exon 1 with the initiation ATG. The targeting vectors were designed to disrupt exon 1 by the in-frame insertion of a lacZ gene and a loxP flanked neomycin cassette immediately downstream of the ATG codon. Red and green arrows denote the regions from where primers were derived to screen for heterozygous and knockout ES cells, respectively. (B, C) Homologous recombination in ES cells. PCR screening was done on selected ES cell clones with the indicated primers (see panel A) to identify homologous recombinants. A 4021 bp fragment is indicative of the presence of the recombined mutant ZO-1 allele (panel B), while the 255 bp fragment denotes the WT allele (panel C).*

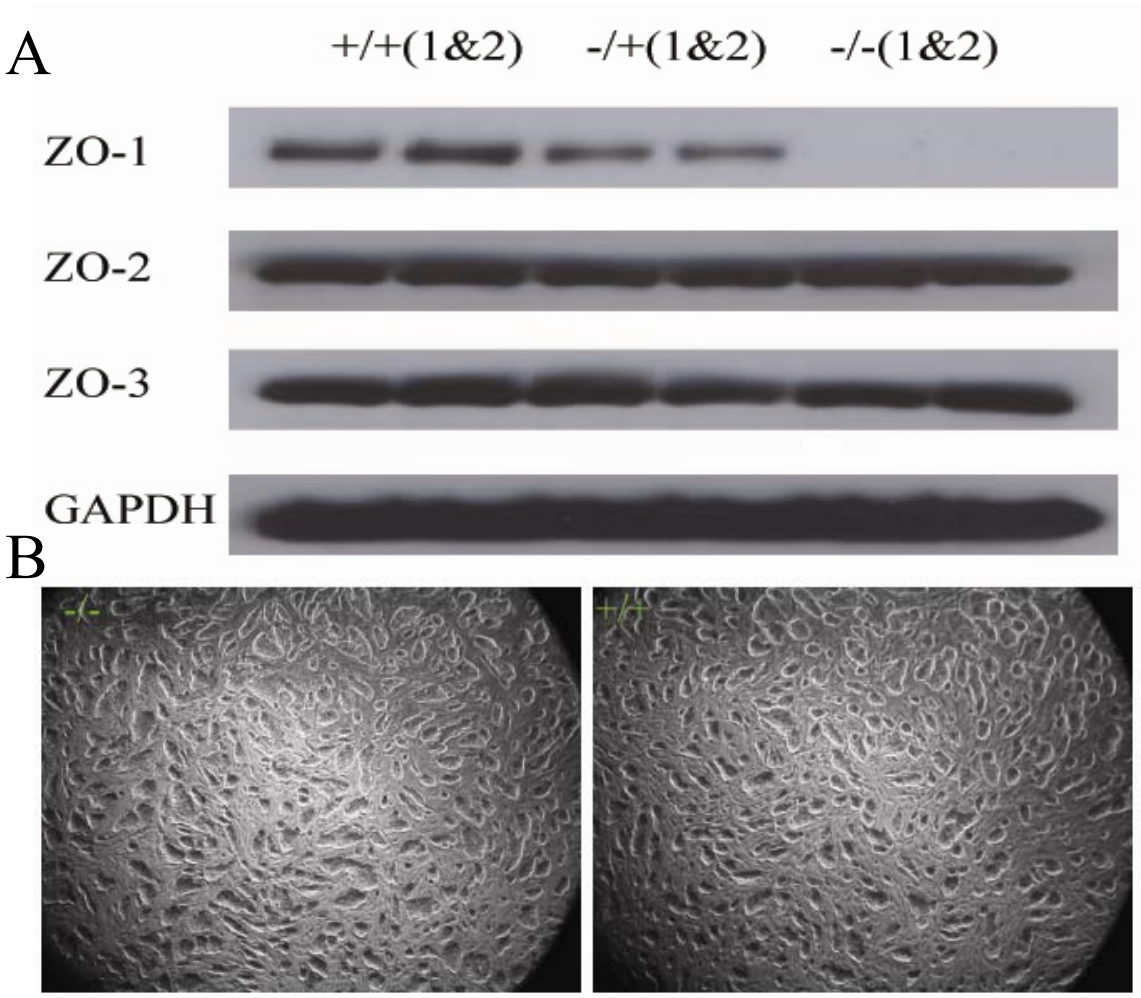

Figure 6 Characterization of ZO-1-/- ES cell lines. *(A) Western blot analysis was done on lysates from 6 ES cell lines to access the expression of ZO-1, ZO-2, and ZO-3. No ZO-1 expression was detected in ZO-1-/- ES cell lines and expression was downregulated in ZO-1-/+ ES cell lines, while the expression of ZO-2 and ZO-3 was unaffected. (B) Morphology of ZO-1-/- ES cells was undistinguishable from that of ZO-1+/+ ES cells.*

3.2 ZO-1 chimeric mice

ZO-1-/+ ES cells were injected into blastocysts in an attempt to generate ZO-1-/+;+/+ chimeric mice and possibly obtain germline transmission. However, injection of ZO-1 heterozygous ES cells did not yield chimeric mice with a high percentage Agouti coat color and no germ line transmission was obtained.

Chimeric embryos generated by injecting ZO-1-/- cells into blastocysts died at early embryonic stages around E9.5. As shown in Figure 7, chimeric embryos carrying ZO-1-/- cells were smaller in size than the ZO-1+/+ embryos. Variablity in the size of the ZO-1-/-;+/+ chimeric embryos could be due to differences in the number of ZO-1-/- cells they carried. The reason for the embryonic lethality will be elucidated in a future study.

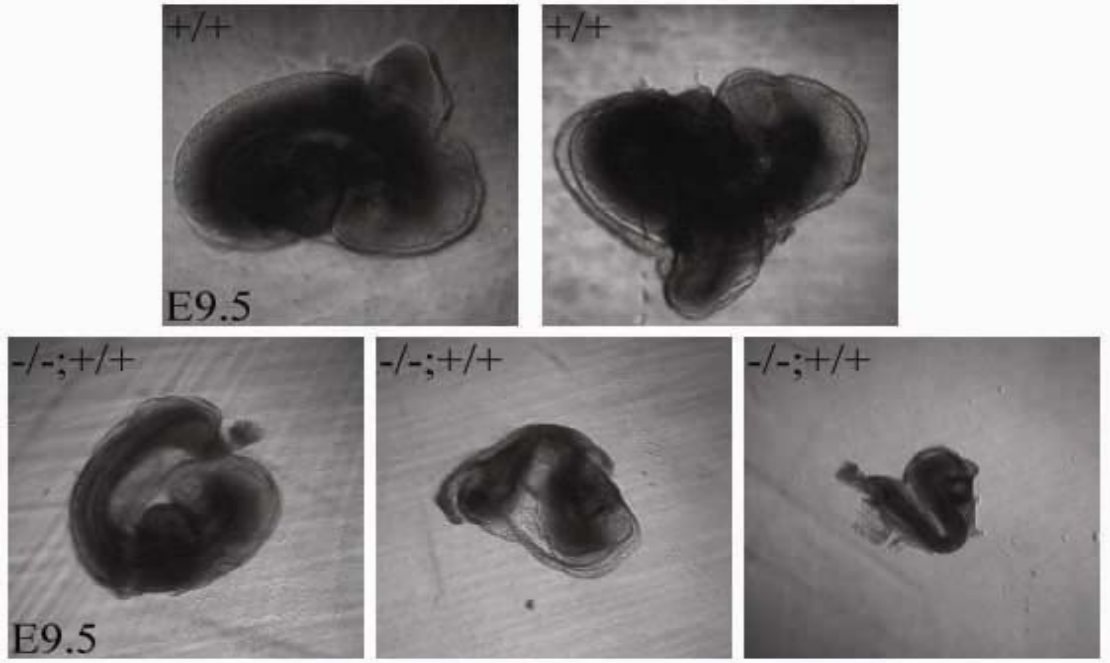

Figure 7 ZO-1-/-;+/+ chimeric mice are embryonic lethal. *ZO-1-/-;+/+ embryos die around E9.5, possibly depending on the contribution of ZO-1-/- ES cells.*

3.3 Discussion

While we have not been able to generate ZO-1-/- mice so far, chimeric embryos derived from ZO-1-/- ES cells died around E9.5. Thus, it is likely that ZO-1-/- mice will also die at the embryo stage, probably at or before E9.5. Our analysis of ZO-1-/- EBs, however, suggests that ZO-1 plays a role in different aspects of embryo development (see Chapter 8). We found that ZO-1 deficiency affects the structure of TJs in the epithelia of the EBs. This is in contrast to reports that inactivation by homologous recombination or silencing of ZO-1 in Eph4 cells or MDCK cells, respectively, does not alter the structure of TJs (Umeda et al., 2004; Mcne et al., 2006). Since EBs recapitulate the early stages of embryo development (Doetschman et al., 1985), the structure of TJs in ZO-1-/- embryos is probably also affected. In addition, we found that ZO-1 deficiency led to the overexpression of T-gene, which is crucial for mesoderm development (Rashbass et al., 1991). Thus, ZO-1 deficiency may affect mesoderm development via the deregulation of T-gene expression. Furthermore, cell proliferation in EBs lacking ZO-1 was enhanced. ZO-1 has been linked to the regulation of proliferation and differentiation through its association with ZONAB (Balda et al., 2003) and its link to the Wnt pathway (Reichert et al., 2000; Polette et al., 2006) and it will be of interest to determine in future studies whether these events and pathways are affected in ZO-1-/- chimeric embryos.

Chapter 4 Generation and phenotypic analysis of ZO-2 null mice

4.1 Generation of ZO-2-/+ ES cells

Genomic fragments containing the ZO-2 locus were isolated from a mouse 129Sv genomic library and subcloned into pBluescript II KS+ vector. A targeting vector designed to replace the exon containing the first transcriptional ATG was constructed using a LacZ neo cassette flanked by short and long arms of 1.8 kb and 5.9 kb for ZO-2 (Figure 8A). This insertion leads to a null mutation of the corresponding gene and in principle allows the expression of the β-gal marker under the control of the endogenous transcriptional regulatory elements of ZO-2.

The targeting vector was linearized with Sal I restriction enzyme and electroporated into the W4 ES cells. After 36 to 48 hours in culture, the transfected ES cell were subjected to selection of G418. The growing clones were screened for homologous recombination at the ZO-2 locus by means of long-range PCR using the primers indicated in Figure 8A. A band of ~1.9 kb was amplified for the targeted ES cell clones and two out of 96 clones analyzed were positive. PCR results were confirmed by Southern blot hybridization using the probes shown in Figure 8A. For each of the 2 targeted clones (#105 and #133), a 6.7 kb wild-type and an 11.5 kb mutant band was detected, while wild type clones (lane3) only showed the 6.7 kb band (Figure 8B).

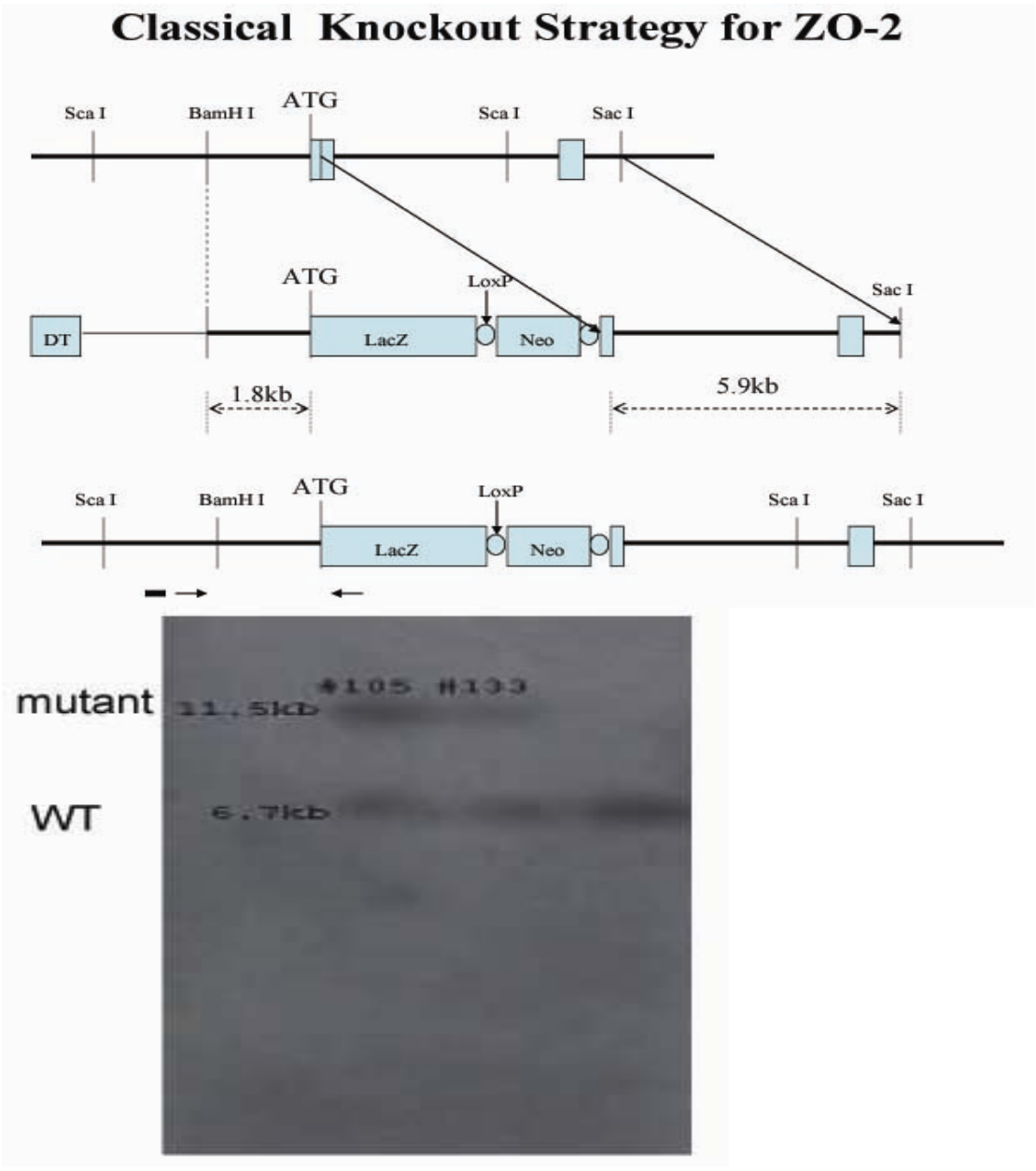

Figure 8 Targeting of the ZO-2 gene *(A) Schematic representations of the genomic locus of the ZO-2 gene shows exon 2 with the initiation ATG. The targeting vector was designed to disrupt exon 2 by the in-frame insertion of a lacZ gene and a loxP flanked neomycin cassette immediately downstream of the ATG codon. Bars indicate the regions to which the probes used for Southern blot analysis hybridize; arrows denote the regions used to design the primers for genotyping. (B) Southern blot analysis of ScaI digested genomic DNA of selected ES cell clones hybridized with labeled DNA probes (see panel A) for the identification of homologous recombination. A 6.7 and 11.5kb ScaI fragment corresponding to the WT or targeted mutant allele, respectively, is detected in -/+ ES cell clones, whereas only the fragment corresponding to the WT allele is present in +/+ controls.*

4.2 Generation of ZO-2-/- mice

Correctly targeted independent ZO-2-/+ ES cell clones were injected into C57BL/6 blastocysts to produce chimera mice with germ line transmission of the mutated allele. Nine chimeric mice with ~100% Agouti coat color and a few chimeric mice with a lower Agouti coat were obtained. These chimeric mice were mated with either C57BL/6 or 129Sv strain mice to establish the F1 generation of heterozygous mice. ZO-2-/+ mice were apparently normal and crossed to obtain homozygous animals.

4.3 Embryonic lethality for ZO-2-/- mice

ZO-2-/+ male and female mice were crossed and genomic DNA was extracted from offspring tails and genotyped (Figure 9). ZO-2-/- pups were absent in litters from ZO-2-/+ crossings (Table 1), indicating embryonic lethality of ZO-2-/- mice. In order to find out at which stage ZO-2-/- embryos die, ZO-2-/+ mice were crossed and the pregnant mothers sacrificed at different stages. Embryos from E9.5-E17.5 were genotyped and no ZO-2-/- embryos were detected, suggesting that ZO-2-/- embryos die before E9.5. Dissection of embryos at E6.5, E7.5 and E8.5 revealed grossly undeveloped and abnormal embryos as compared to corresponding ZO-2+/+ embryos (Figure 10). Histological analysis showed that these abnormal embryos were much smaller than corresponding ZO-2+/+ embryos and apparently underwent absorption (Figure 11). Consistent with Mendelian ratios, about one forth of the total embryos were small and undergoing resorbtion and thus presumed to be ZO-2-/- (Table 1). At E8.5, the putative ZO-2-/- embryos were completely absorbed, whereas at E7.5, their structure was disorganized. At E6.5 and E5.5, the structure of putative ZO-2-/- embryos was still well organized, but growth was retarded. These findings thus reveal that ZO-2 is critical for embryonic development in mice.

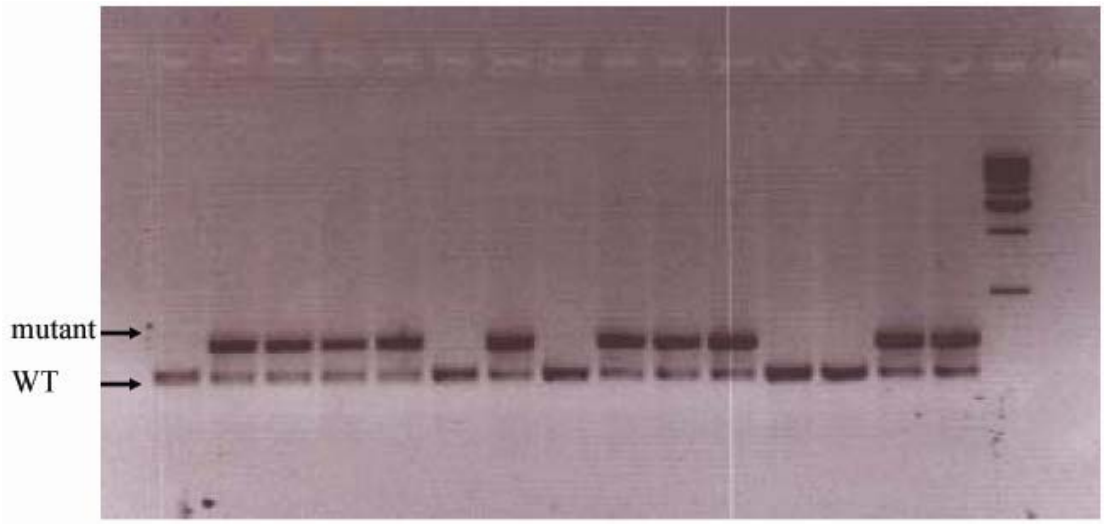

Figure 9 Genotyping of transgenic mice. *Genomic DNA was amplified by PCR using primers designed to distinguish between WT and mutant alleles. Fragment of 580 bps is indicative of the presence of the recombined mutant allele of ZO-2, while the 367 bps fragment denotes the WT allele. No ZO-2 -/- mice were detected in newborn litters.*

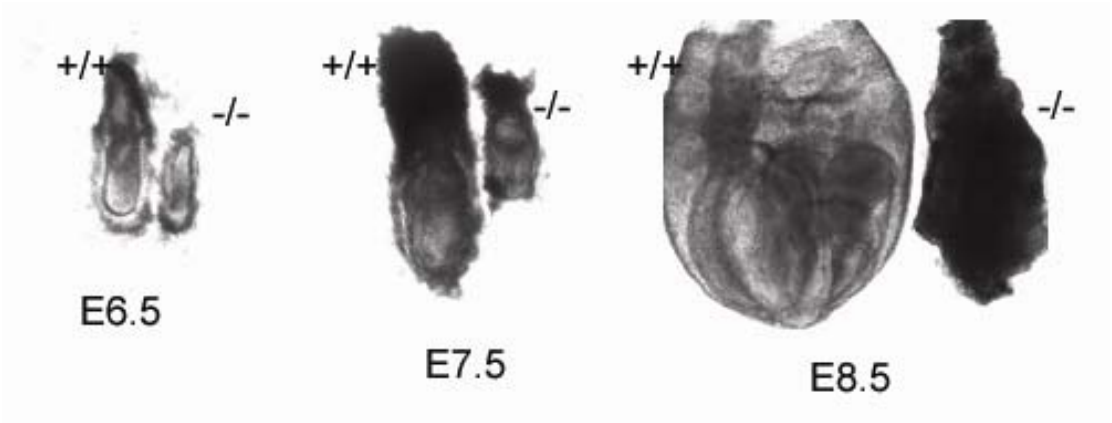

Figure 10 Developmental arrests of ZO-2-/- embryos. *ZO-2+/+ and ZO-2-/- embryos dissected from their deciduas at E6.5, E7.5 and E8.5. Note the overall smaller size and developmental arrest of ZO-2-/- embryos.*

Table 1. Genotypic analysis of offspring from heterozygous x heterozygous breeding pairs

Stage	No. of indicated genotypes					
	Wild-type (25%)	heterozygous (50%)	Homozygous (25%)	abnormal	absorbed	Total
Weaning	27	53	0			80
E9.5-17.5	14	29	11	0	11	54
E8.5	7	12	4	3	1	23
E7.5	ND	ND	57	22	35	211
E6.5	ND	ND	34	19	15	141
E5.5	ND	ND	4	3	1	14
E3.5	16	37	15			68

Table 1 Genotypic analysis of offspring and embryos from crossing of ZO-2-/+ mice. *No alive ZO-2-/- mice were not found among the offspring. About one forth of the embryos between E5.5 to E8.5 were abnormal or showed deciduas were absorbed.*

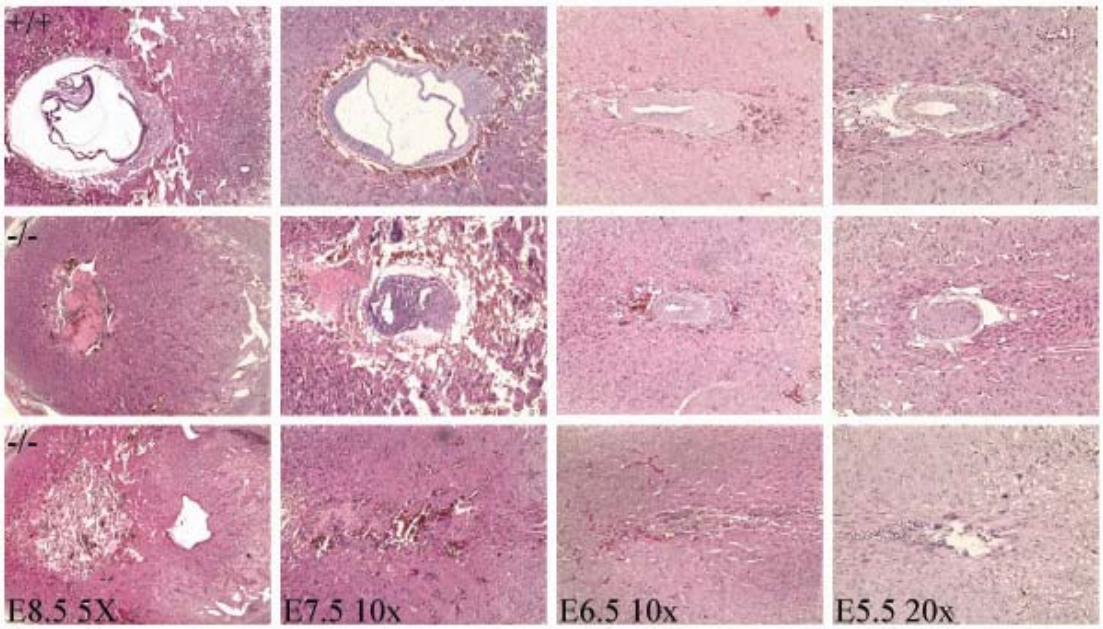

Figure 11 Postimplantation development of ZO-2-/- embryos. *Histology of embryos with normal or typical abnormal appearances at E5.5, E6.5, E7.5 and E8.5. Note the developmental arrest of ZO-2-/- embryos from E5.5 onwards and their eventual resorption by E8.5.*

4.4 Decreased cell proliferation in ZO-2-/- embryos

Given the apparent smaller size of ZO-2-/- embryos, we determined if alterations in proliferation contributed to this developmental arrest. Bromodeoxyuridine (BrdU) was peritoneally injected into pregnant female mice two hours before sacrifice. E6.5 embryos were dissected out from the deciduas, sectioned and stained to detect BrdU incorporation. Based on this assay, few if any proliferating cells were found in ZO-2-/- E6.5 embryos when compared to ZO-2+/+ controls (Figure 12). These data suggests that decreased cell proliferation contributes to the retarded growth of ZO-2-/- embryos.

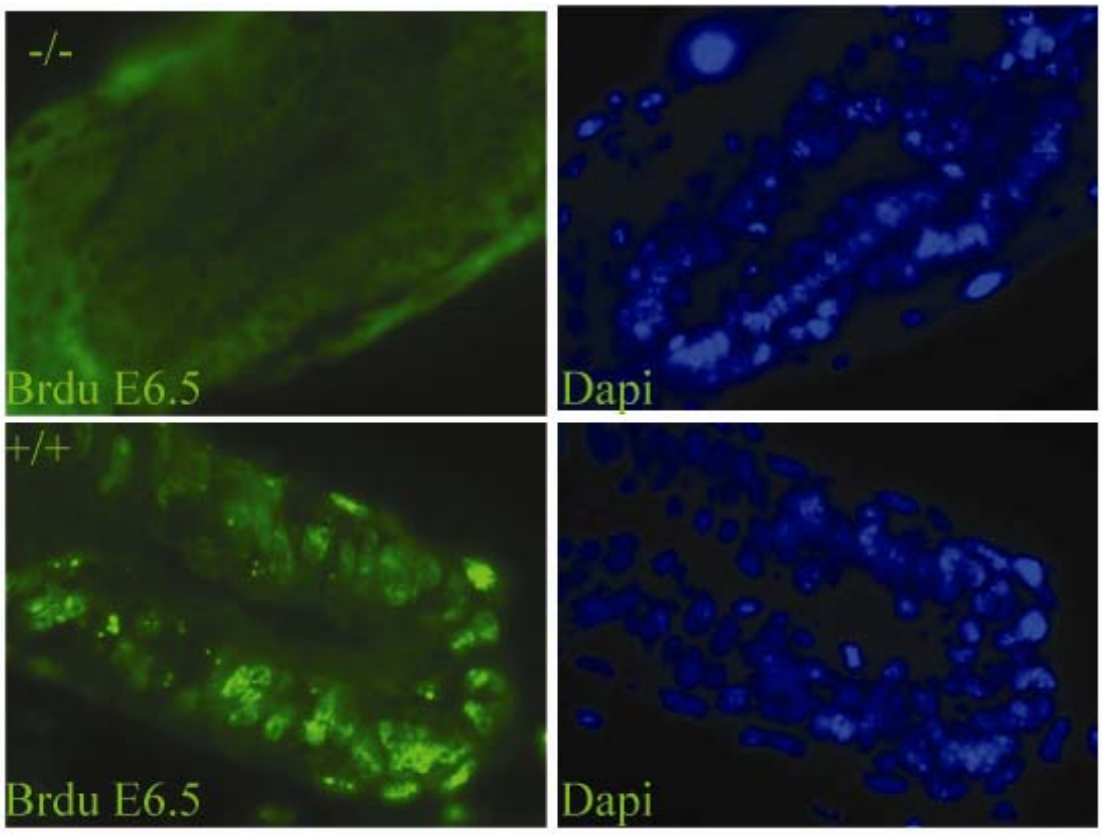

Figure 12 Cell proliferation is compromised in E6.5 ZO-2-/- embryos. *E6.5 embryos were labeled with BrdU and incorporated BrdU (green) and nuclei (blue) were visualized in sections by fluorescence microscopy.*

4.5 Increased apoptosis in E7.5 ZO-2-/- embryos

Given the apparent degeneration of ZO-2-/- embryos, we determined if apoptosis contributed to this developmental arrest. Tunnel staining was carried out on cryo-sections of mouse embryos from E6.5 to E8.5 to detect apoptosis. Only low levels of programmed cell death was detected in either ZO-2-/- or ZO+/+ embryos at E6.5. At E7.5, however, ZO-2-/- embryos revealed significant apoptotic activity as compared to ZO-2+/+ controls (Figure 13). These findings suggest that apoptosis might be a consequence of the decreased cell proliferation observed in ZO-2-/- embryos and not the direct cause of lethality for these embryos.

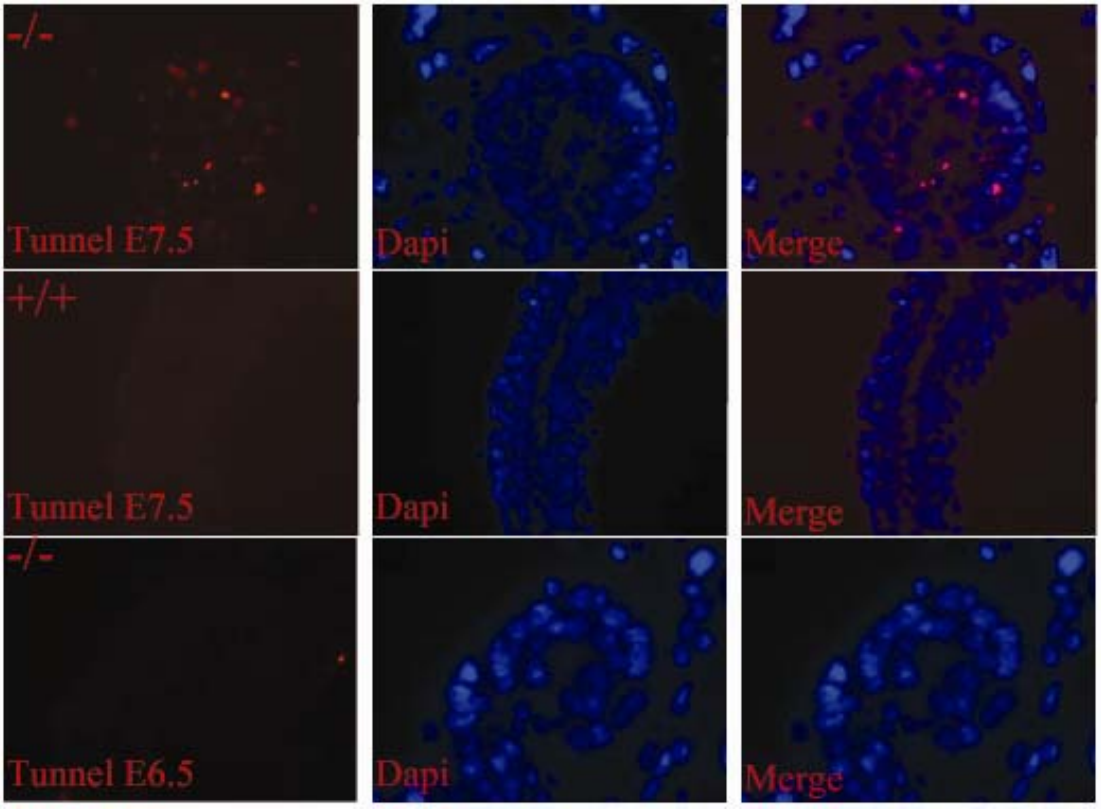

Figure 13 Enhanced apoptosis in E7.5 ZO-2-/- embryos. *Apoptosis in ZO-2+/+ and ZO-2-/- embryos at E6.5 or E7.5 was visualized by fluorescence microscopy using the Tunnel assay (red). Nuclei are stained in blue.*

4.6 ZO-2-/- embryos do not develop mesoderm

Interestingly, ZO-2-/- embryos consistently failed to develop mesoderm as determined by histological analysis. To confirm this observation, expression of the mesoderm marker T-gene (brachyury) was monitored. As shown in Figure 14 (A, B), nuclear T-gene was detected in E7.5 ZO-2+/+ embryos but absent in ZO-2-/- embryos. In *in vitro* differentiated EBs, T-gene expression was normally expressed in ZO-2-/- EBs (Figure 14C). These data indicate that ZO-2-/- embryo growth is arrested before mesoderm formation rather than ZO-2 deficiency affecting mesoderm differentiation.

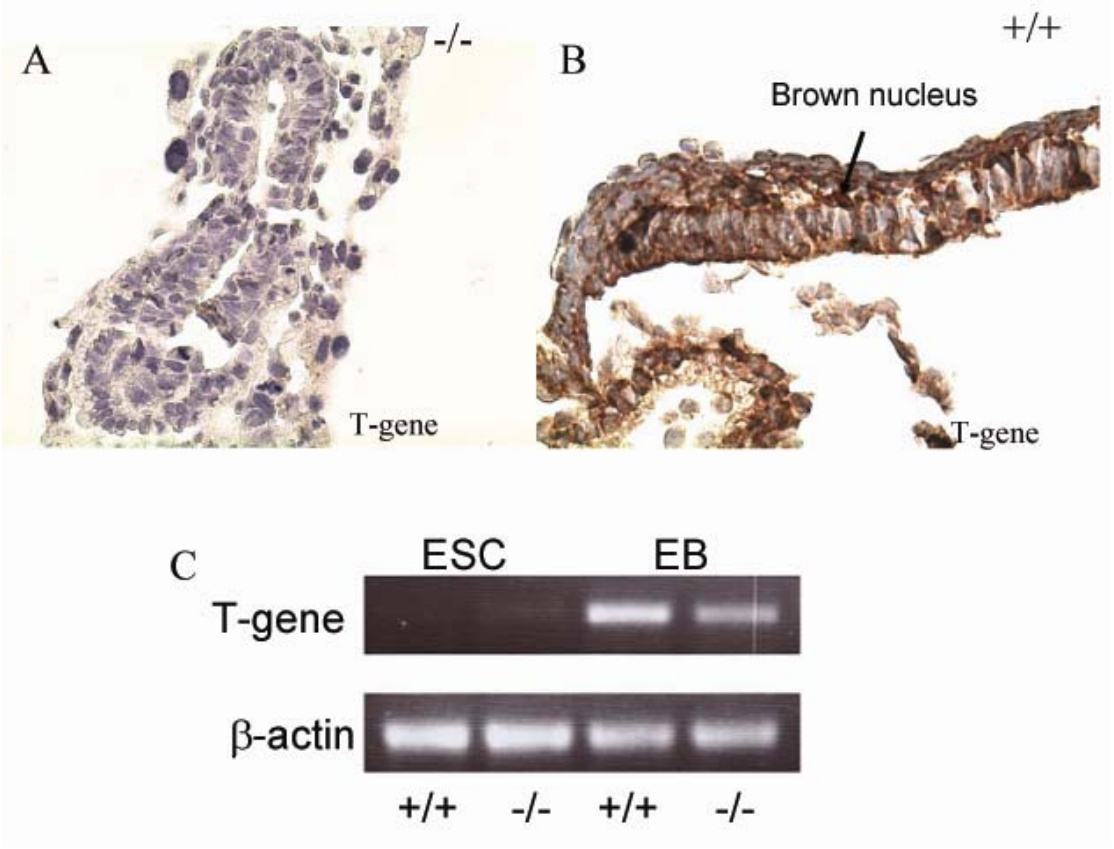

Figure 14 T-gene expressions in E7.5 ZO-2-/- embryos and EBs. *(A, B) T-gene antibody stained the mesoderm of ZO-2+/+ embryos (brown nuclei), but the staining was absent in ZO-2-/- embryos. (C) T-gene was detected in in vitro differentiated ZO-2-/- EBs*

4.7 Expression and localization of TJ and AJ markers is not affected in ZO-2-/- embryos

Given the role of ZO-2 protein as a scaffold that tethers TJ proteins to the cytoskeleton (González-Mariscal et al., 2003), we analyzed by immunostaining if the expression and subcellular distribution of selected TJ and AJ markers was affected. As shown in Figure 15 (A, D), ZO-2 was strongly expressed in ZO-2+/+ embryos at E7.5 and particularly enriched at sites of cell-cell contact. As expected, no specific ZO-2 staining was found in ZO-2-/- embryos. ZO-1 and ZO-3 were also expressed in E7.5 embryos. They were predominantly found on visceral endoderm and ectoderm cells facing either the internal cavity or the extra-embryonic space (Figure 15B, C, E, and F). Neither the expression nor the distribution of ZO-3 and ZO-1 was dramatically altered in ZO-2-/- embryos. Furthermore, the prominent apical localization of prominin, an apical marker, and membrane localization of E-cadherein, a lateral marker, were maintained in ZO-2-/- embryos (Figure 16), indicating that the ability of TJs to maintain the asymmetric distribution of membrane proteins between the apical and basolateral domains is unaffected.

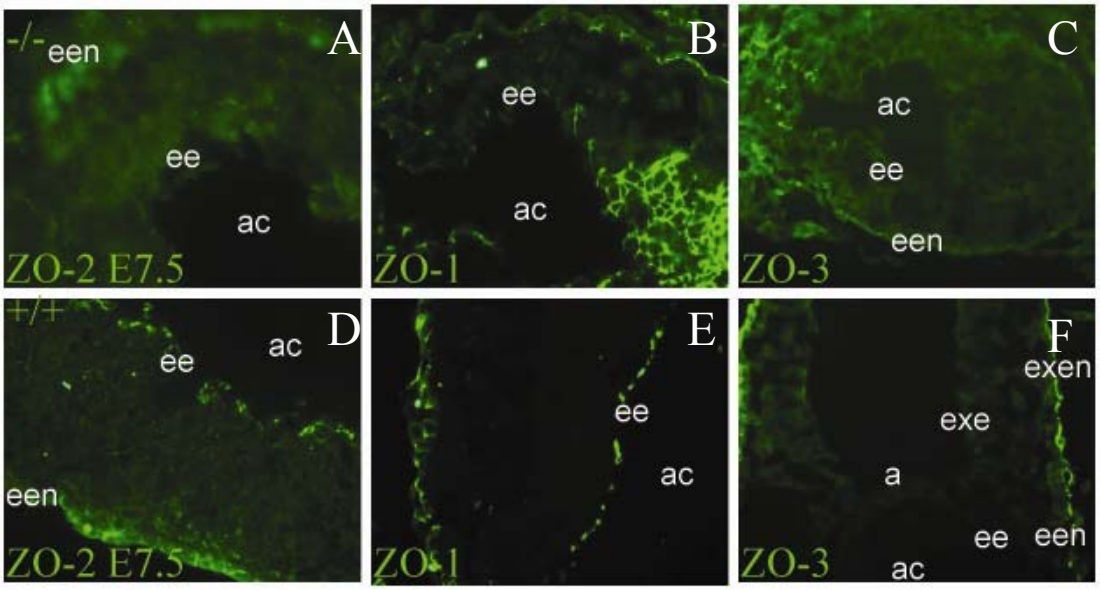

Figure 15 Distribution of ZO-1and ZO-3 in ZO-2-/- embryos is not altered. *Sections of E7.5 ZO-2-/- and ZO-2-+/+ embryos were labeled with antibodies to ZO-2, ZO-1, or ZO-3 and visualized by immunofluorescence microscopy. Ee, embryonic ectoderm; exe, extraembryonic ectoderm; een, embryonic endoderm; exen, extraembryonic endoderm; em, embryonic mesoderm; a, amnion; ac, amniotic cavity*

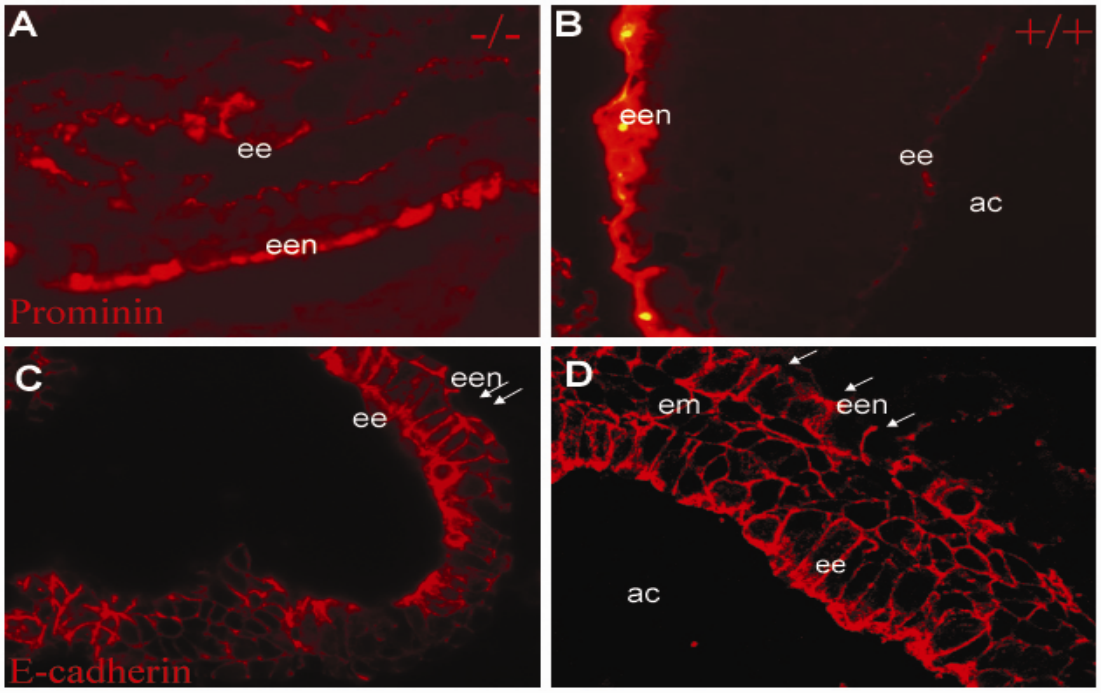

Figure 16 Apical-basal polarity is not affected in ZO-2-/- embryos. *Sections of E7.5 ZO2 -/- (A,C) and ZO-2+/+ (B,D) embryos were labeled with antibodies to the apical marker Prominin (A,B) or the lateral marker E-cadherin (C,D) and visualized by immunofluorescence microscopy. ac, amniotic cavity; ee, embryonic ectoderm; een, extraembryonic endoderm; ee, embryonic ectoderm; embryonic mesoderm.*

4.8 The TJ architecture is altered in ZO-2-/- embryos

To assess the structural integrity of TJs, we analyzed E6.5 and E7.5 embryo sections by EM. As shown in Figure 17 (A, C), the apical junctional complex were readily detected as electron dense plaques in ZO-2+/+ and -/+ embryos, where the intercellular space between adjacent visceral endoderm and ectoderm cells was obliterated. Less frequently, short plaques could be observed (Table 2). In contrast, long electron dense structures were absent in ZO-2-/- embryos and only the occasional short plaque could be detected (Figure 17B, D). These observations indicate that although TJ markers such as ZO-1 and ZO-3 still localize correctly, the structural integrity of TJs is compromised in the developing embryos.

4.9 The function of TJs as a diffusion barrier is affected in ZO-2-/- embryos

Given the apparent structural alterations in TJs, we monitored paracellular permeability in E7.5 ZO-2-/- embryos. Lanthanum permeability was efficiently restricted at the level of TJs in cells of control embryos (Figure 18). In contrast, lanthanum was readily detected in spaces between the lateral plasma membranes of adjacent cells of ZO-2-/- embryos. Quantification showed that, whereas none of the TJs from control embryos allowed diffusion of lanthanum, more than 10% of the TJs from ZO-2-/- embryos were leaky (Table 3).Thus, the structural and functional integrity of the apical junctional complex was compromised in cells of developing ZO-2-/- embryos.

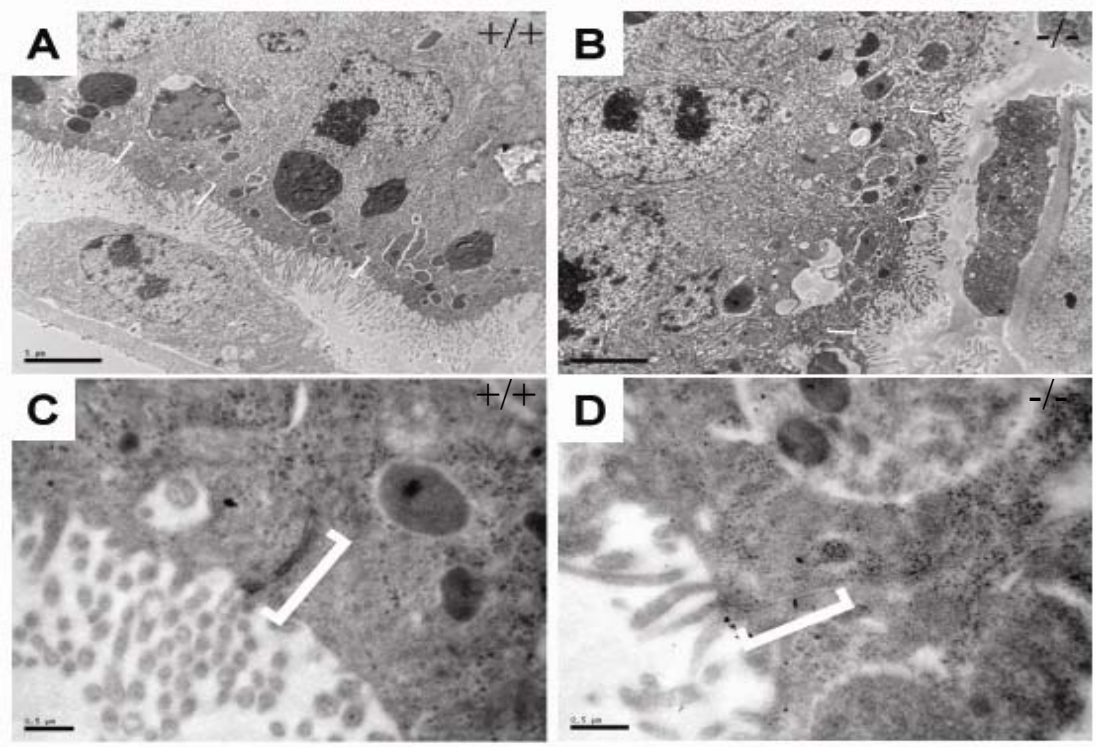

Figure 17 The architecture of the apical junctional complex is altered in cells of ZO-2-/- embryos. *A-D. E6.5 (data not shown) and E7.5 embryo sections were analyzed by TEM to visualize the apical junctional complex. Typical electron dense plaques were readily detected at the apical pole of the lateral membrane of adjacent cells of ZO-2+/+ embryos (A, C) but were rarely observed in cells of ZO-2-/- embryos (B, D). ZO-2-/- embryos were identified based on their small size as compared to wild-type and heterozygous embryos.*

Stage	Embryo Morphology (No)	Normal tight junction	Rudimentary tight junction	Absent tight junction	Total
E6.5	Tiny (2)	0	4	19	23
E6.5	Normal (5)	48	8	0	56
E7.5	Tiny (3)	0	7	37	44
E7.5	Normal(3)	25	6	0	31

Table 2 Statistical analysis of the frequency of TJs with altered structure in ZO-2-/- and ZO-2+/+ embryos

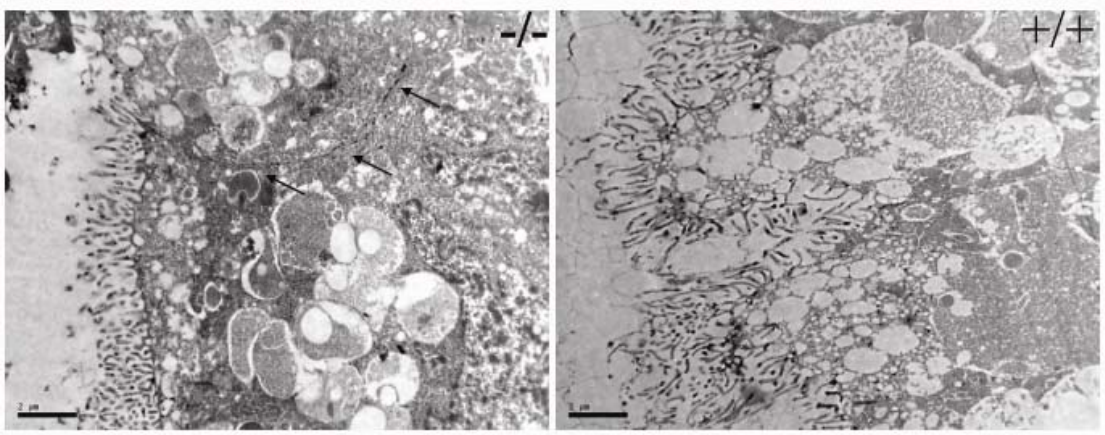

Figure 18 The permeability barrier of the apical junctional complex is altered in cells of ZO-2-/- embryos. *E7.5 embryos were postfixed in lanthanum nitrate and processed for transmission electron microscopy. Note the presence of lanthanum (arrows, black color) in intercellular spaces of ZO-2-/- but not in ZO-2+/+ embryos.*

	Intact TJ	leaky TJ
WT(5)	52	0
ZO-2HO(2)	67	8

Table 3 Statistical analysis of TJ leakiness in ZO-2+/+ and ZO-2-/- embryos.

4.10 ZO-2-/- blastocysts grow normally in vitro

Given the embryonic lethality of ZO-2-/- embryos *in vivo*, we analyzed whether ZO-2 deficiency affects the growth of blastocysts in vitro. ZO-2-/+ males and females were mated, pregnant females sacrificed and blastocysts at E3.5 flushed from the uterus and cultured. As shown in Figure 19A, there was no obvious difference between ZO-2+/+ and ZO-2-/- blastocysts after 4 days in culture. The culture was kept for 9 days and no defect was observed for the ZO-2-/- cells. After 9 days in culture, cells were collected and genotyped (Figure 19B). Of the 68 blastocysts checked by PCR, 15 blastocysts were ZO-2 deficient (Table 1). The number of ZO-2-/- blastocysts was about one fourth of the total blastocysts isolated and thus consistent with Mendelian ratio. This finding thus suggests that ZO-2 deficiency does not affect the survival of blastocysts.

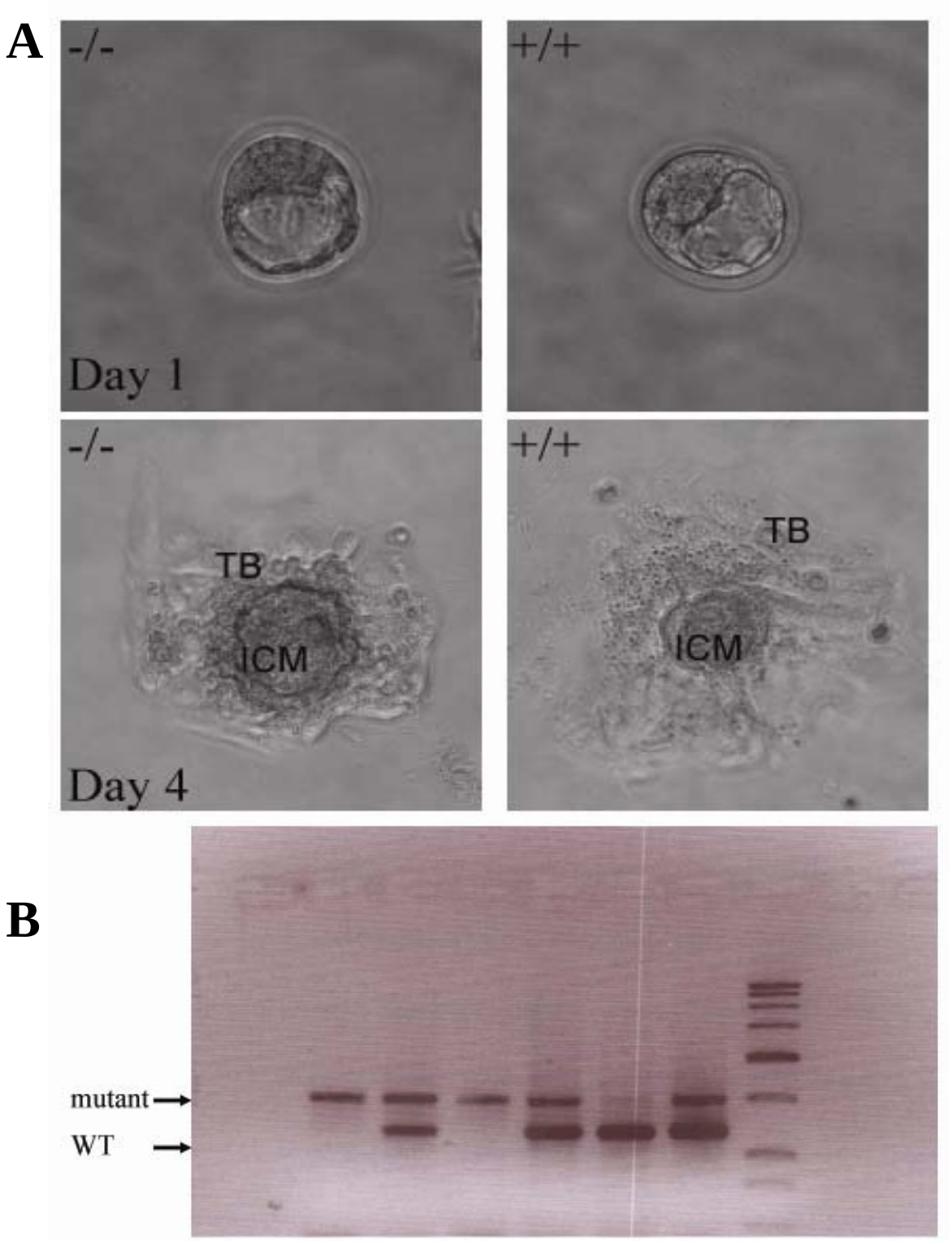

Figure 19 In vitro blastocyst culture and PCR genotyping. *(A) E3.5 ZO-2-/-, ZO-2-/+ or ZO-2+/+ blastocysts after 1 and 4 days in culture. Note the normal development of the inner cell mass (ICM) and trophoblast outgrowh (TG) for ZO-2-/- blastocysts. (B) Blastocysts were genotpyped by RT-PCR, yielding 367 bp and 580 bp fragments indicative of the WT and inactivated ZO-2 alleles, respectively.*

4.11 Discussion

We successfully generated ZO-2-/- mice and found that these mice show early embryonic lethality. This finding provides the first evidence for a critical and non-redundant role for a single ZO protein in mammalian development. In ZO-2-/- embryos, TJs displayed structural defects, manisfested in the absence of the electron dense apical junctional plaque typically observed by TEM. Experiments are currently underway to determine if the absence of the junctional plaque correlates with alterations in the TJ strands that can be observed in freeze fractures. While apical-basal polarity was not affected in epithelia of ZO-2-/- embryos, the barrier function of TJs was compromisd. However, given the loss of proliferation and the increased in apoptosis of ZO-2-/- around E6.5-E7.5, it is not clear whether the increased leakiness of E7.5 ZO-2-/- embryos reflects a bona-fide defect in the TJs or the general degradation of embryo viability. Intriguingly, however, in vitro studies on ZO-2-/- EBs indicated that ZO-2 is dispensable for normal TJ structure (e.g. the presence of an electron dense junctional plaque by TEM) and function (e.g. polarity and barrier) (see Chapter 9). These differences might be explained by the notion that minor defects in TJ structure may lead to more pronounced phenotypes under physiological stress. Furthermore, the relevance of individual ZO proteins may depend on particular tissue and/or developmental stage of the organism. Consistent with this speculation, silencing of ZO-2 in cell lines either shows no effect on TJ structure or function, only a minor delay in TJ formation (Adachi et al., 2006), or dramatic effects on TJ structure, epithelial polarity and barrier function (Hernandez et al., 2007).

Chapter 5 ZO-2 rescue and phenotypic analysis

5.1 Expression pattern of ZO-2 in early embryo development stage

ZO-2 is expressed as early as in 16-cell stage mouse embryos (Eckert et al., 2004). As shown in figure 20A, ZO-2 is strongly expressed in E6.5 embryos and particularly enriched at sites of cell-cell contact. ZO-2 staining is detected in both extra-embryonic and embryonic tissue and the strongest expression of ZO-2 is in the visceral endoderm. Similarly, ZO-2 is also expressed in ectoderm and endoderm of E7.5 embryos (Figure 20B), but not in mesoderm.

A

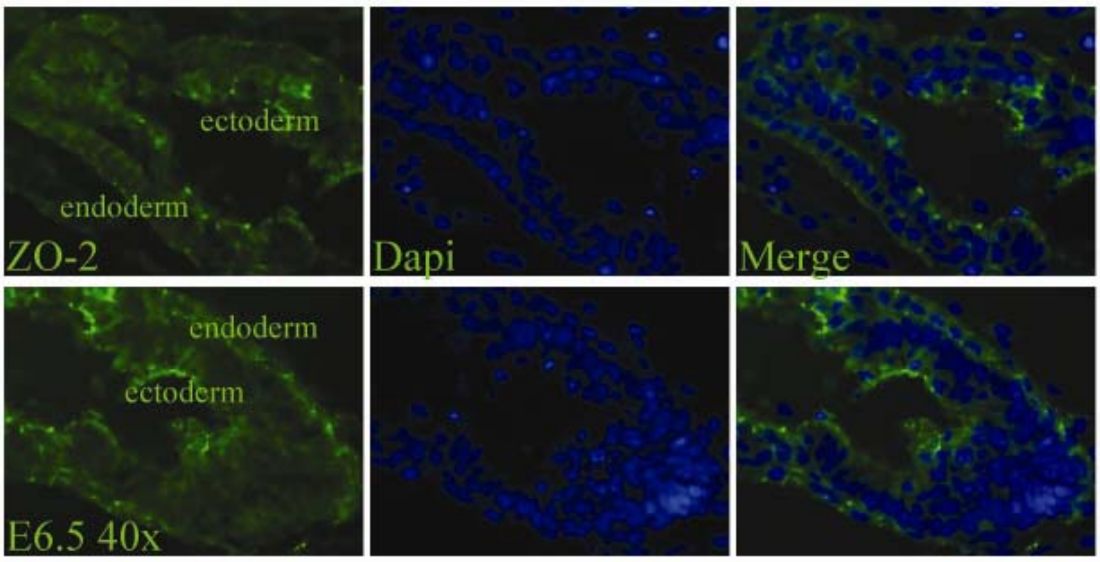

Figure 20 Expression of ZO-2 in early stage embryos. *(A) ZO-2 is expressed in both ectoderm and endoderm of E6.5 embryos.*

B

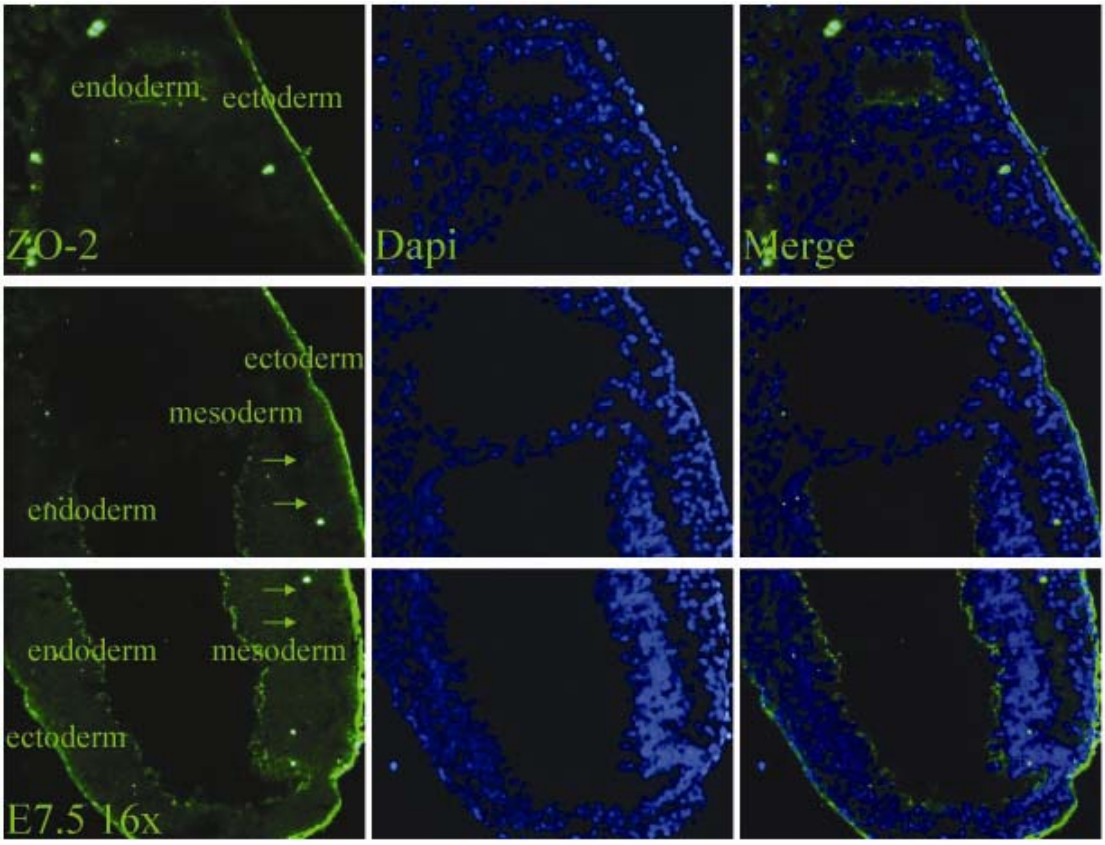

(B) ZO-2 is expressed in both ectoderm and endoderm, but not in mesoderm (indicated with arrows) of E7.5 embryos.

5.2 Generation of ZO-2 chimeric embryos

As mentioned in Chapter 4, ZO-2 deficiency led to embryonic lethality around E6.5 and E7.5. In order to assess whether extra-embryonic ZO-2 expression is critical for the embryo development, ZO-2-/- ES cells were injected into C57BL/6 blastocysts to produce ZO-2 chimeric embryos. One of the pregnant mothers was sacrificed at E15.5 and embryos were dissected. Genotyping of yolk sac tissue indicated that all 6 embryos carried ZO-2-/- cells (data not shown). The embryos were sectioned and stained with ZO-2 antibody. As shown in Figure 21, ZO-2 is strongly expressed in the skin of WT embryos but was either absent or only weakly expressed in the skin of the chimeric embryos.

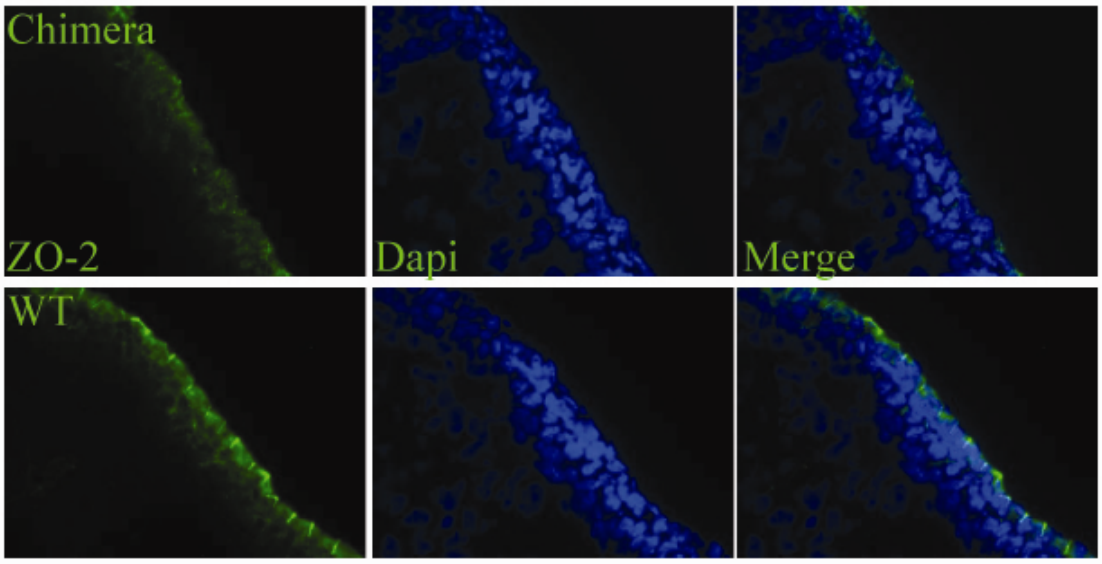

Figure 21 Expression of ZO-2 in the skin of E15.5 embryos. *ZO-2 is strongly expressed in the skin of WT embryos, while its expression in chimeric embryos is greatly reduced.*

5.3 ZO-2 is dispensable for epiblast development

When ZO-2 chimeric embryos where allowed to develop to term, viable mice were born. Table 4 summarizes the analysis of the chimeric mice derived from two independent ZO-2-/- ES cell clones, clone 54 (derived from the ZO2+/- ES cell used to generate the ZO-2+/- and ZO-2-/- mice described in Chapter 4) and clone 91. Thirty-three offspring were obtained from clone 54 and 17 of them had apparently 100% Agouti coat color. Twenty-nine offspring were obtained from clone 91, 15 of them with apparently 100% Agouti coat color. 3 Agouti males and 1 Agouti female were crossed with C57BL/6 WT females and males, respectively, and all 30 offspring were Agouti (Table 5). Genotyping indicated that all the offspring were ZO-2 heterozygotes.

The expression of the different ZO proteins in different organs was checked by Western blot. As shown in Figure 22, ZO-2 expression was greatly reduced in several organs analyzed, while the expression of ZO-1 and ZO-3 was not visibly affected. These data suggest that ZO-2-/- ES cells can contribute efficiently to various tissues and ZO-2 protein is dispensable for epiblast development. The embryonic lethality of ZO-2-/- embryos (see Chapter 4) may thus be due to a requirement for ZO-2 in the extra-embryonic tissue.

Table. Early embryonic lethality rescue by injecting ZO-2-/- ES cell into WT blastocysts.

Clone No	Offspring No	100% Agouti Offspring No
#54	33	17
#91	29	15

Table 4 Rescue of embryonic lethality by injecting ZO-2-/- ES cell into WT blastocysts. *Two independent ZO-2-/- ES clones, #54 and #91, both gave rise to offspring with high percentage Agouti coat color.*

Table. Offspring from cross of 100% agouti ZO-2 chimera mice with C57BL/6 wild type mice.

Mice* Type	Offspring No	Agouti Offspring No	Genotype
3 Male	23	23	ZO-2-/+
1 Female	7	7	ZO-2-/+

* The Chimera mice are around 3-month old when they were mated

Table 5 Cross between chimeric mice and C57BL/6 WT mice*. Both male and female chimeric mice gave rise to high percentage offspring with mutant allele.*

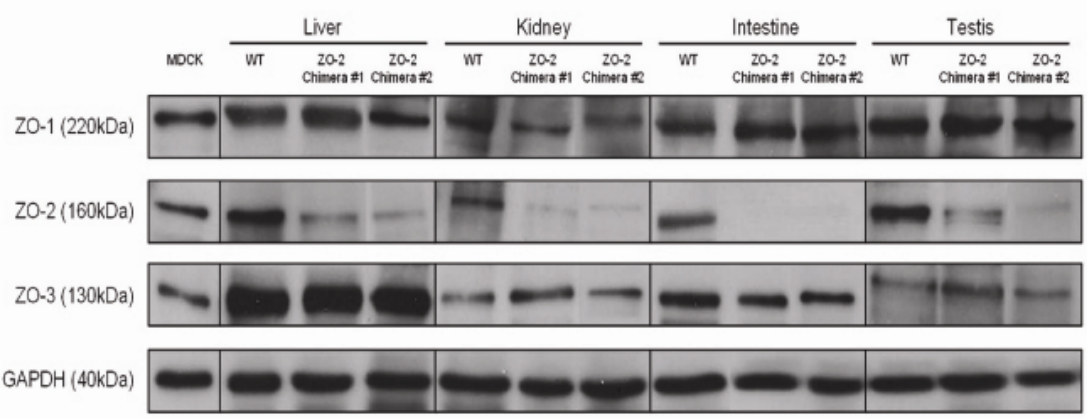

Figure 22 Expression of ZO proteins in chimeric mice. *The expression of ZO-2 is greatly reduced in chimeric mice, while the expression of ZO-1 and ZO-3 is not obviously altered in these mice.*

5.4 Chimeric expression of ZO-2-/- cells in testis results in reduced fertility of male chimeric mice

Mating experiments showed that male ZO-2 chimeric mice had difficulties impregnating C57BL/6 females. In order to assess whether the fertility of ZO-2 male chimeric mice was affected by the chimeric expression of ZO-2, the following mating experiment was carried out. One ZO-2 male chimeric mouse was paired with two C57BL/6 females and allowed to mate for up to 4 weeks. Once a female was identified to be pregnant in the course of the 4 weeks, she was separated from the male before giving birth to prevent a second pregnancy. As shown in Table 6, only 4 out of 8 male ZO-2 chimeric mice were able to impregnate female mice. In contrast, all WT, ZO-2+/- heterozygous and ZO-2+/- chimeric male mice were able to impregnate all available female mice. These data shows that the fertility of male ZO-2 chimeric mice is reduced, likely dependent on the contribution of ZO-2-/- cells to the testis of the individual male. In contrast, the fertility of female ZO-2 chimeric mice was not apparently affected based on the results from a small scale experiment where 3 WT males were able to impregnate three ZO-2 chimeric females.

Table 6 Cross between different types of male mice with C57BL/6 female mice.

Mouse type	Male[A] No.	Female[B] No.	Pregnant No.	Offspring No.
ZO-2 chimera (-/-;+/+)	4	8	7	54
ZO-2 chimera (-/-;+/+)	4	8	0	0
ZO-2 heterozygote (-/+)	5	10	10	75
ZO-2 chimera (-/+;+/+)	5	5	5	37
WT(+/+)	6	12	12	86

A. The age of ZO-2 chimera (-/+;+/+) ranges from 6 months to 10 months. All other males are about 6 months old.

B. All the females are of C57BL/6 background and aged from 8 to 12 weeks.

5.5 Chimeric expression of ZO-2-/- cells in the testis results in apoptosis

Since the fertility of male ZO-2 chimeric mice was affected, we analyzed whether the presence of ZO-2-/- cells altered the morphology of the testis. Male ZO-2 chimeric mice were sacrificed from 6 to 10-months of age and the testis dissected, sectioned and stained with hematoxylin and eosin. As shown in Figure 23, cells were absent from several seminiferous tubules, resulting in empty tubules. Multiple apoptotic bodies were observed in several seminiferous tubules, where cells were apparently undergoing cell death. To assess whether the loss of cells in the seminiferous tubules was due to apoptosis, tunnel analysis was carried out. As shown in Figure 24, no or only an occasional apoptotic cell was found in seminiferous tubules of WT mice. However, extensive apoptosis was observed in the seminiferous tubules of ZO-2 chimeric animals, confirming that the observed loss of cells was due to programmed cell death.

In the testis, ZO-2 is expressed at the blood-testis barrier region of adjacent Sertoli cells (Fink et al., 2006). Immuno-staining confrimed the absence of ZO-2 at many contact sites of adjacent Sertoli cells in the testis of ZO-2 chimeric mice (Figure 25A). Expression of ZO-1 in these regions was normal (Figure 25B). As previsouly shown for the barrier function on TJs in embryos (Chapter 4), the lack of ZO-2 could affect the blood-testis barrier. This could alter the ionic environment in the different compartments of the testis and lead to cell death.

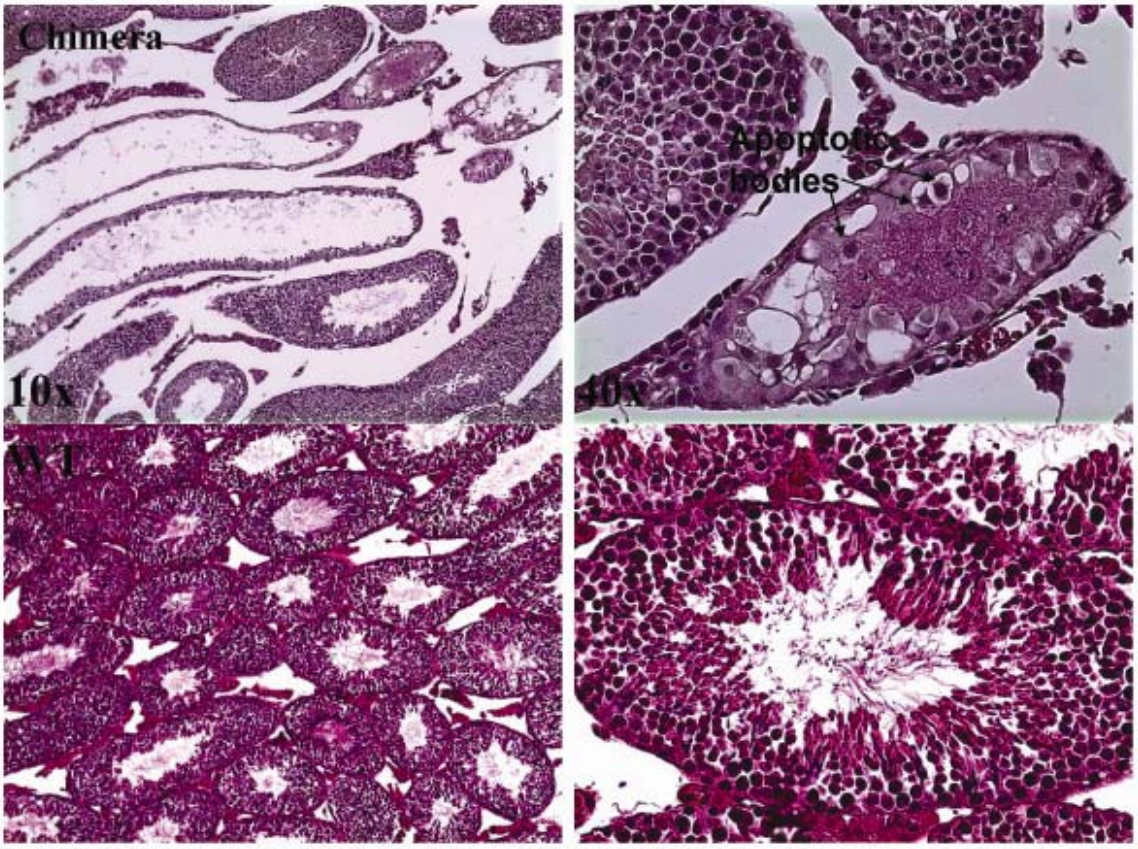

Figure 23 Histological analysis of the testis. *The cells in the testis of ZO-2 chimeric mice undergoing cell death and empty seminiferous tubules are indicated.*

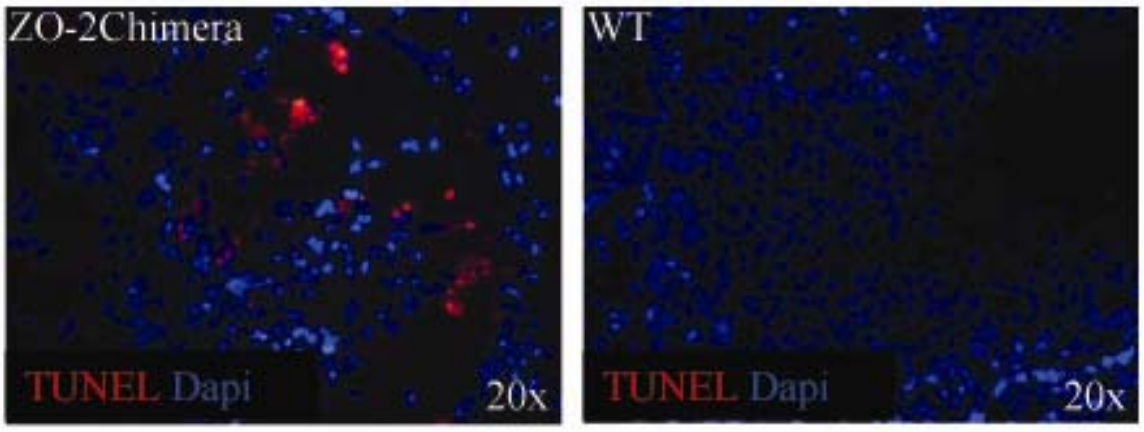

Figure 24 Apoptosis in the testis of ZO-2 chimeric mice. *Apoptosis signal was detected in the seminiferous tubules of ZO-2 chimeric mice, while rarely seen in the testis of WT mice.*

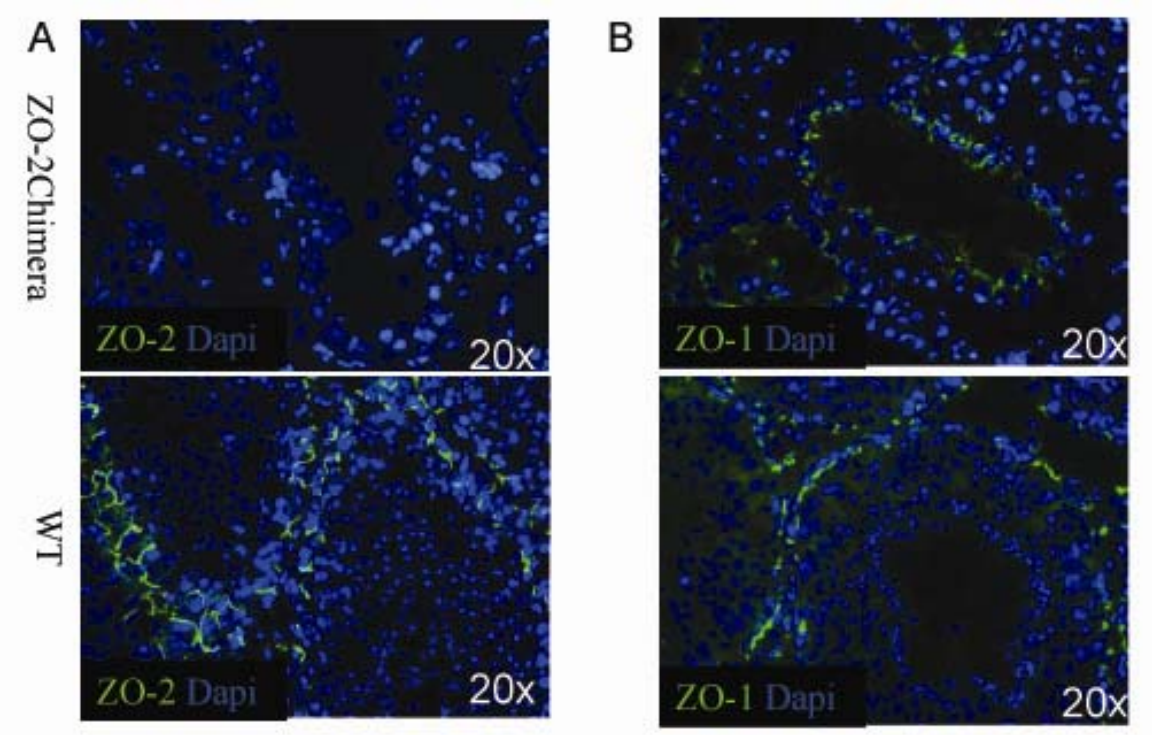

Figure 25 ZO-2 and ZO-1 expression in testis. *(A) ZO-2 expression is greatly reduced in the testis of ZO-2 chimeric mice. (B) ZO-1 expression is not altered in the testis of ZO-2 chimeric mice.*

5.6 ZO-2 chimeric mice present with defects in balance and hearing

ZO-2 chimeric mice showed obvious problems in coordinated walking and often tilted their head to a side (Video 1). Since this behavior is typical for animals with defects in maintaining balance control (Torres et al., 1998), this phenotype was followed up. About 75% of the ZO-2 chimeric mice with 100% Agouti coat color "circled" when lifted by their tails (Table 7), a behavior characteristic for loss of balance control. In contrast, this was never observed for WT or ZO-2+/- heterozygous animals. This phenotype indicates that the vestibular system in the inner ear might be affected. Analysis of the vestibular system in these mice will be the focus of a future study.

Defects in balance control are often linked to hearing defects. We therefore assessed the hearing capability of ZO-2 chimeric mice using Preyer Reflex analysis (Hulander et al., 1998). Briefly, a mouse kept in silent environment was subjected to a sudden sound by clapping the hand and the response was evaluated. Based on this test, the lack of a response of the animal to the sound is taken as an indication for an impairment of hearing. As shown in Table 8, 50% of the mice with a loss in balance control also showed hearing defects. A detailed analysis of the role of ZO-2 in the inner ear, in particular the vestibular system and the organ of Corti, will be the basis for future studies.

5.7 Defects in other organs of ZO-2 chimeric mice

In addition to testis and inner ear, other organs of ZO-2 chimeric mice showed obvious anomalies. These included an enlarged calyx in the kidney and an abnormal loss of fur (data not shown).

Cell line	Coat color	Mouse No	Unbalanced No
ZO-2-/+	100% agouti	9	0
ZO-2-/-	<50% agouti	17	0
ZO-2-/-	100% agouti	32	22

Table 7 Balance defect in ZO-2 chimeric mice. *About 70% of the ZO-2 chimeric mice (-/ ;+/+) with high percentage Agouti coat lost balance control. ZO-2 chimeric mice (-/-;+/+) with low percentage Agouti coat, ZO-2 chimeric mice (-/+;+/+) with high percentage Agouti coat, and ZO-2-/+ mice (not shown) are normal.*

Mice type	Mice No	Agouti(%)	Balance	Prayer reflex No
ZO-2Chimera	10	100%	lost	5
ZO-2Chimera	6	>50%	normal	6
ZO-2-/+	10	Nil	normal	10

Table 8 Prayer Reflex analysis for hearing. *For Prayer Reflex analysis, the mouse was kept in a silent atmosphere and was subjected to a sudden sound by clapping the hand and the response was evaluated. If the mouse responded, it's judged to be normal. If not, the hearing was impaired. 50% of those mice lost balance control also lost hearing.*

5.8 Discussion

ZO-2 is expressed in both embryonic and extra-embryonic tissue during the early developmental stages. ZO-2-/- ES cells were injected into WT blastocyst to determine whether ZO-2 is indispensable for both embryonic and extra-embryonic tissue based on the fact that injected cells only contribute to embryonic tissue but not extra-embryonic tissue. Surprisingly, ZO-2 chimeric mice were viable, even when ZO-2-/- cells highly contributed to chimeric mice based on their ~100% Agouti coat color. Furthermore, the injected ZO-2-/- ES cells gave rise to germ cells and most born offspring were from the injected ZO-2-/- ES cells. These data indicate that embryonic lethality may reflect an extra-embryonic requirement for ZO-2 rather than a prerequisite for development of the epiblast.

In testis, the germ cells are separated from the external environment by the blood-testis barrier (Dym et al., 1970). ZO-2 is a major component for forming the TJ in the blood-testis barrier, which is a highly dynamic structure. In contrast to TJs in other organs, TJ in the testis express both the ZO-1 alpha+ and alpha- splice forms. The distribution of these two isoforms, however, differs within the testis. ZO-1 alpha+ is restricted to TJs that join Sertoli cells to spermatogonia and preleptotene and leptotene spermatocytes, while ZO-1 alpha- is found in TJs between Sertoli cells to all classes of germ cells (Pelletier et al. 1997). In ZO-2 chimeric male mice, strong apoptosis was observed in the seminiferous tubules. Abnormal apoptosis might result from the disruption of the testis barrier. In the testis, ZO-1alpha+ expression levels are relatively low and other ZO proteins may not be able to compensate for the loss of ZO-2. Thus, the

loss of ZO-2 might result in blood-testis barrier defects, likely leading to cell death in the seminiferous tubules and thereby affecting the fertility of the ZO-2 chimeric male mice.

Chapter 6 Generation and phenotypic analysis of ZO-3-/- mice

6.1 Generation of ZO-3-/- mice

Genomic fragments containing the ZO-3 locus were isolated from a 129Sv mouse genomic library and subcloned into pBluescript II KS+ vector. A targeting vector designed to replace the exon containing the first transcriptional ATG was constructed using a LacZ neo cassette flanked by short and long arms of 2.2 kb and 4.8 kb for ZO-3 (Figure 26). This insertion results in a null mutation of the corresponding gene and allows in principle the expression of the β-gal marker under the control of the endogenous transcriptional regulatory elements of ZO-3.

The targeting vector was linearized, electroporated into the W4 ES cells and the cells subjected to selection in G418. The growing clones were screened for homologous recombination at the ZO-3 locus by long-range PCR using the primers indicated in Figure 26A. A band of ~ 2.5 kb was amplified for the targeted ES cell clones and 5 positive clones out of 96 picked were obtained (data not shown). PCR results were confirmed by Southern blot hybridization using the probes shown in Figure 26A. For the 5 targeted clones, the expected 5.8 kb wild-type and 10.6 kb mutant bands were detected, while for wild type clones, only one 5.8 kb wild-type band was present (Figure 26B).

Clone 48 and 50 were injected into C57BL/6 blastocysts to produce chimeric mice. Both clones produced chimeric mice with ~100% Agouti coat color and germ line

transmission of the mutated allele. These chimeric mice were mated with either C57BL/6 or 129Sv strain mice to establish the F1 generation of heterozygous animals. ZO-3 heterozygous mice were apparently normal and crossed to obtain homozygous animals.

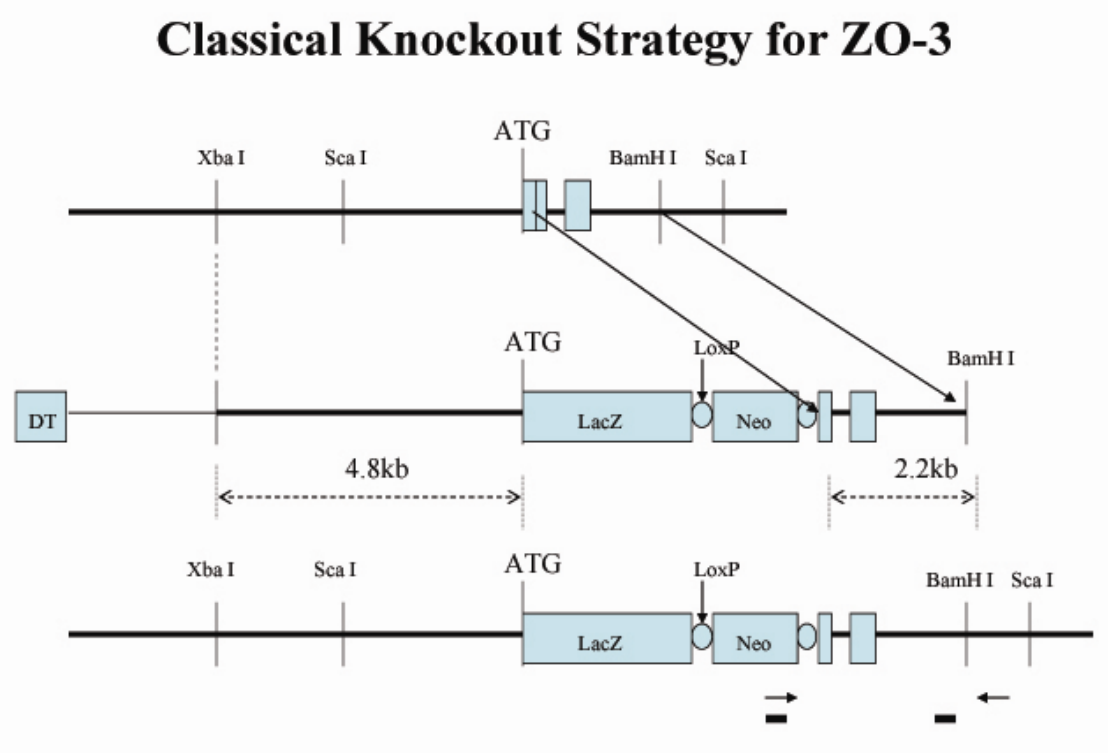

Figure 26 Targeting of the ZO-3. *(A) Schematic representation of the genomic locus of ZO-3 shows exon 3 with the initiation ATG. The targeting vector was designed to disrupt exon 3 by the in-frame insertion of a lacZ gene and a loxP flanked neomycin cassette immediately downstream of the ATG codon. Bars indicate the regions to which probes used for Southern blot analysis hybridize; arrows denote the regions from where primers used for screening of the targeted clones were derived.*

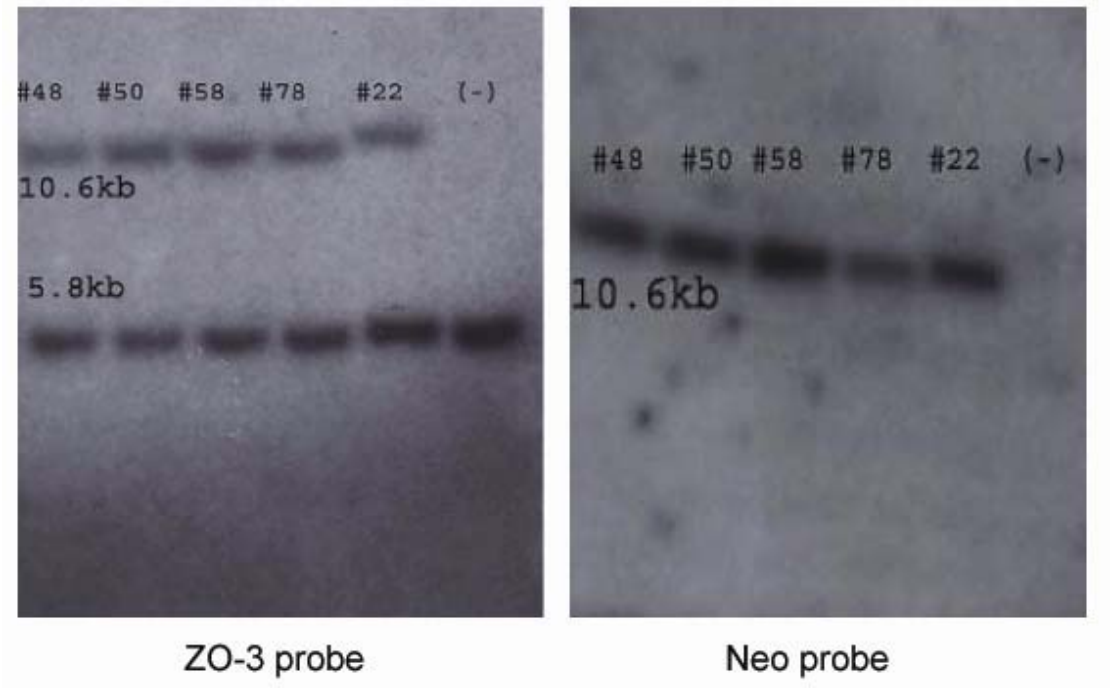

(B) Southern blot of ScaI digested genomic DNA of selected ES cell clones probed with labeled DNA probes hybridizing to genomic DNA (see panel A) or the neomycin gene for the identification of homologous recombinants. a 10.6 and 5.8 kb ScaI fragment corresponding the targeted mutant or WT allele, respectively, is detected in targeted (+/-) ES cell clones, whereas only the fragment corresponding to the WT allele is present in controls (+/+).

6.2 ZO-3-/- mice are born and viable

To generate ZO-3 null mice, ZO-3-/+ male and female mice were crossed. Genomic DNA was extracted from the tails of offspring and genotyped. As shown in Figure 27, ZO-3+/+, -/+ and -/- offspring were found in the litter, in a ratio consistent with Mendelian inheritance (Table 9) and suggesting that ZO-3 deficiency does not affect embryo development. Furthermore, born mice were fully viable. In order to corroborate the genotype, Western blot analysis was done using tissue lysates from ZO-3+/+ and ZO-3-/- mice (Figure 28). ZO-3 protein was absent in the lysate of liver and small intestine obtained from ZO-3-/- mice, thus confirming the PCR genotyping.

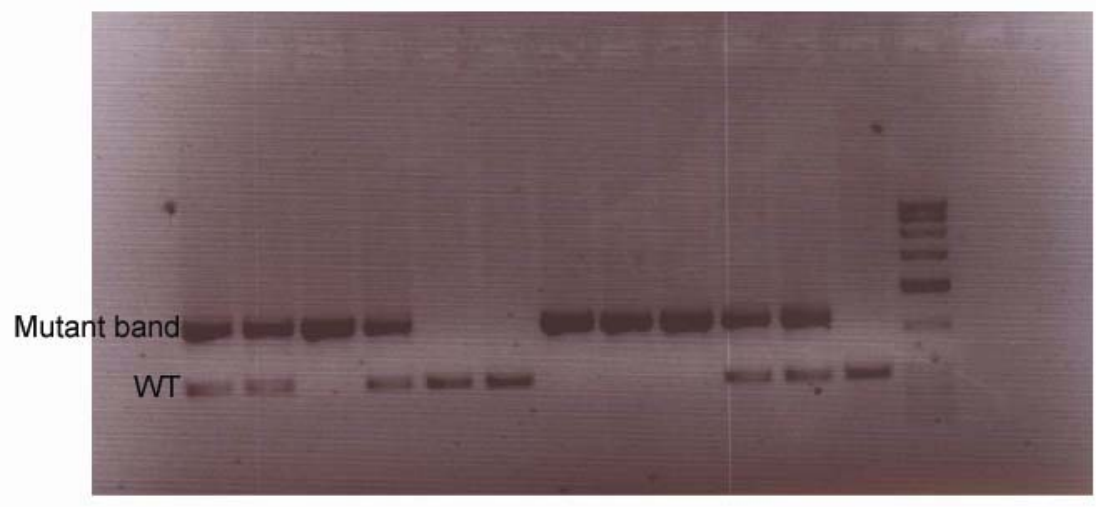

Figure 27 Genotyping of transgenic mice. *Genomic DNA was amplified by PCR using primers designed to distinguish between WT and mutant alleles. A fragment of 679 bps is indicative of the presence of the recombined mutant ZO-3 allele, while the 297 bp fragment denotes the WT allele.*

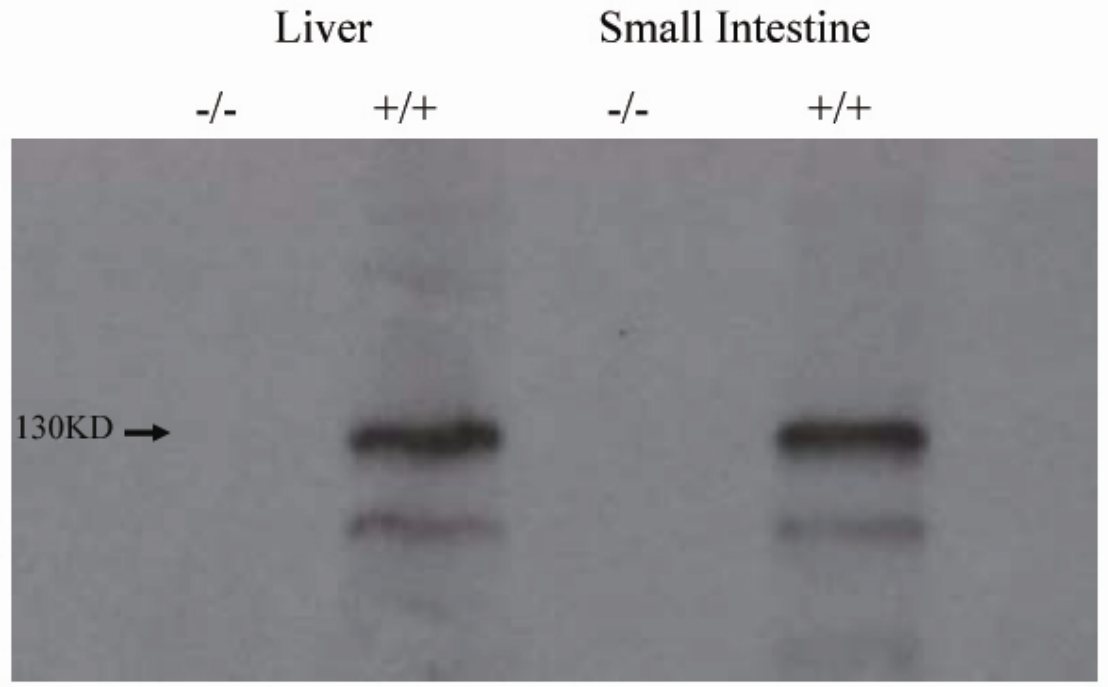

Figure 28 Western blot detection of ZO-3 protein*. Lysates of small intestine and liver from ZO-3+/+ and ZO-3 -/- littermates were fractionated by SDS/PAGE, transferred to membranes, and blotted with antibodies to ZO-3.*

Table 1. Genotypic analysis of offspring from heterozygous x heterozygous breeding pairs

No. (%) of indicated genotypes			
Wild-type	heterozygous	Homozygous	Total
17	57	23	97

Table 9 Genotypic analysis of offspring from ZO-3-/+ mice crossing. *ZO-3-/- mice are born at a Mendelian ratio and survive normally in the postnatal life.*

6.3 Organs of ZO-3-/- mice are histologically normal

ZO-3 is predominantly expressed in epithelial cells (Inoko et al., 2003).The tissue distribution of ZO-3 was monitored by Western blot analysis of selected major organs and ZO-3 was found to be highly expressed in stomach, intestine, liver, lung, kidney, and skin (Figure 29). These organs were sectioned and stained with hematoxylin and eosin. As shown in Figure 30, there was no histological difference detected in small intestine of ZO-3-/- mice. Similarly, ZO-3-/- mice monitored from birth to two years of age had no detectable defects in the other organs analyzed (data not shown).

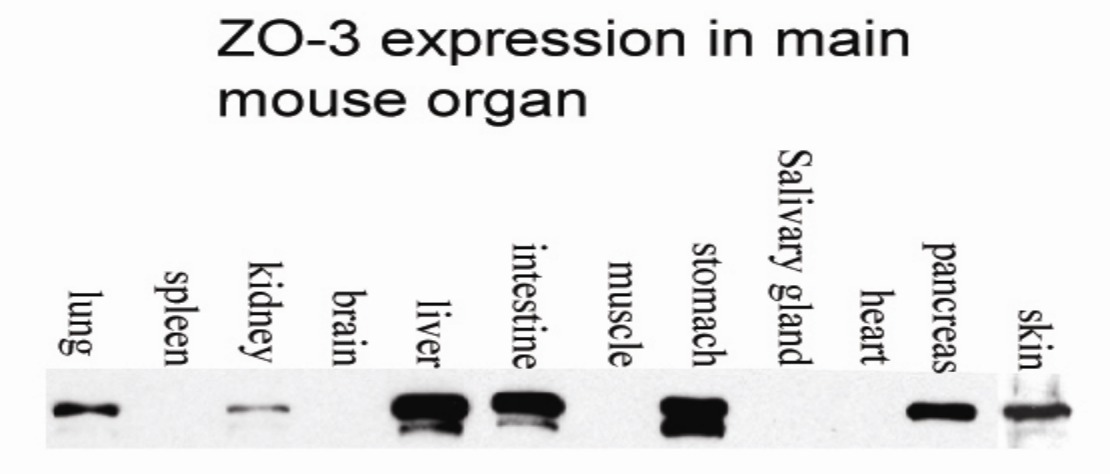

Figure 29 ZO-3 expressions in major mouse organ.

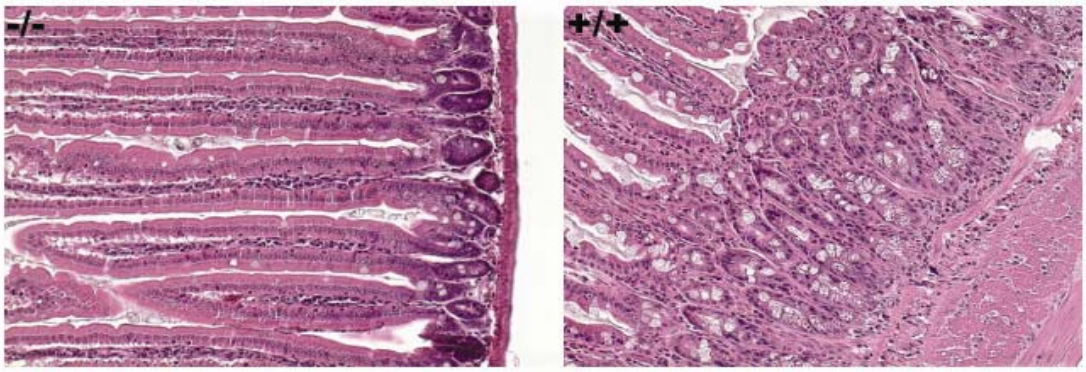

Figure 30 H&E staining of small intestine of ZO-3-/- and ZO-3+/+ mice. *Up to 24 months of age, ZO-3-/- mice did not show any morphological differences in the intestine and other major organs (data not shown).*

6.4 Expression and localization of TJ and AJ markers are unaffected in the small intestine of ZO-3-/- mice

Given the role of the ZO-3 protein as a scaffolds that tethers TJ integral membrane proteins to the cytoskeleton, we analyzed by immunostaining if the expression and subcellular distribution of selected TJ and AJ markers is affected. As shown in Figure 31A, ZO-3 is strongly expressed in the small intestine of wild type mouse and particularly enriched at the apical pole of the lateral membrane of cells, facing the intestinal lumen. As expected, no specific ZO-3 staining was found in the small intestine of ZO-3-/- mice (Figure 31A). ZO-1 and ZO-2 proteins are also expressed in the small intestine and showed a similar distribution as ZO-3. Neither the expression nor the distribution of ZO-1 and ZO-2 was apparently altered in the small intestine of ZO-3-/- mouse (Figure 31 B, D). Similarly, the expression and distribution of occludin and E-cadherin were not affected in the absence of ZO-3 (Figure 31D). The expression and localization of these proteins in other major organs such as stomach and liver was also analyzed and found to be similar between ZO-3+/+ and ZO-3-/- animals (data not shown).

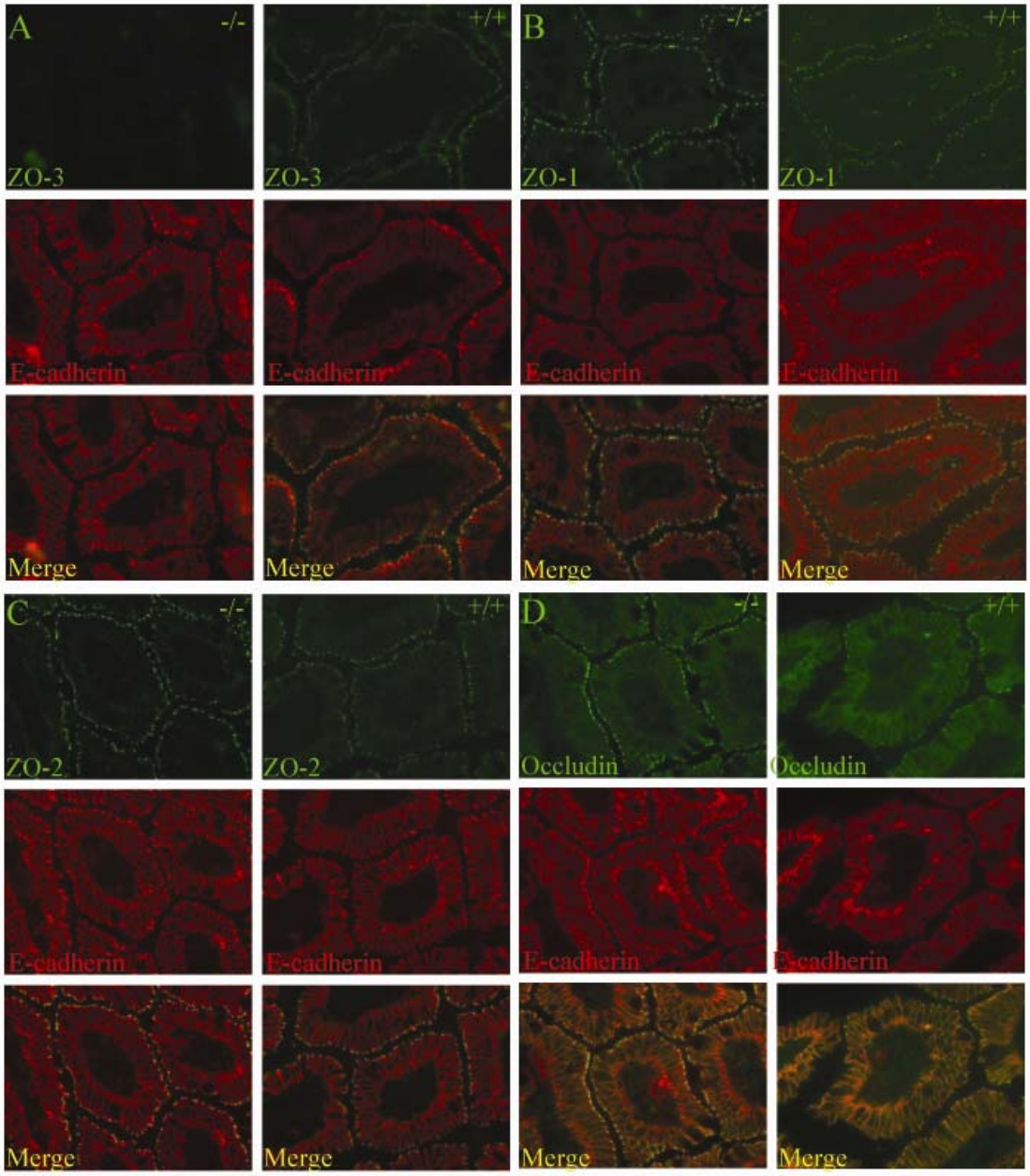

Figure 31 Protein distributions in small intestine. *(A) ZO-3 is not expressed in the small intestine of ZO-3-/- mouse; E-cadherin staining marks the lateral plasma membrane. (B, C, D) the distribution of ZO-1, ZO-2 and occludin is not altered in the small intestine of ZO-3-/- mice.*

6.5 TJ architecture is intact in ZO-3 null mice

To assess the structural integrity of TJs, we analyzed sections of the small intestine by EM. As shown in Figure 32, TJs were detected as typical electron dense plaques in the small intestine of ZO-3+/+ mice. In contrast to the loss of the plaque observed in ZO-2-/- embryos (see Figure 17 of Chapter 4), no structural difference was apparent for TJs in the intestine of ZO-3-/- mice as compared to controls (Figure 32).

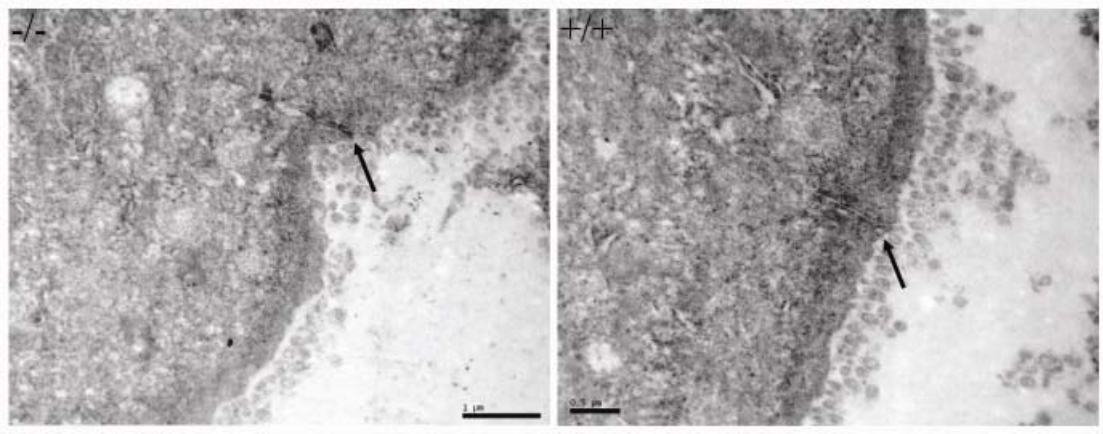

Figure 32 TJ morphology. *Electron micrographs of intestinal sections of ZO-3-/- and ZO-3+/+ mice show the presence to the typical electron dense plaques of the apical junctional complex between adjacent epithelial cells.*

6.6 ZO-3 deficiency does not affect mouse growth.

Given the strong expression of ZO-3 in the gastrointestinal tract (e.g. stomach, small intestine and colon), we reasoned that defects in the epithelial tissue of these organs may affect nutrient uptake and postnatal growth of ZO-3-/- pups. As shown in Figure 33, growth rates from 2 weeks to 12 weeks of age did not differ for ZO-3+/+ and ZO-3-/- mice, suggesting that the digestive and absorptive functions of the gastrointestinal tract is not compromised in ZO-3-/- mice.

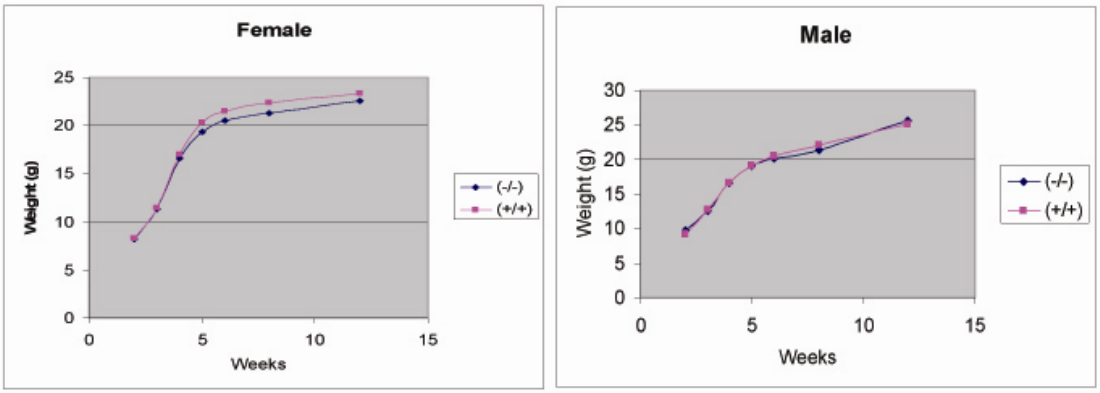

Figure 33 Postnatal growth curves of ZO-3-/- and ZO-3+/+ mice. *From 2 weeks to 12 weeks, ZO-3-/- mice show no apparent differences compared to ZO-3+/+ mice.*

6.7 Discussion

Unlike ZO-2-/- mice, ZO-3-/- mice were viable and the different organs analyzed were histologically normal. This finding is consistent with a recent report (Adachi et al. 2006). Among the three ZO proteins, ZO-3 is the shortest member and all of its functional domains have their corresponding sequence in ZO-1 and ZO-2. Unlike ZO-1 and ZO-2, ZO-3 is exclusively expressed in epithelia and not in endothelia, and is also not present in sites of cadherin-based cell-cell adhesion (Inoko et al. 2003). Thus, knockout of ZO-3 may not affect the development and viability of the mice if the function of ZO-3 can be compensated by ZO-1 and/or ZO-2. Alternatively, ZO-3 may be important for less critical physiological functions. A more detailed analysis in conjunction with the exposure of mice to different stress situations will likely be required to unravel physiological processes in which ZO-3 is important.

Chapter 7 Generation and phenotypic analysis of ZO-2-/-ZO-3-/- mice

7.1 Generation of ZO-2-/- ZO-3-/- mice

ZO-2-/+ mice were crossed with ZO-3 -/- mice to generate ZO-2-/+ZO-3-/+ mice. The ratio between the number of ZO-2+/+ZO-3-/+ and ZO-2-/+ZO-3-/+ offsprings was about 1:1, consistent with Mendelian ratio (data not shown). ZO-2-/+ZO-3-/- mice were obtained by crossing ZO-2-/+ZO-3-/+ mice, but as expected, no ZO-2-/-ZO-3-/- animals were found. ZO-2-/+ZO-3-/- mice were crossed and the ratio between the number of ZO-2+/+ZO-3-/- and ZO-2-/+ZO-3-/- offsping was around 1:2, consistent with Mendelian ratio (Table 10). Several pregnant mothers were sacrificed at different stages to obtain embryos. Similar to ZO-2-/-, ZO-2-/-ZO-3-/- embryos died at an early embryonic stage.

Table 1. Genotypic analysis of offspring from ZO-2He/ZO-3Ho breeding pairs

	No. (%) of indicated genotypes		
ZO-2Wt/ZO-3Ho	ZO-2He/ZO-3Ho	ZO-2Ho/ZO-3Ho	Total
40	74	0	114

Table 10 Cross between ZO-2-/+ZO-3-/- mice does not yield any ZO-2-/-ZO-3-/- mice.

7.2 ZO-2-/+ZO-3 -/- mice are histologically normal

ZO-2-/+ZO-3-/- mice were born and viable. Main organs, including liver and lung, were dissected from mice aged between 2 to 24 months and their histology was analyzed. As shown in Figure 34, there were no obvious histological differences between ZO-2-/+ZO-3-/- and WT mice in the liver and lung. Also other major organs of ZO-2-/+ZO-3-/- animals, in particular intestine and kidney, were normal (data not shown). In order to assess whether upregulation of the expression of other ZO family members was responsible for functional redundancy, protein expression levels for the different ZO proteins was quantified in WT, ZO-2-/+, ZO-3-/-, and ZO-2-/+ZO-3-/- mice (Figure 35). ZO-2 expression levels were downregulated in ZO-2-/+ and ZO-2-/+ZO-3 -/- mice, but not changed in ZO-3-/- mice. As expected, ZO-3 was not expressed in ZO-3-/- and ZO-2-/+ZO-3 -/- mice, but its expression was unchanged in ZO-2-/+ animals. ZO-1 expression was similar in WT, ZO-2-/+, ZO-3-/-, and ZO-2-/+ZO-3-/- mice. These data suggest that ZO proteins either do not compensate for each other or that compensation does not require increased expression levels.

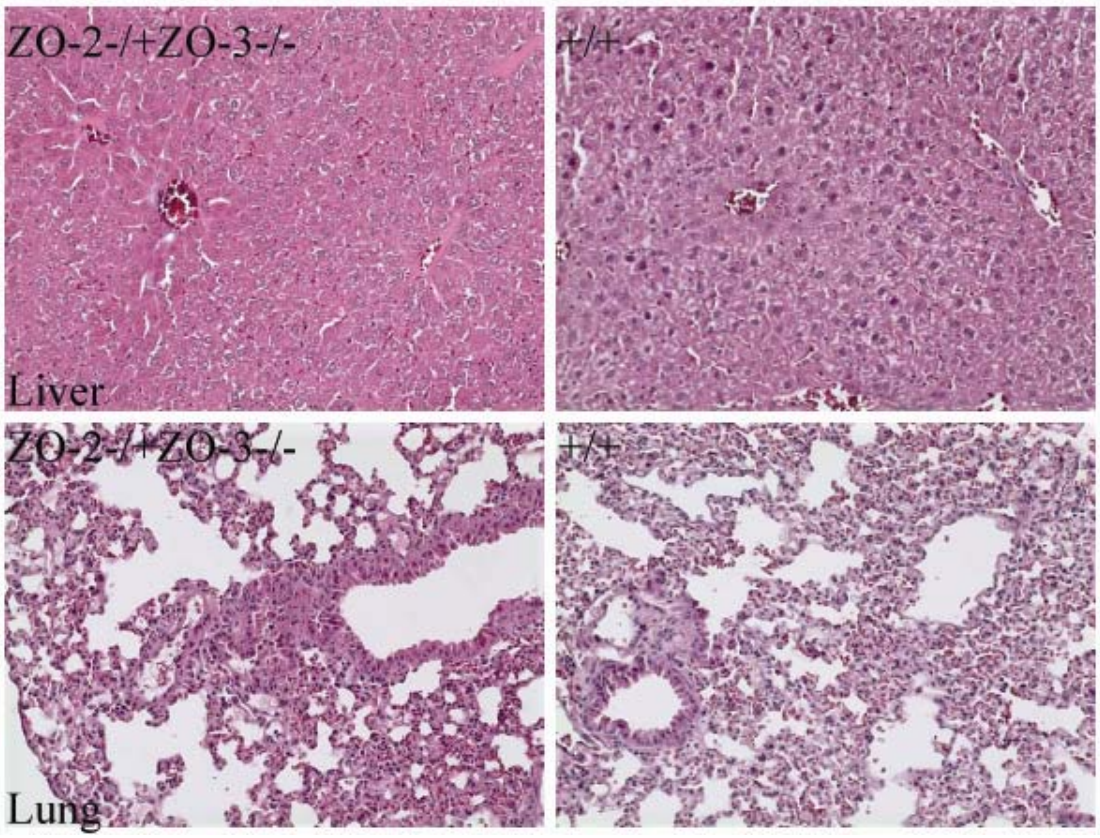

Figure 34 Histological analysis of ZO-2-/+ZO-3-/- mice. *No histological abnormality was found in the liver and lung of ZO-2-/+ZO-3-/- mice.*

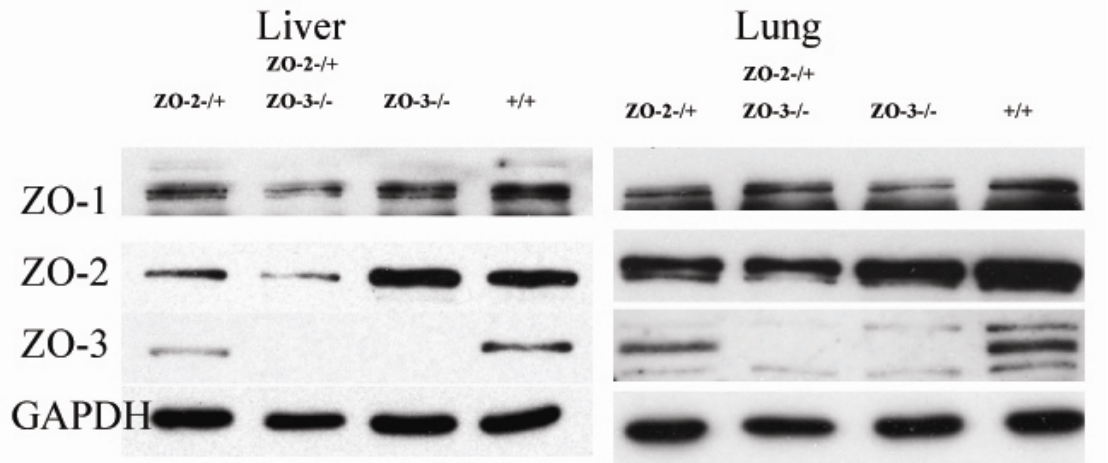

Figure 35 Western blots for ZO protein expression. *ZO protein expression in liver and lung of WT, ZO-2-/+, ZO-3-/-, and ZO-2-/+ZO-3-/- mice*

7.3 ZO-2-/-ZO-3-/- embryos die earlier than ZO-2-/- embryos

In order to determine the embryonic stage at which ZO-2-/-ZO-3-/- embryos die, ZO-2-/+ZO-3-/- mice were crossed and the pregnant mothers sacrificed at E6.5 and E7.5. Approximately one fourth of the deciduas dissected at E6.5 and E7.5 were small in size as compared to control deciduas (Table 11). Histological analysis showed that these deciduas were empty (Fig. 36) and did not contain small embryos as found for deciduas from the crossing of ZO-2-/+ mice (see Chapter 4), although empty deciduas were also occasionally observed in crossings of ZO-2-/+ mice, these were of normal size. These data indicate that ZO-2-/-ZO-3-/- embryos die earlier than ZO-2-/- embryos and thus ZO-3 might partially compensate a function of ZO-2 required during early stages of embryo development.

Table. Cross of ZO-2HeZO-3WT and ZO-2HeZO-3HO, respectively

Mice type	Stage	Normal No.	Tiny No.	Absorbed No.
ZO-2HeZO-3WT	E7.5	76	8	19
ZO-2HeZO-3HO	E7.5	47	0	19
ZO-2HeZO-3WT	E6.5	43	6	7
ZO-2HeZO-3HO	E6.5	57	0	18

Table 11 Statistical analysis of embryo morphology (normal or small and undergoing absorption) at E6.5 and E7.5. *While some ZO-2-/- embryos appear to survive up to E7.5, no ZO-2-/-ZO-3-/- embryos survive past E6.5.*

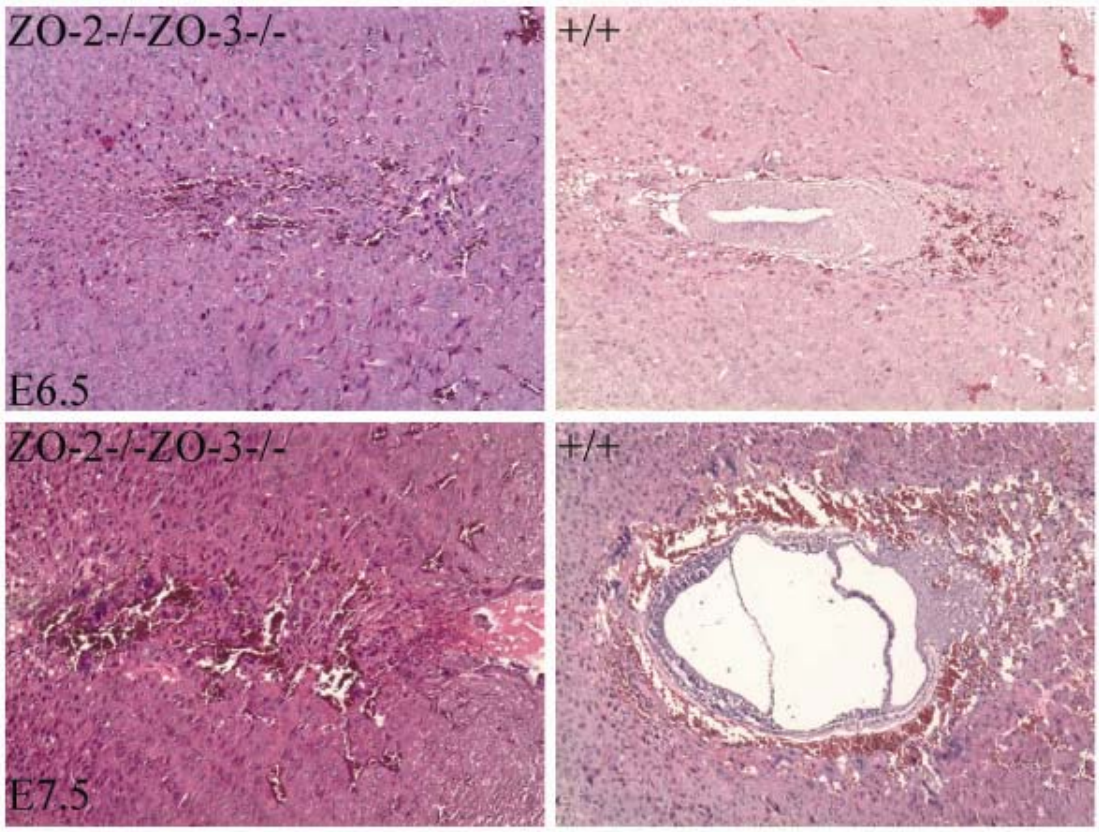

Figure 36 Histological analysis of ZO-2-/-ZO-3-/- embryos. *The ZO-2-/-ZO-3-/- embryos are completely absorbed by E6.5.*

7.4 ZO-2-/- ZO-3-/- blastocysts grow normally in vitro

Given the early embryonic lethality of ZO-2-/-ZO-3-/- embryos in vivo, we analyzed whether ZO-2 and ZO-3 deficiency affected the growth of blastocysts in vitro. ZO-2-/+ZO-3-/- male and female mice were crossed, pregnant mothers sacrificed at E3.5 and blastocysts flushed out from the uterus. As shown in Figure 37, there was no obvious difference in growth of ZO-2+/+ZO-3-/-, ZO-2-/+ZO-3-/-, and ZO-2-/-ZO-3-/- blastocysts after 4 days culture. The culture was kept for up to 9 days and again no obvious difference among the cultures was observed (data now shown). After 9 days in culture, cells were collected and genotyped. 18 blastocysts were checked by PCR and 4

blastocysts were ZO-2 and ZO-3 deficient (Figure 38). The number of ZO-2-/-ZO-3-/- blastocysts was about one fourth of the total blastocysts and thus consistent with Mendelian inheritance. These data thus indicate that ZO-2 and ZO-3 deficiency does not affect the growth of blastocysts in vitro.

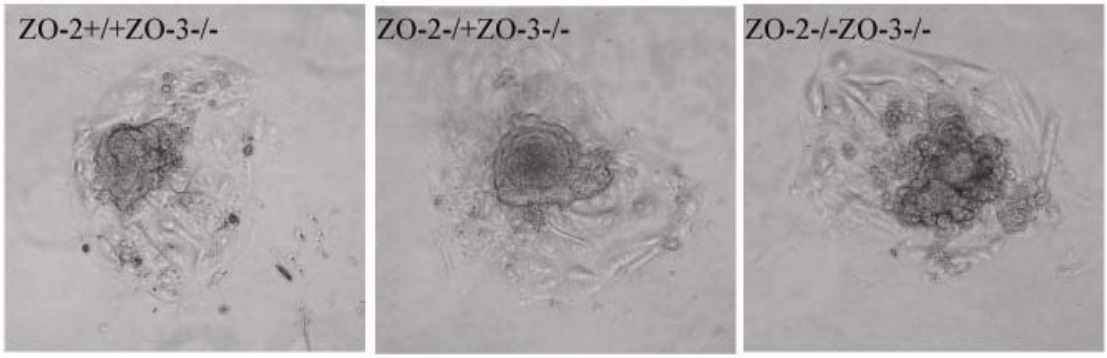

Figure 37 In vitro culture of blastocysts. *ZO-2+/+ZO-3-/-, ZO-2-/+ZO-3-/-, and ZO-2-/-ZO-3-/- blastocysts didn't show morphological difference.*

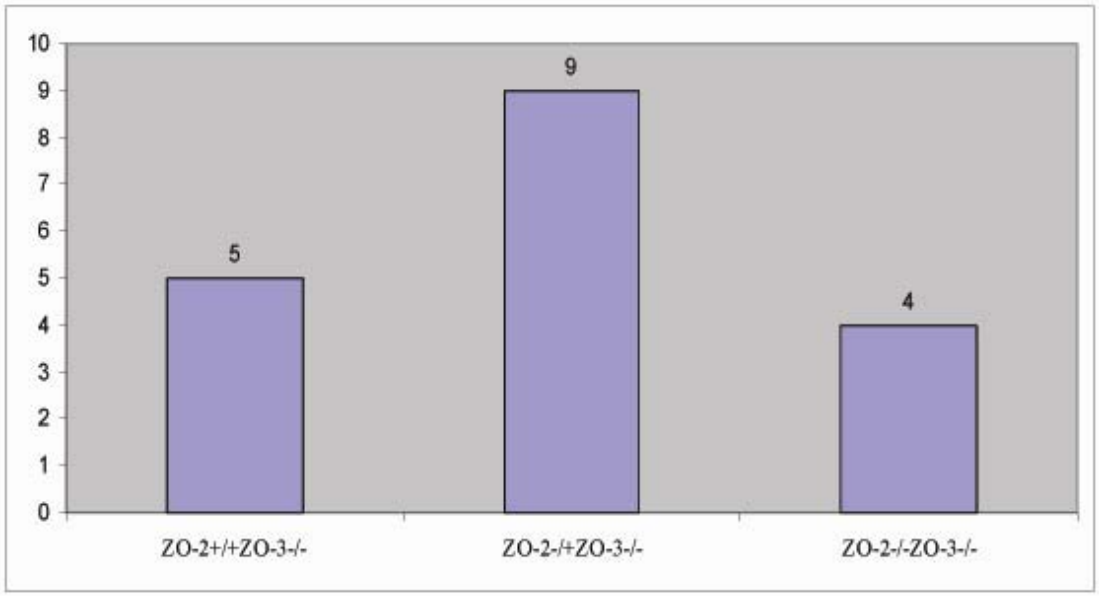

Figure 38 Statistical analysis of the number blastocysts in different genotype. *The number of ZO-2+/+ZO-3-/-, ZO-2-/+ZO-3-/-, and ZO-2-/-ZO-3-/- blastocysts obtained from the crossing of ZO-2-/+ZO-3-/- mice is consistent with Mendelian ratio.*

7.5 Discussion

In order to assess whether ZO-2 and ZO-3 can compensate for each other, ZO-2+/- heterozygous and ZO-3-/- homozygous mice were crossed. As expected, ZO-2-/-ZO-3-/- mice were embryonic lethal. However, the ZO-2-/-ZO-3-/- embryos died earlier than ZO-2-/- embryos and no ZO-2-/-ZO-3-/- embryos were found at E6.5. Smaller empty deciduas were found, indicating that ZO-2-/-ZO-3-/- blastocysts were implanted but died shortly after implantation. As discussed above, ZO-2 is likely indispensable for the normal function of the extra-embryonic tissue but dispensable for the growth of epiblast. ZO-3 is highly expressed in the extra-embryonic tissue (data not shown). Since ZO-2-/-ZO-3-/- embryos died earlier than ZO-2-/- embryos, ZO-3 might partially compensate for the function of ZO-2 in extra-embryonic tissue at early stages of embryonic development. ZO-2-/-ZO-3-/- blastcysts grew normally in vitro, suggesting that ZO-2 and ZO-3 are dispensable for blastocyst development prior to implantation.

We can not exclude that ZO-2 and ZO-3 could also compensate for each other at later stages of embryonic development and/or during postnatal life. Derivation of chimeric mice from ZO-2-/-ZO-3-/- ES cell could be a possible approach to further explore the roles of ZO-2 and ZO-3 at those later stages.

ZO-2 expression levels were reduced by ~50% in the mice carrying one inactivated allele. Furthermore, ZO-3 partially compensated for the function of ZO-2 during the early embryonic development stage. Therefore, although both ZO-2 heterozygous and ZO-3 homozygous mice were phenotypically normal, it was interesting to analyze the phenotype of ZO-2-/+ZO-3-/- mice. Phenotypic analysis in terms of survival, health and fertility showed that ZO-2-/+ZO-3-/- mice were viable and indistinguishable from WT

mice. Western blot analysis indicated that ZO-2 expression levels were reduced by half and ZO-1 expression levels were not altered in ZO-2-/+ZO-3-/- mice. These data thus show that even in the absence of ZO-3, half the ZO-2 protein levels might be sufficient for the normal development and function of various tissues.

Chapter 8 Phenotypic analysis of ZO-1-/- embryonic stem cells

8.1 Protein expression in ZO-1-/- EBs

Given the strong expression of ZO-1 protein in EBs, the expression levels of other TJ and AJ markers were analyzed by Western blot. ES cells were differentiated to form EBs and on day 10, EBs were lysed and the expression of selected proteins analyzed. As expected and shown in Figure 39, ZO-1 was not expressed in ZO-1-/- and downregulated in ZO-1-/+ EBs. The expression of ZO-2 was not significantly affected but, interestingly, ZO-3 protein levels were reduced in ZO-1-/- EBs. The expression levels of occludin, cingulin, E-cadherin and claudin-3 were not altered in either ZO-1-/+ and ZO-1-/- EBs. These data show that expression of ZO-3, but not that of ZO-2 or the other junction proteins analyzed, is altered in EBs lacking ZO-1.

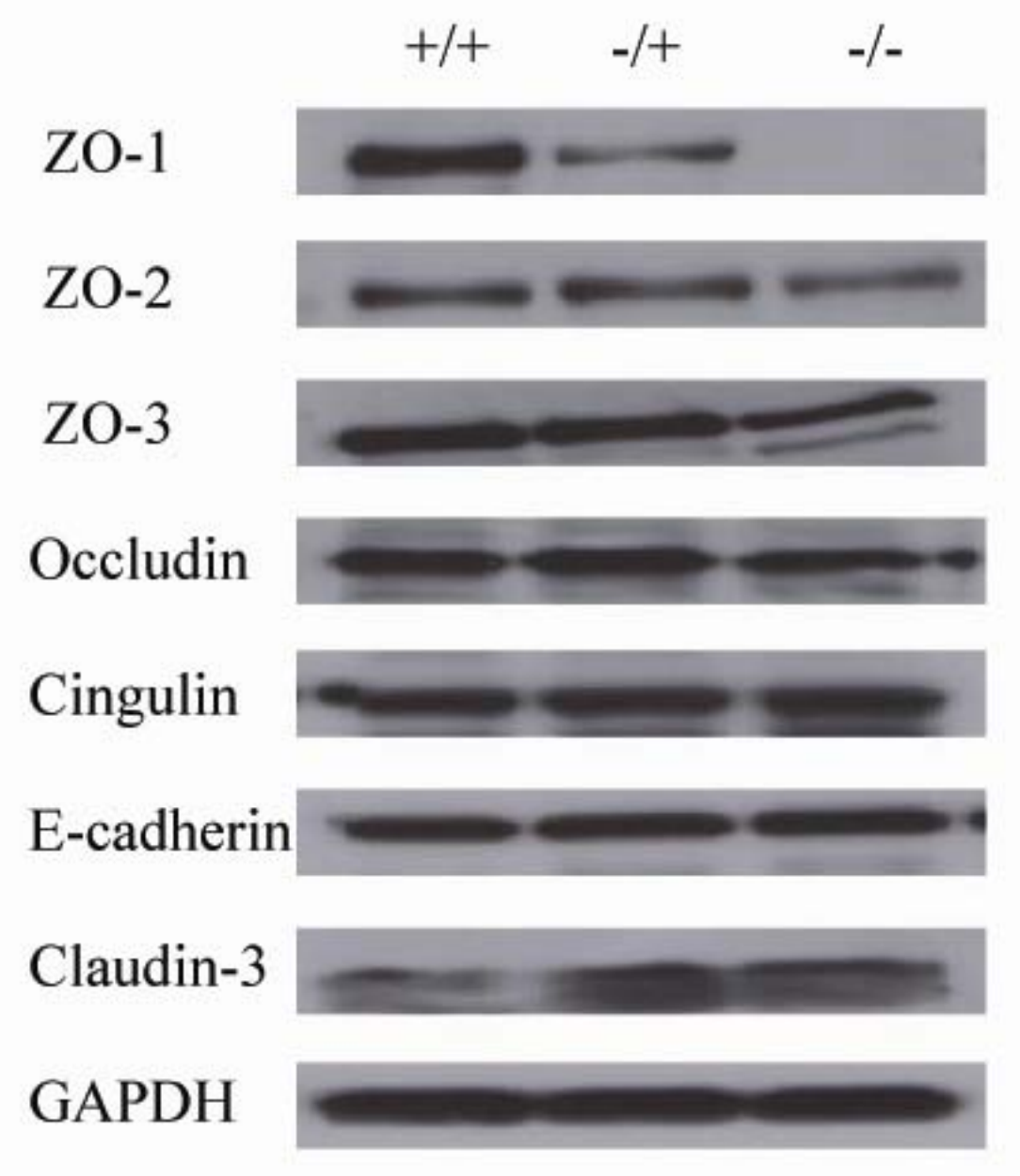

Figure 39 Expression levels of selected junction-associated proteins in ZO-1-/- EBs. *Western blot was done on lysates from day 10 EBs to assess the expression of ZO proteins and selected TJ and AJ markers. ZO-1 was not expressed in ZO- -/- EBs and downregulated in ZO- -/+ EBs; ZO-3 was downregulated in ZO-1 -/- EBs, while the expression of ZO-2 and the other TJ and AJ markers analyzed was not altered in either ZO-1 -/- or ZO-1 -/+ EBs.*

8.2 The subcellular localization of several TJ and AJ markers is altered in ZO-1-/- EBs

Given the role of ZO-1 as a scaffold protein that links TJ proteins to the cytoskeleton, we analyzed by immunostaining if the subcellular distribution of selected TJ and AJ markers was affected. As shown in Figure 40A, ZO-1 was strongly expressed in the epithelia of ZO-1+/+ EBs, where it was enriched at sites of cell-cell contact. As expected, no specific ZO-1 staining was observed in ZO-1-/- EBs (Figure 40A). EBs also expressed ZO-2, ZO-3 and other TJ and AJ markers such as occludin and cingulin. While ZO-2 remained well localized to the sites of cell-cell contact in the epithelia or ZO-1-/- EBs, ZO-3 showed a diffused distribution (Figure 40B, C). The localization of occludin and cingulin was not altered in the epithelia of ZO-1-/- EBs (Figure 40D, 4E). Claudin-1, claudin-3, claudin-4, claudin-5, claudin-6 and claudin-7, however, no longer showed plama membrane localization but instead were diffused throughout the cytoplasm (Figure 40F, G, H, I, J, K). The localization of the apical maker moesin and the lateral marker E-cadherin was unaffected in ZO-1-/- EBs (Figure 41), indicating that the ability of TJs to maintain the asymmetric distribution of proteins between the apical and the basolateral domain was not affected.

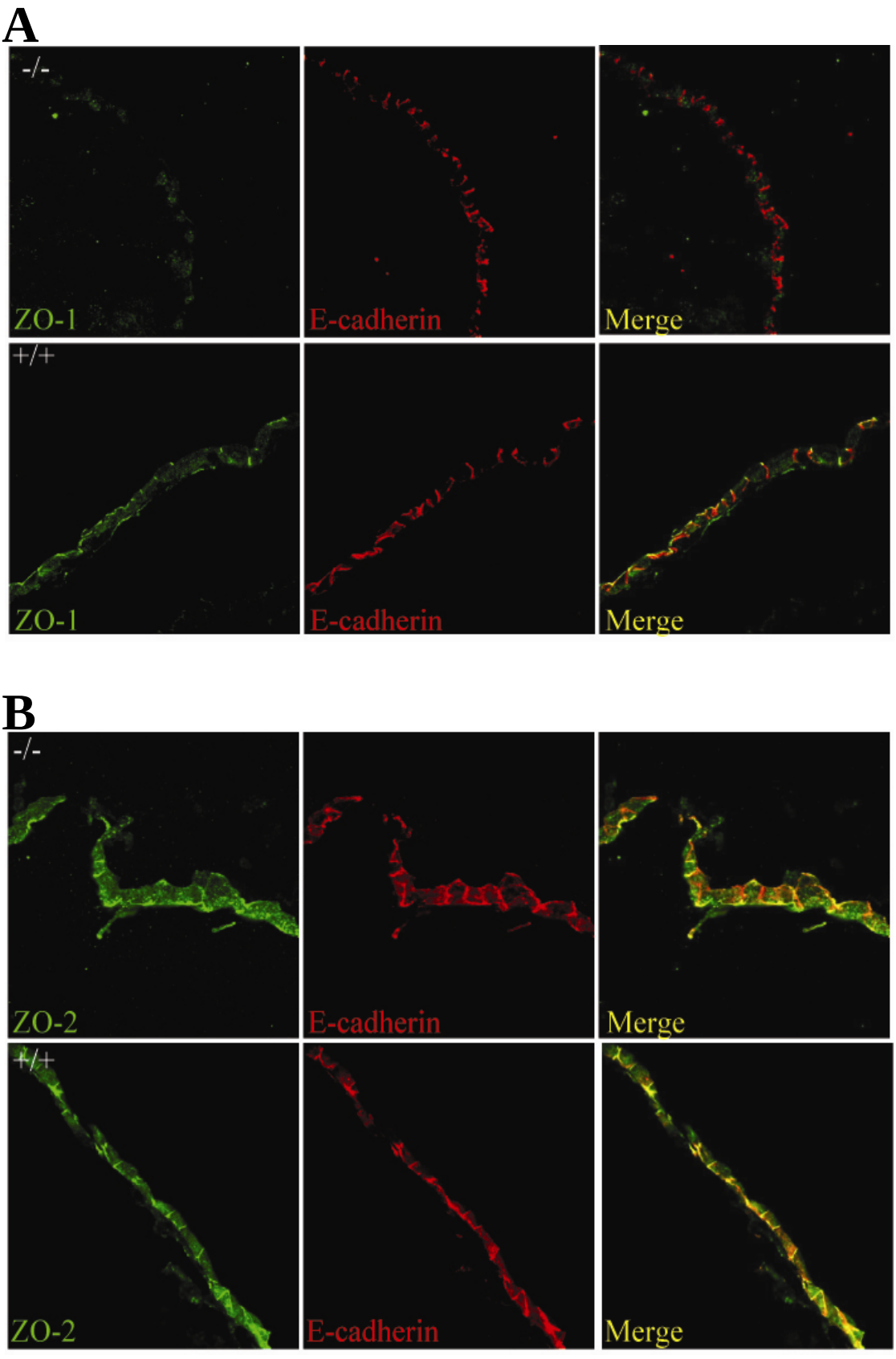
A
-/-
ZO-1
E-cadherin
Merge
+/+
ZO-1
E-cadherin
Merge
B
-/-
ZO-2
E-cadherin
Merge
+/+
ZO-2
E-cadherin
Merge

C

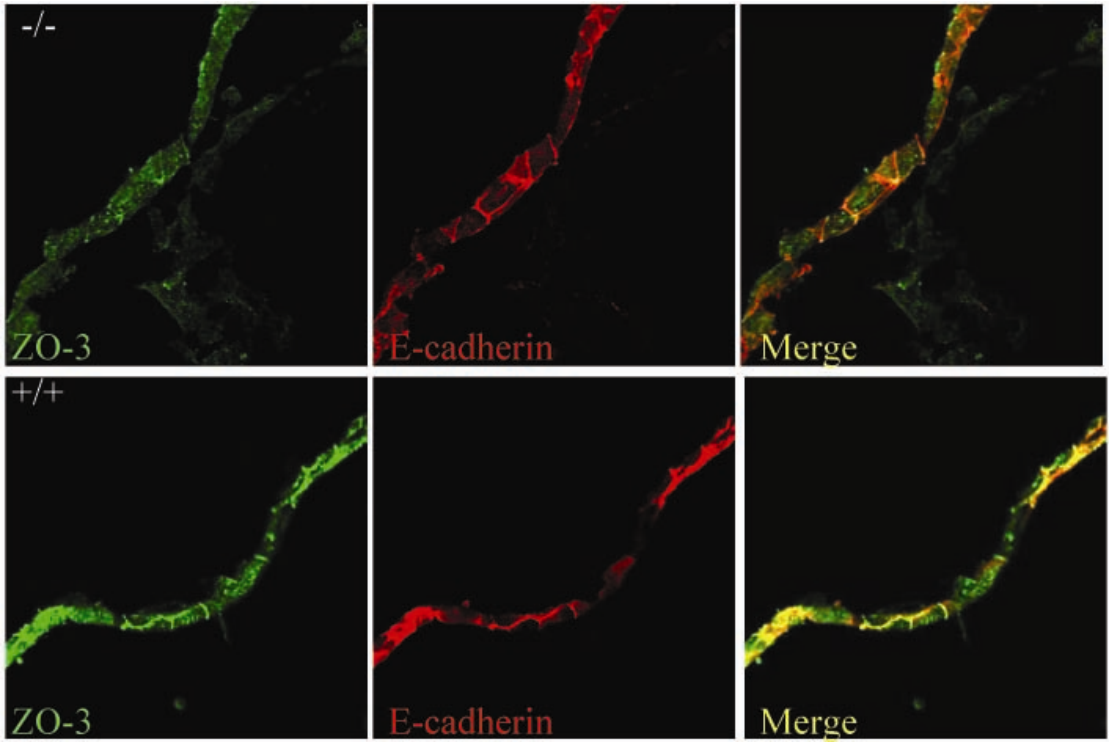
-/-
ZO-3
E-cadherin
Merge
+/+
ZO-3
E-cadherin
Merge

D

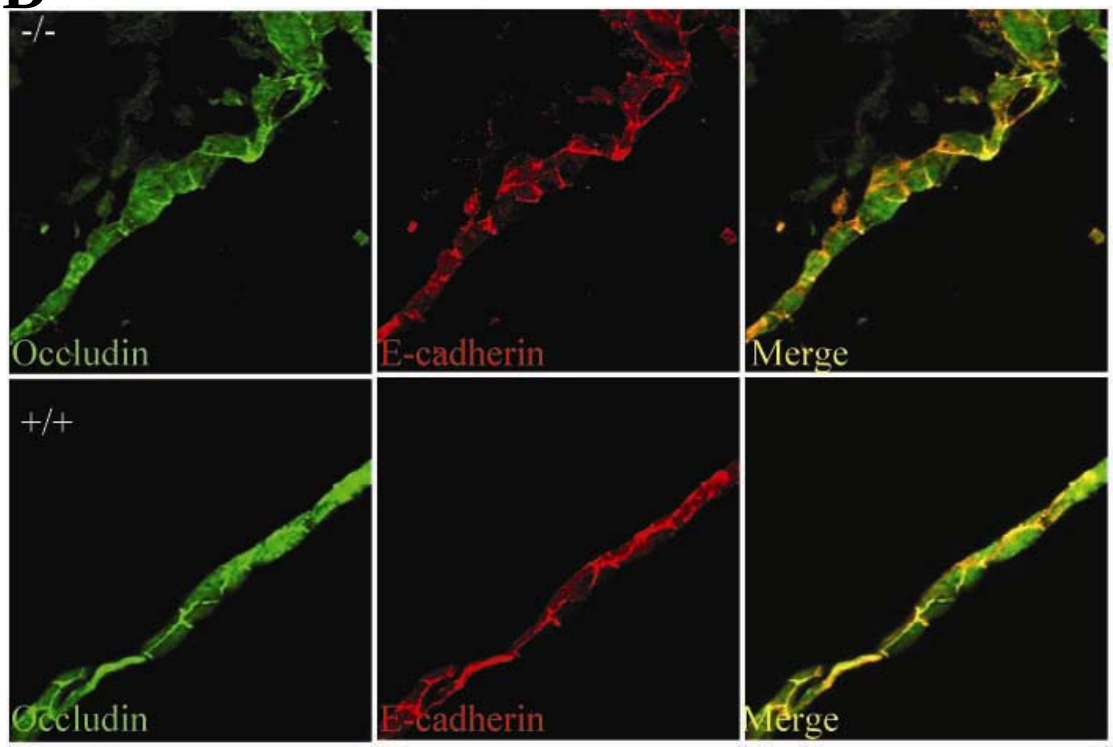
-/-
Occludin
E-cadherin
Merge
+/+
Occludin
E-cadherin
Merge

E

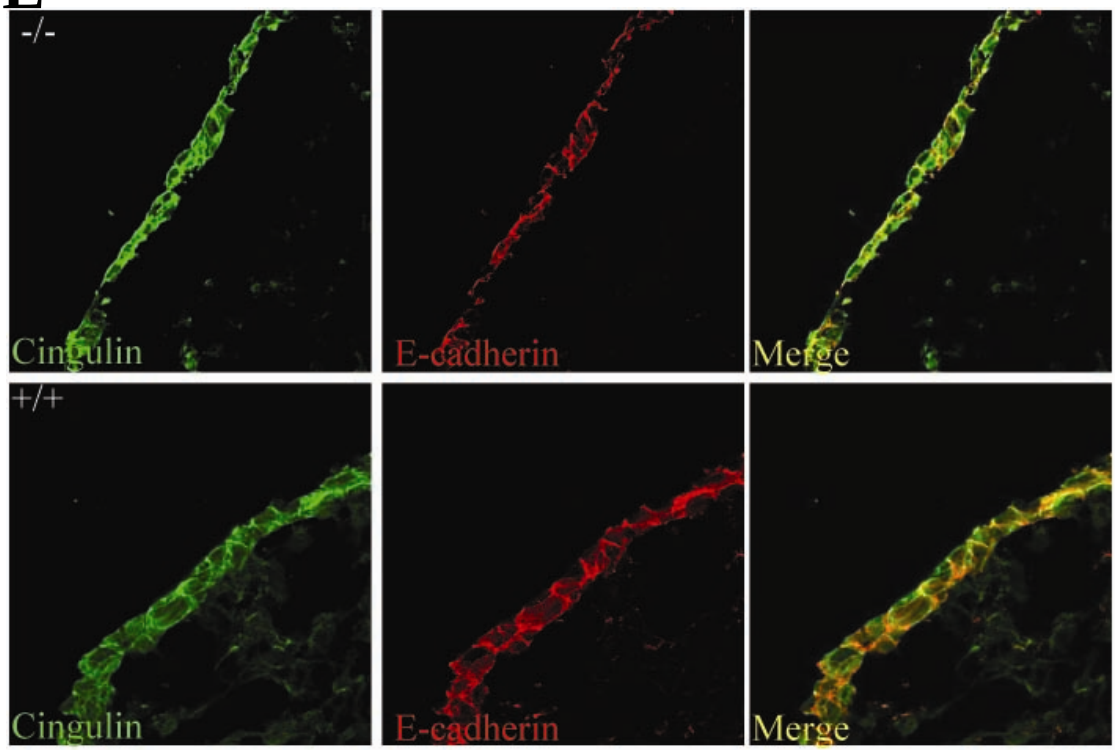
-/-
Cingulin
E-cadherin
Merge
+/+
Cingulin
E-cadherin
Merge

F

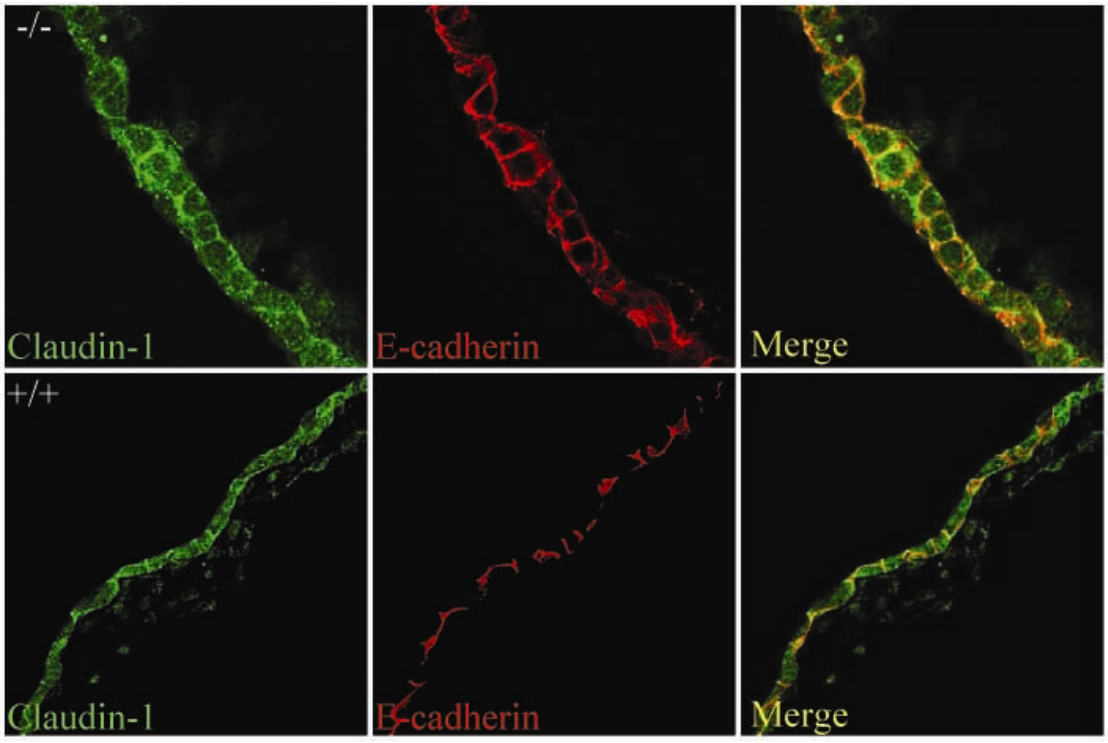
-/-
Claudin-1
E-cadherin
Merge
+/+
Claudin-1
E-cadherin
Merge

G

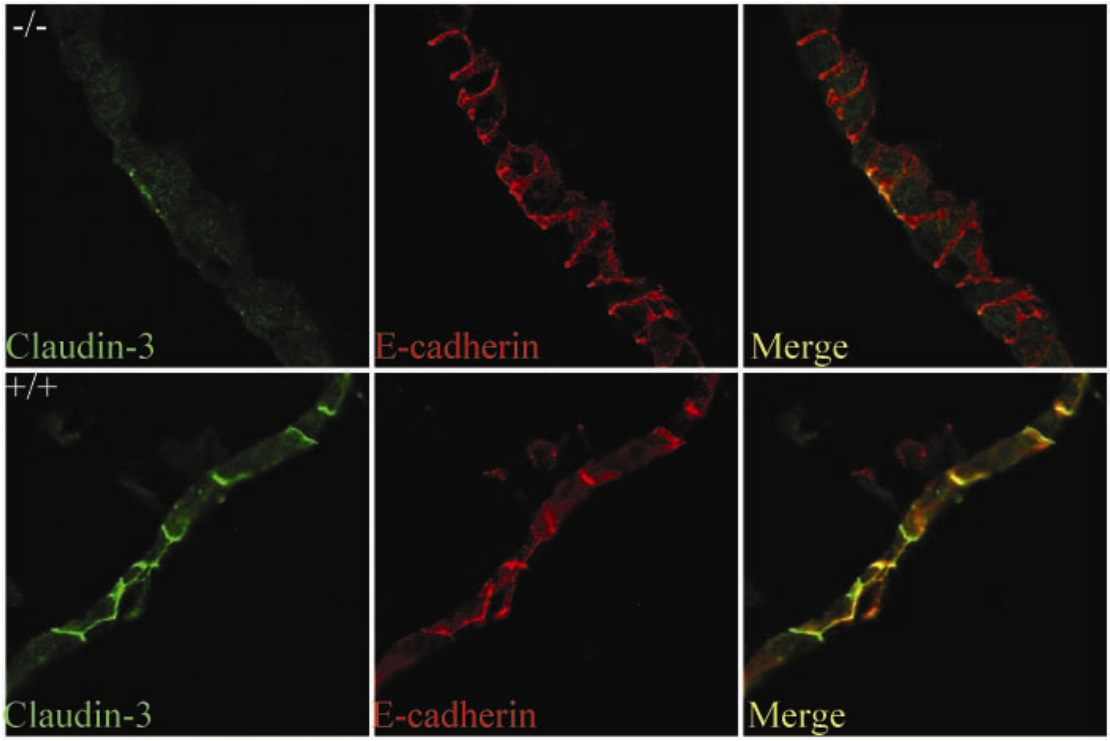
-/-
Claudin-3
E-cadherin
Merge
+/+
Claudin-3
E-cadherin
Merge

H

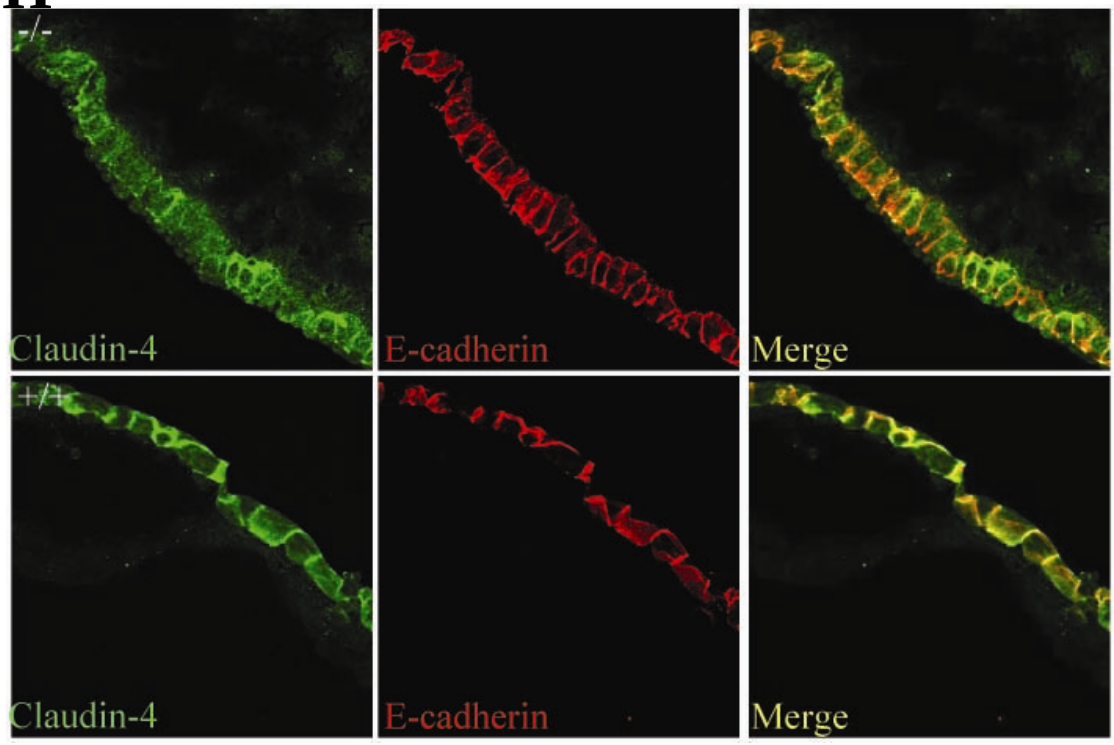
-/-
Claudin-4
E-cadherin
Merge
+/+
Claudin-4
E-cadherin
Merge

I

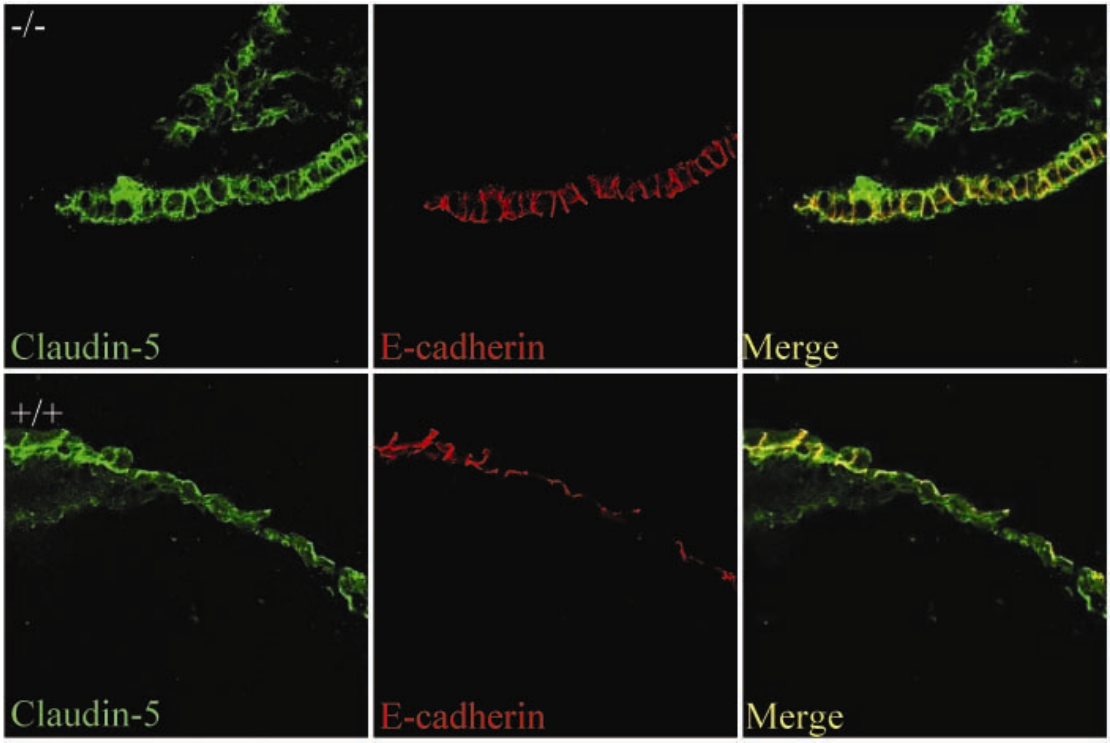
-/-
Claudin-5
E-cadherin
Merge
+/+
Claudin-5
E-cadherin
Merge

J

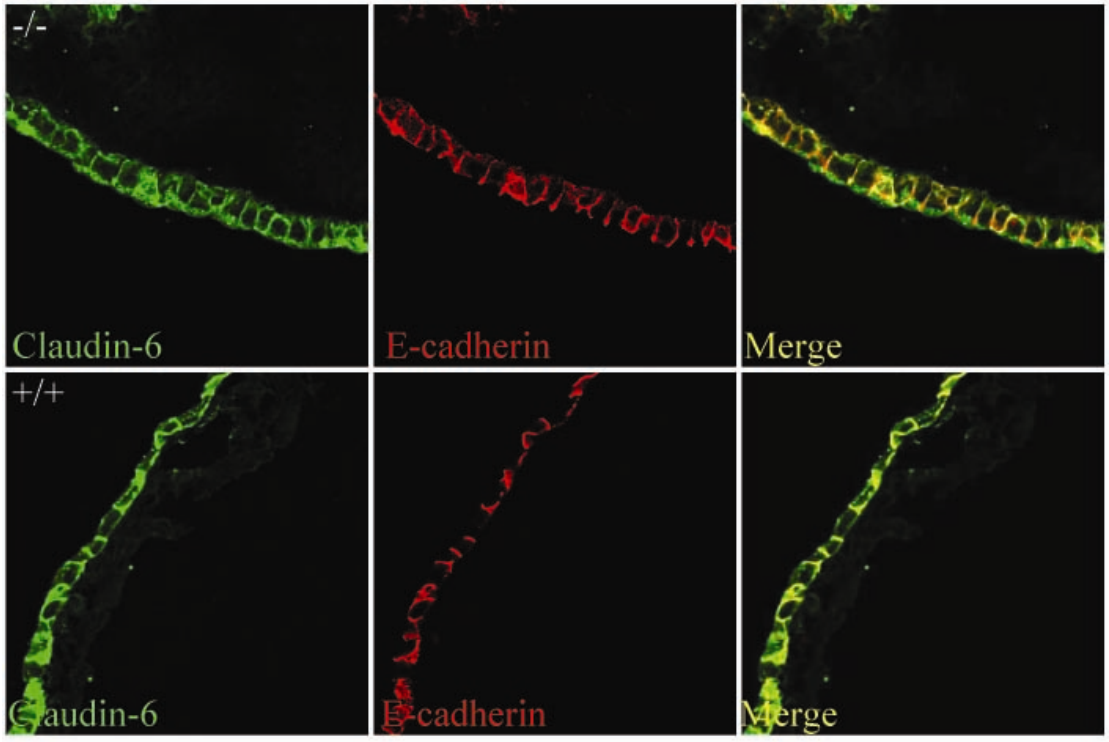
-/-
Claudin-6
E-cadherin
Merge
+/+
Claudin-6
E-cadherin
Merge

K

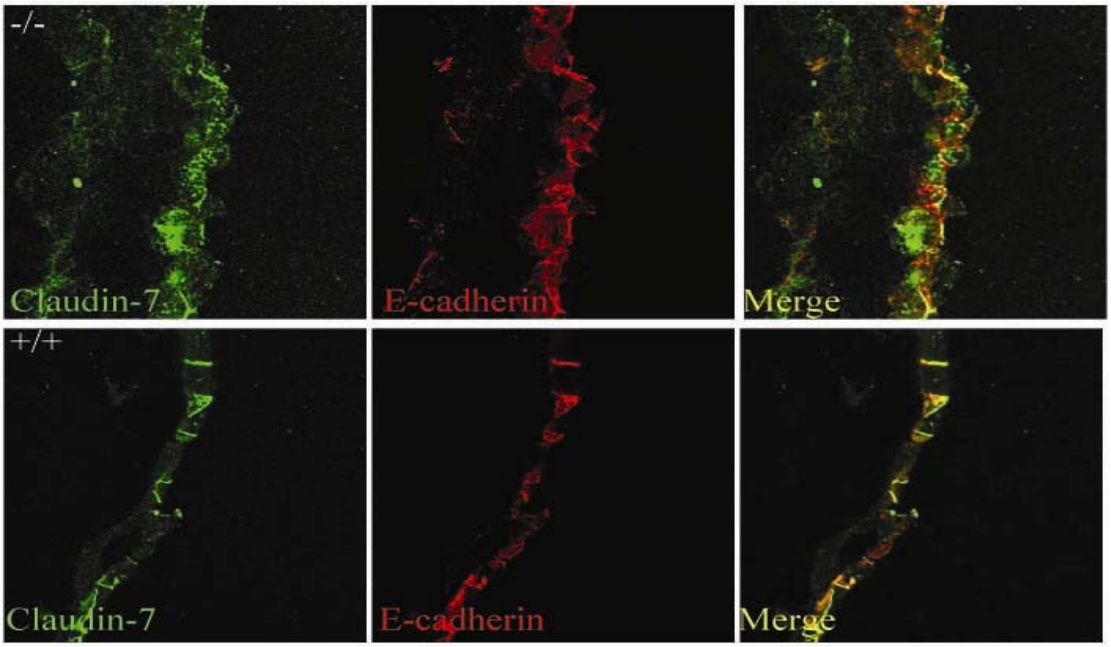

Figure 40 Distribution of ZO proteins, TJ and AJ markers in ZO-1-/- EBs. *(A) ZO-1 is not expressed in ZO-1-/- EBs. (B) Distribution of ZO-2 is not altered. (C) ZO-3 is diffused to the cytoplasm in ZO-1-/- EBs. (D, E) Distribution of occludin and cingulin is not alterd. (F, G, H, I, J, K) Claduin-1, claudin-3, claudin-4, claudin-5, claudin-6 and claudin-7 are diffused to the cytoplasm in ZO-1-/- EBs.*

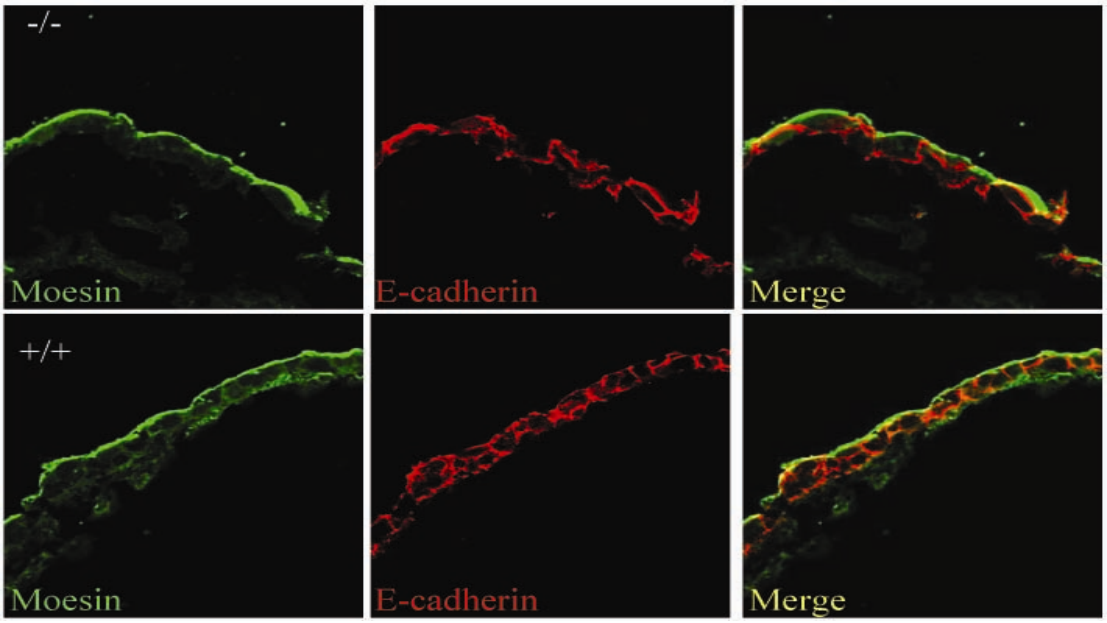

Figure 41 Apico-basolateral polarities are not affected in ZO-1-/- EBs. *Sections of day 15 ZO-1-/- and ZO-1+/+ EBs were labeled with antibodies to the apical marker moesin and the lateral marker E-cadherin. The distribution of both moesin and E-cadherin was not altered.*

8.3 The TJ structure is affected in ZO-1-/- EBs

To assess the structural integrity of TJs, we analyzed sections of 5-day and 10-day EBs by EM. As shown in Figure 42A, the apical junctional complex was readily detected as electron dense plaques in ZO-1+/+ EBs, where the intercellular space between adjacent epithelial cells was obliterated. However, in ZO-1-/- EBs, distinct TJ plaques were rarely detected. Quantification by counting the presence of well established plaques between adjacent cells revealed that they were present at ～100% of the cell-cell contact sites in ZO-1+/+ EBs, but only at ~13% of the contacts between cells in ZO-1-/- EBs (Figure 42B). These data indicate that ZO-1 deficiency affects the formation of well developed TJ plaques.

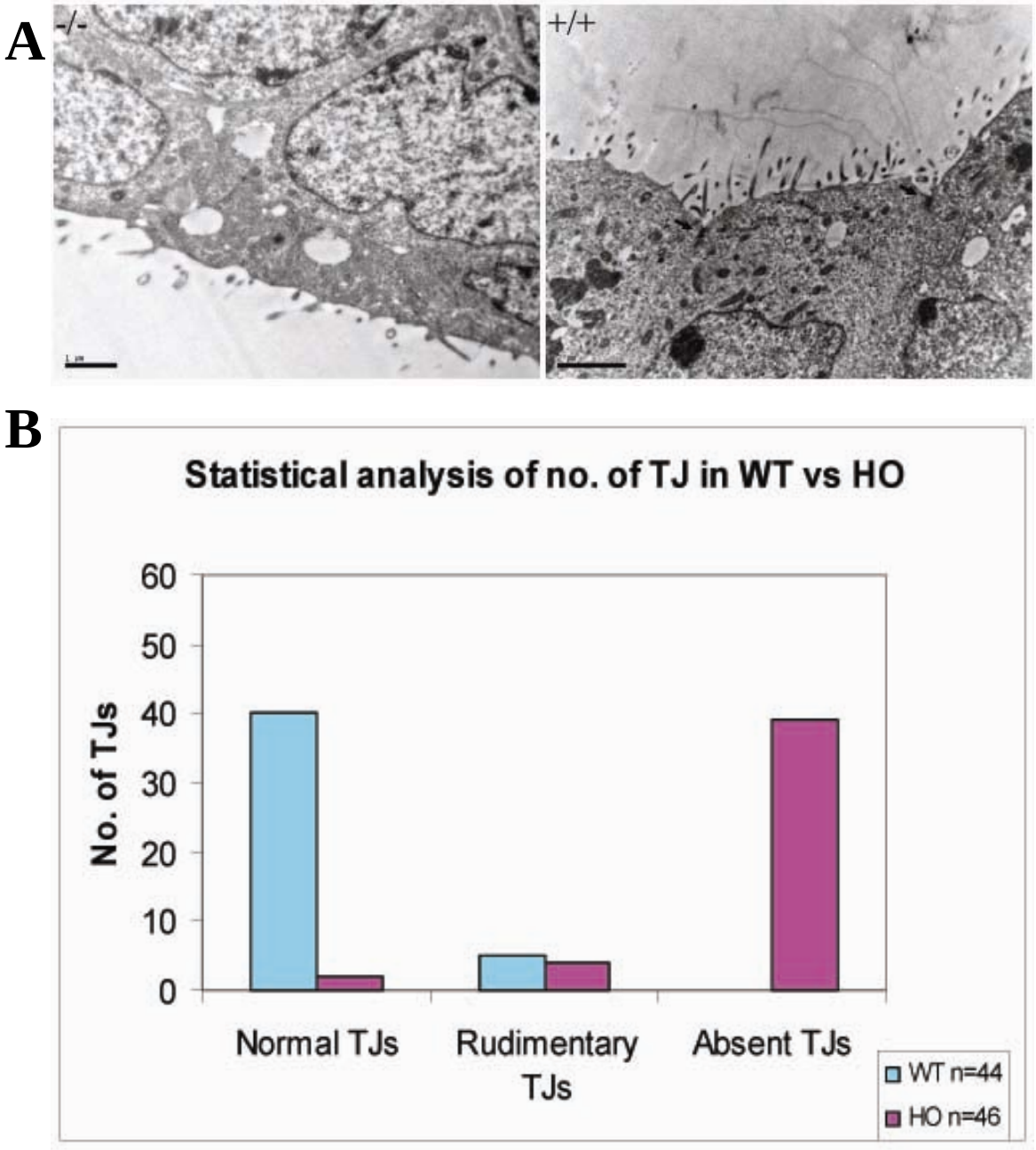

Figure 42 The architecture of the apical junctional complex is altered in cells of ZO-1 -/- EBs. *(A) Day 10 EBs were sectioned and analyzed by TEM to visualize the apical junctional complex. Typical electron dense plaques were readily detected at the apical pole of the lateral membrane of adjacent cells of ZO-1+/+ EBs, but were rarely observed in cells of ZO-1-/- EBs. (B) Statistic analysis of number of tight junctions in ZO-1+/+ vs ZO-1-/- EBs.*

8.4 ZO-1 deficiency promotes mesoderm development

ZO-1 has been implicated in the regulation of cell proliferation and differentiation. To determine if the absence of ZO-1 had an effect on gene expression and to elucidate possible signaling pathways affected, we embarked on microarray analysis of day 10 ZO-1+/+ and ZO-1-/- EBs. Interestingly, and as shown in Table 12, genes related to mesoderm development were strongly upregulated. The mRNA level of the mesoderm marker T-gene/Brachyury, for example, was more than 20-fold higher in ZO-1-/- as compared to ZO-1+/+ EBs. Furthermore, the genes involved in Wnt signaling were also upregulated. In order to confirm the microarray results, RT-PCR was used to check the expression of T-gene. As shown in Figure 43A, T-gene mRNA expression was much higher in ZO-1-/- EBs. Western blots indicated that T-gene was also upregulated at the protein level (Figure 43C). These data suggest that ZO-1 might be involved in the regulation of gene expression during the early stages of embryo development and ZO-1 deficiency facilitates mesoderm development.

8.5 ZO-1deficiency promotes mesoderm development via a β–catenin/Wnt dependent signaling pathway.

ZO-1 indirectly interacts with β–catenin (Itoh et al., 1997), which is a central player in the Wnt signaling pathway. Furthermore, Wnt proteins regulate the expression of T-gene. To assess whether the upregulation of T-gene in the ZO-1-/- EBs involves the β–catenin/Wnt signaling pathway, β–catenin expression levels were analyzed by Western blot. This analysis revealed that total β–catenin protein levels were the same in ZO-1+/+,

ZO-1-/+ and ZO-1-/- EBs. β –catenin can be present in an inactive form and a phosphorylated active form (Sinha et al., 2004). Since only the ser33/ser37 phosphorylatyed form can activate Wnt signaling (Sinha et al., 2004), we used a phospho-specifc antibody against with phospho-amino acid ser33/ser37 to monitor the activation state of β –catenin in the different EBs. Interestingly, phosphorylated β –catenin levels were significantly upregulated in ZO-1-/- as compared to ZO-1+/+ EBs (Figure 43C). As a positive control, 293T cells were treated with LiCl, which is known to activate β –catenin (Figure 43B).

Thus, the absence of ZO-1 results in increased levels of active β –catenin, likely resulting in the activation of the Wnt signaling pathway and the upregulation of the expression of genes involved in mesoderm development, including T-gene.

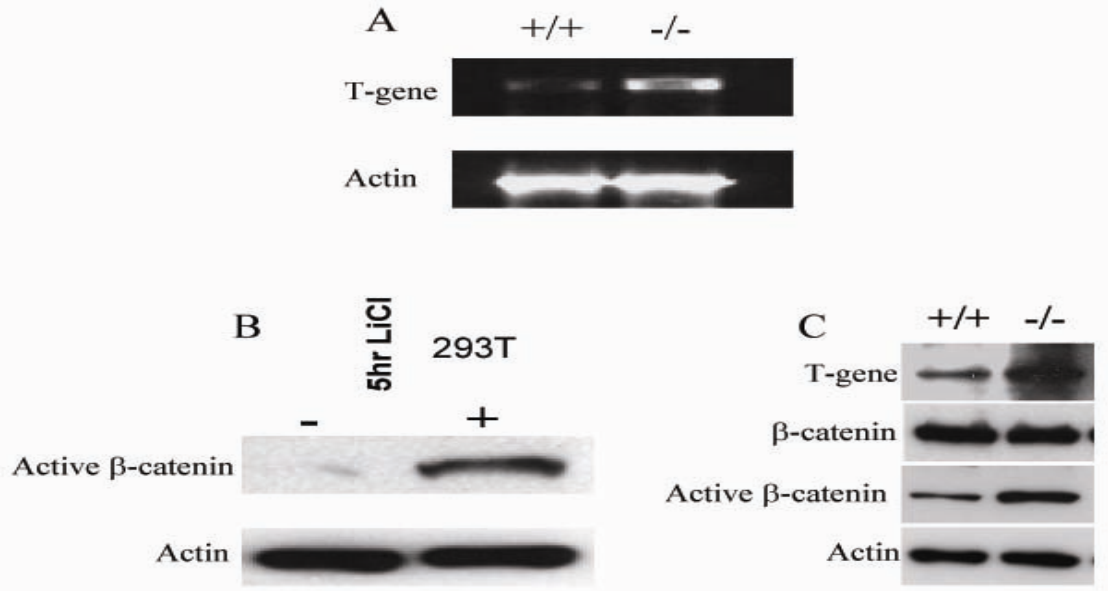

Figure 43 ZO-1 deficiency results in the upregulation of T-gene expression. *(A), RT-PCR showed upregulation of T-gene mRNA in day 10 ZO-1-/- EBs. (B), An antibody specific for the activated form of β-catenin antibody detcts increased levels of activated β –*catenin *in 293T cells treated with LiCl. (C), T-gene and active β-catenin are upregulated in day 10 ZO-1-/- EBs, but the total β-catenin protein levels remain unchanged.*

A

Mesoderm development	Fold change
Eomesdermin homolog (Eomes)	Up 8.6
PKKARIA	Up 1.5
Mesoderm specific transcript (Mest)	Up 3.5
T-gene/ Brachyury	Up 21.1
LHX2	Up 9.8
Neural adhesion molecule 1 (NCAM 1)	Up 16.0
PitX2	Up 2.3
Goosecoid	Up 16.0
Cytochrome P450, family 26, subfamily A polypeptide 1 (CYP26A1)	Up 4.3
Foxhead box H1	Up 1.6
Kruppel like factor 4	Up 3.7
Iroquosis homeobox 3 (IRX3)	Up 1.6
neuropilin 1 (NRP)	Up 9.2

B

Wnt signaling	Fold Change
secreted frizzled-related protein 1 (SFRP-1)	Up 4.0
serum/ glucoticoid regulated kinase	Up 1.6
Pitx2	Up 2.3
N-cadherin/cadherin 2, type2	Up 4.0
inhibitor of DNA binding 1, ID1	Up 2.6
inhibitor of DNA binding 2, ID2	Up 1.5
inhibitor of DNA binding 3, ID3	Up 1.9
Neural adhesion molecule (NCAM1)	**Up 16.0**
Goosecoid (GSC)	**Up 16.0**
T-gene/ Brachyury	**Up 21.1**
LIM homeobox 1 (LHX1)	**Up 6.1**
Transcription factor 12 (TCF12)	Up 1.5
Cerberus 1 (Cer1)	Up 4.6
SOX-4	Up 1.6
cytochrome P450, family 26, subfamily A, polypeptide 1(CYP26A1)	Up 4.3
heterogeneous nuclear ribonucleoprotein U-like 1	Up 2.0
heterogeneous nuclear ribonucleoprotein A2/B1	Up 1.5
follistatin	Up 4.9
BAMBI	Up 2.0
Dikkopff (Dff1)	Up 4.6
Four and half LIM domains (FHL1)	Up 1.5
Patched homolog (PTCH)	Up 1.5
Protein tyrosine phosphatase recelptor G (PTPRG)	Up 3.2
Reticulocalbin 1 (RCN)	Up 1.7
Smoothened homolog	Up 1.7
SOX11	Up 2.3
SOX17	Up 2.8
Thyrotrophin releasing hormone	Up 3.2
frizzled-related protein	Up 2.5
protein phosphatase 2 regulatory subunit A (PR 65), beta isoform	Up 1.9
adenomatosis polyposis coli down-regulated 1 (APCCD1)	Up 7.0
Frizzled homolog 8 (FRZ 8)	Up 2.2
Necdin	Up 2.1
kelch domain containing 2 (KLHDC2)	Up 1.9
transducer of ErBB2 (TOB2)	Up 7.0
Foxhead box A2 (FOXA2)	Up 4.6
Zic family member 1 (ZIC1)	Up 14.9
microtubule-associated protein, RP/EB family, member 2	Up 3.0

Table 12 Microarray analysis. *Microarray analysis to detect the expression levels of genes involved in mesoderm development (A) and Wnt signaling (B) in day 10 EBs.*

8.6 EBs derived from ZO-1-/- ES cells have a larger volume compared to ZO-1+/+ EBs.

We observed that on average the volume of ZO-1-/- EBs was larger than that of ZO-1+/+ EBs (Figure 44A). In additions, ZO-1-/- EBs displayed a smoother surface and appeared darker than ZO-1+/+ EBs. To assess whether the ZO-1-/- EBs contained more cells as compared to ZO-1+/+ controls, EBs were cultured in hanging drops. On day 5, 50 EBs each were randomly picked, trypsinized and the number of cells counted. As shown in Figure 44B, the 50 ZO-1-/- EBs contained on average ~1.5 fold more cells than an equal number of ZO-1+/+ EBs.

To determine if the higher number of cells in ZO-1-/- EBs was the result of an increased cell proliferation rate, BrdU incorporation was monitored in day 5 EBs. Indeed, as shown in Figure 44C, BrdU incorporation was enhanced in ZO-1-/- as compared to ZO-1+/+ EBs, suggesting a higher cell proliferation rate in the absence of ZO-1. The precise role of ZO-1 in the regulation of cell proliferation in EBs will be the subject of future studies.

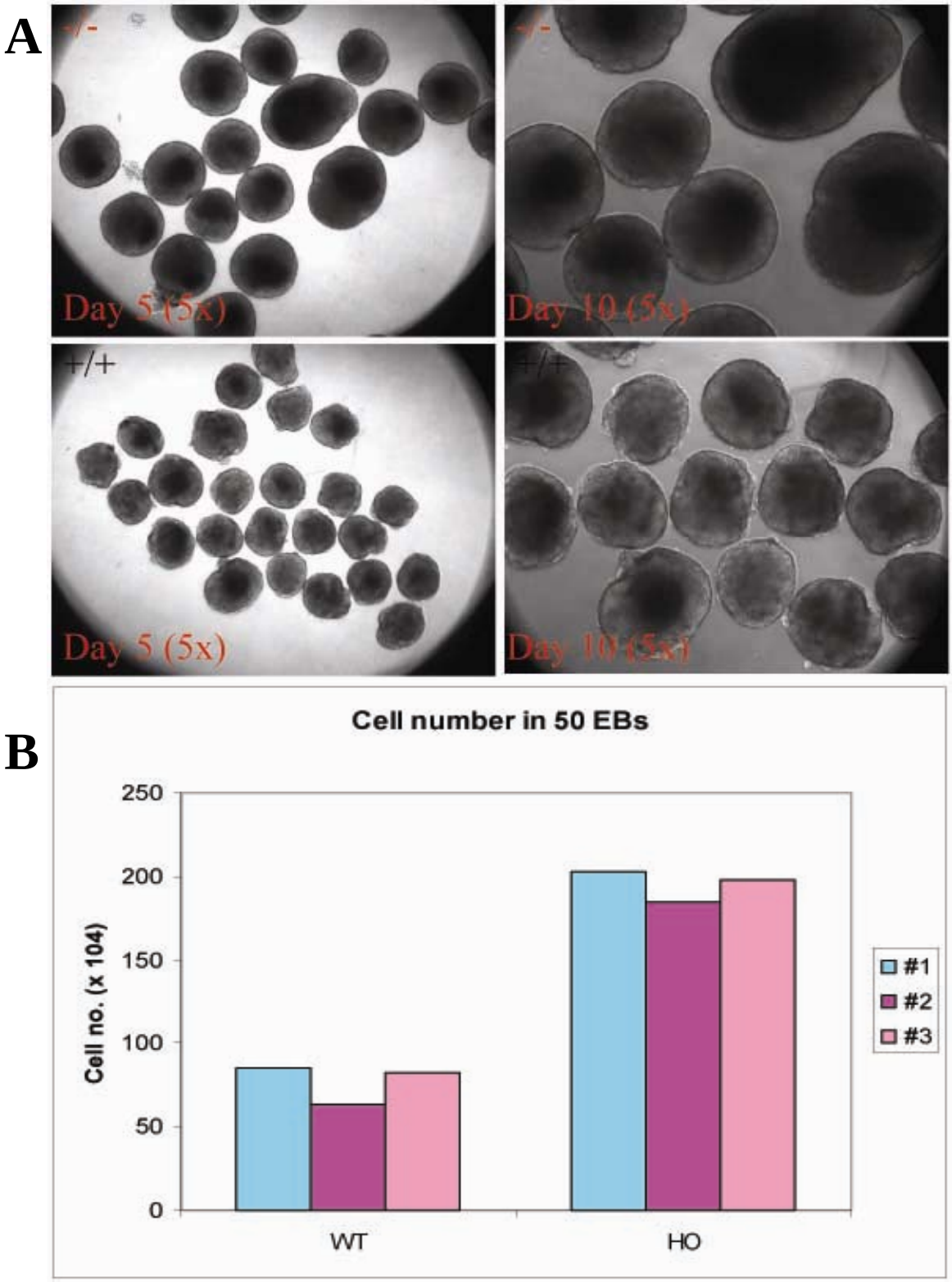

Figure 44 Proliferation of ZO-1-/- EBs*. (A) ZO-1-/- EBs are larger than ZO-1+/+ EBs. (B) Cell number in EBs. ZO-1-/- EBs contain more cells than ZO-1+/+ EBs.*

C

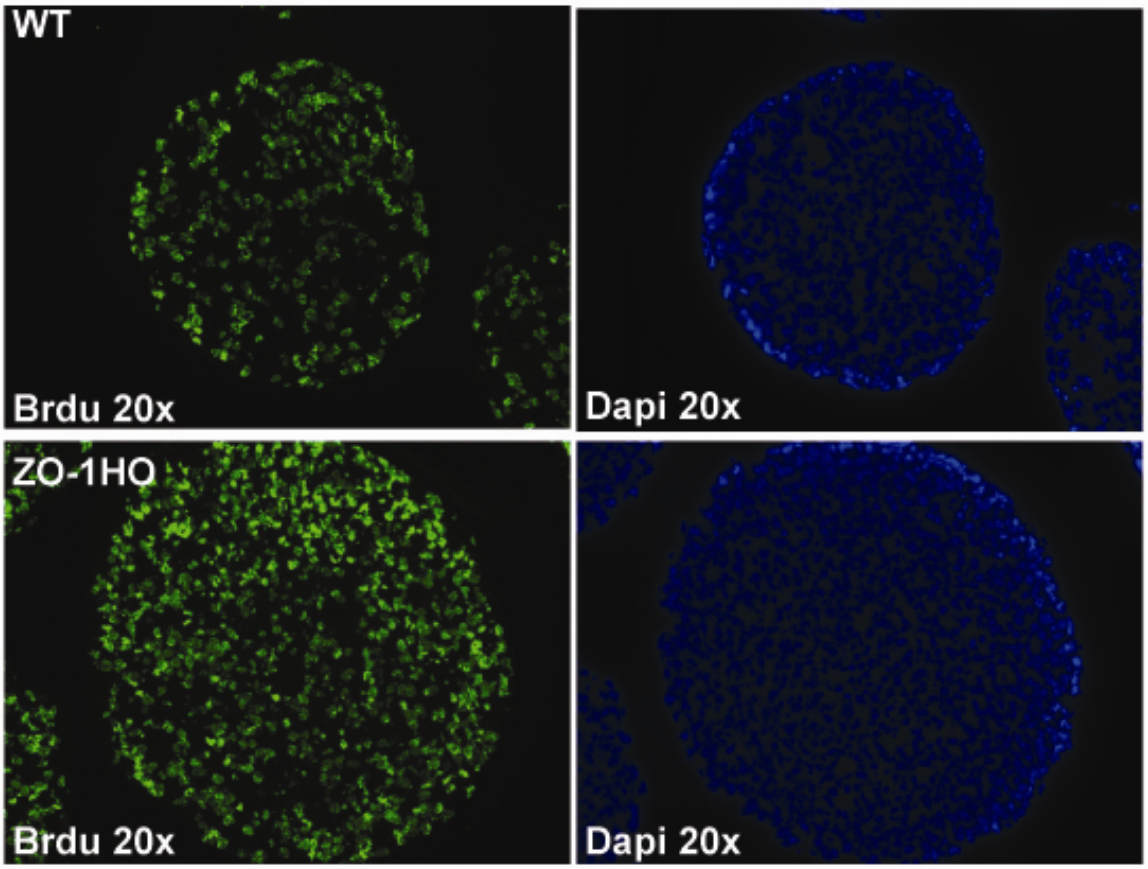

(C) BrdU incorporation. Enhanced BrdU incorporation in ZO-1-/- as compared to ZO-1+/+ EBs.

8.7 Discussion

Analysis of selected proteins showed that the expression levels of some were altered in ZO-1-/- EBs. For example, ZO-3 was downregulated. In addition, the membrane localization of ZO-3 and several claudins was disturbed. Furthermore, EM analysis indicated that the TJs were either not well developed or absent in ZO-1-/- EBs. Our findings differ from those of a recent report, in which ZO-1 was demonstrated to be dispensable for TJ function in Eph 4 epithelial cells (Umeda et al. 2004). In ZO-1-/- Eph4 cells, TJ plaques were indistinguishable from those of WT Eph4 cells and only the recruitment of a few proteins to TJs was delayed. Furthermore, the localization of TJ proteins was not changed in ZO-1-/- Eph4 cells, with the sole exception of cingulin, which was diffused in the cytoplasma. In contrast, cingulin still localizes to the plasma membrane in ZO-1-/- EBs. The differences observed between ZO-1-/- EBs and ZO-1-/- Eph4 cells might be due to the distinct nature of these two cell lines. First, EBs are derived from ES cells, while Eph4 cells are a cancer cell line. Normal and cancer cells may display different properties, in particular with respect to cell-cell adhesion. Second, different protein sets are expressed in EBs and EpH4 cells. For example, ZO-3 is expressed in EBs but absent from Eph4 cells (Umeda et al., 2006). Different expression patters are also found for claudins (González-Mariscal et al., 2003), among other proteins. Third, Eph4 cells have at least four alleles for ZO-2 (Umeda et al. 2006), while EBs are diploid. Finally, EB formation recapitulates early stages of embryonic development with its dynamic regulation of gene expression, whereas Eph4 cells represent fully differentiated epithelial cells. Thus, at least during the development of EBs from ES cells, ZO-1 is critical for the integrity of epithelial TJs.

After 5 days in culture ZO-1-/- EBs were significantly larger than WT EBs. BrdU incorporation experiments revealed that cell proliferation was enhanced as compared to control EBs. On the other hand, apoptotic activity in ZO-1-/- EBs remained similar to that in WT EBs. These findings suggest that ZO-1 plays a crucial role in cell cycle regulation. Previous reports revealed that ZONAB regulates cell proliferation by controlling PCNA and cyclin D1 expression and that ZO-1 can influence the activity of ZONAB by sequestering it to the plasma membrane (Balda et al. 2000). However, based on Western blot and immunoflurescence analysis, we found no evidence for altered ZONAB expression levels or ZONAB localization in ZO-1-/- EBs (data not shown). Furthermore, microarray analysis showed that the expression of PCNA and cyclin D1 is not affected in ZO-1-/- EBs. Based on preliminary RT-PCR analysis, cyclin D2 appears to be strongly upregulated in ZO-1-/- EBs (data not shown). These data indicate that ZO-1 might regulate cell proliferation in EBs independent of ZONAB.

In ZO-1-/- EBs, expression of the mesoderm maker T-gene/brachyury was upregulated at both the mRNA and protein levels. T-gene is regulated by the Wnt/β-catenin pathway (Yamaguchi et al. 1999; Kemler et al. 2004; Chen et al. 2006). Although there is not evidence for a direct interaction of ZO-1 with β-catenin, ZO-1 can interact with α-catenin to form a complex with E-cadherin and β-catenin (Itoh et al.1997). More interestingly, however, mislocalization of intact ZO-1 to the cytosol in breast cancer cell lines lacking occludin (Polette et al., 2005) or overexpression of ZO-1 mutants that do not associate with the plasma membrane (Reichert et al., 2000) has been shown to activate β-catenin/Tcf/Lef transcriptional activity. Thus, ZO-1 might be able to regulate β-catenin indirectly. Although the protein expression level and localization of β-catenin

was not affected in ZO-1-/- EBs, more of the active, Ser33/Ser37 phosphorylated form of β-catenin, was found. Therefore, ZO-1 deficiency may favor β-catenin phosphorylation, resulting in the activation of canonical Wnt signaling and upregulation of T-gene expression. In contrast to EBs, silencing of β-catenin via siRNA in breast cancer cells abrogated β-catenin signaling, suggesting differences between EBs and cancer cell lines which will be explored in future studies. These findings however confirm that ZO-1 is not only involved in TJ formation, but also play a crucial regulatory role in cell differentiation during development and in particular mesoderm differentiation.

Chapter 9 Generation and phenotypic analysis of ZO-2-/- embryonic stem cells

9.1 Generation of ZO-2-/- ES cells

To obtain ZO-2-/- ES cells, previously generated ZO-2-/+ ES cells (see Chapter 4) were selected with 20 mg/ml G418 and screened by PCR (Figure 45A). The ZO-2+/+ ES cell clones displayed only the WT band of 254 bps; the ZO-2-/+ ES cell clones had both WT and mutant bands, and the ZO-2-/- ES cell clones had only the mutant band of 368 bps. The ZO-2 deficiency was confirmed by Western blot (Figure 45B). All three ZO proteins were expressed in control ES cells. ZO-2 expression was reduced in ZO-2-/+ ES cells and absent in ZO-2-/- ES cells. The expression of ZO-1 and ZO-3 was not significantly different in ZO-2+/+, -/+ and -/- ES cells. ZO-2-/- ES cells were morphologically undistinguishable from ZO-2+/+ ES cells (Figure 45C).

A

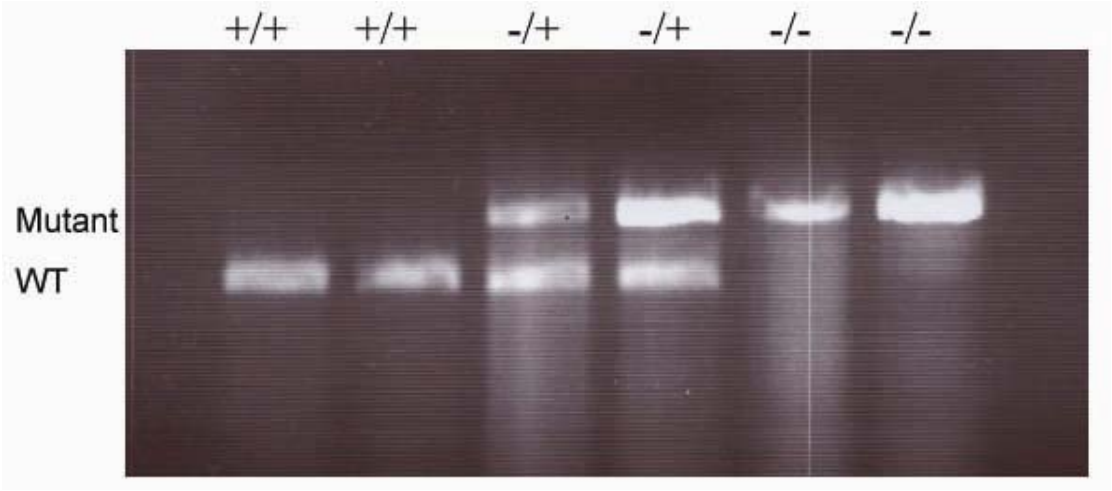

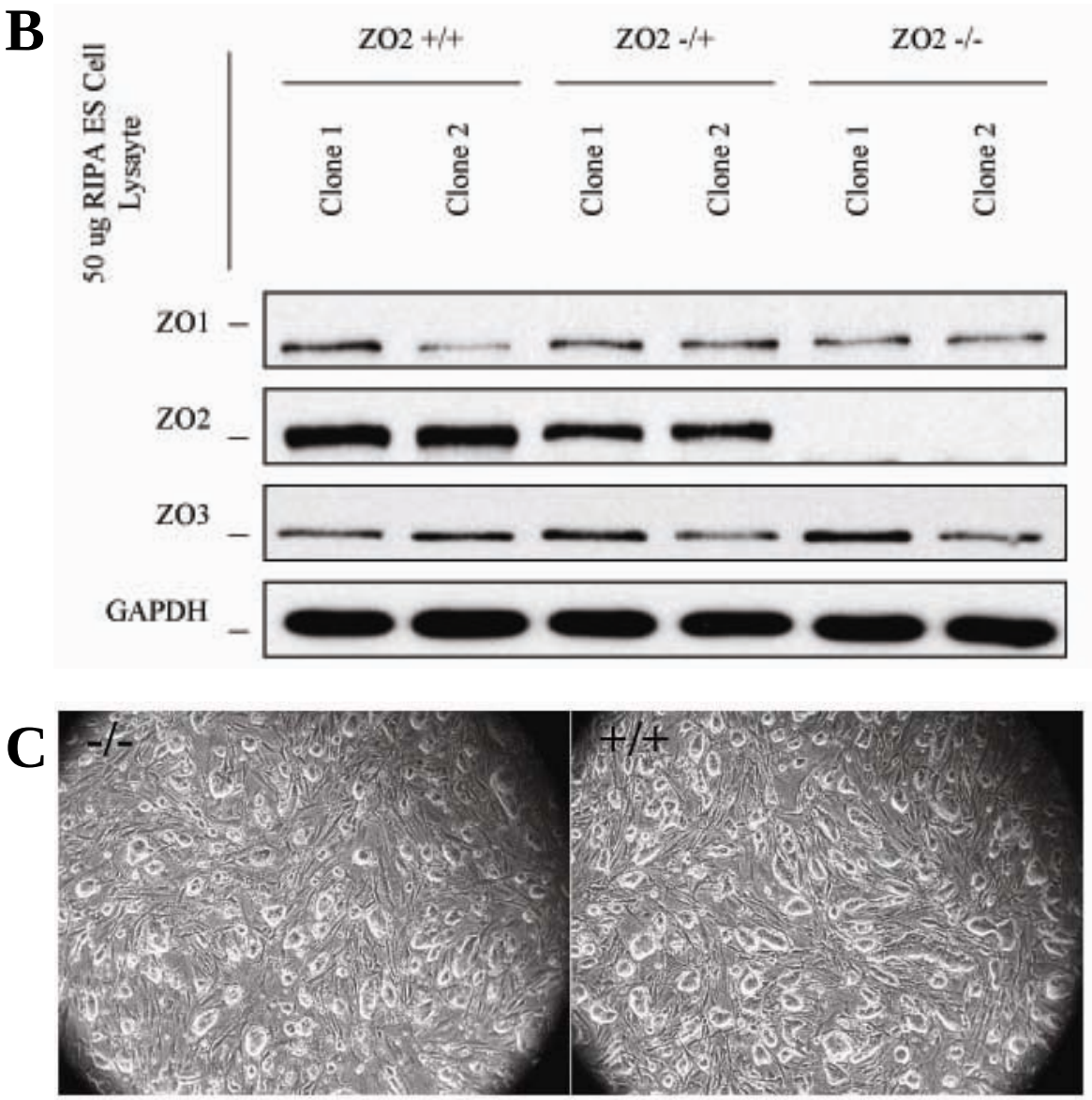

Figure 45 Generation of ZO-1 -/- ES cell lines. *(A) Six different ES cell clones were genotyped. ZO-1+/+ clones only present the WT band(254 bps), ZO-1-/+ clones yield both the WT and mutant band(368 bps), and ZO-1-/- clones only have the mutant band.(B) Western blot was done on lysates from 6 ES cell lines to access the expression of ZO-1, ZO-2, and ZO-3. ZO-1 was not expressed in ZO-1-/- ES cell lines and downregulated in ZO-1 -/+ ES cell lines, while the expression of ZO-2 and ZO-3 was not altered in ZO-1 -/- and ZO-1 -/+ ES cell lines. (C) Morphology of ZO-1 -/- ES cells was similar to that of WT ES cells.*

9.2 Normal expression levels of TJ and AJ markers in ZO-2 -/- EBs

Given the strong expression of ZO-2 protein in the EBs (Figure 46, 47A), expression levels of selected TJ and AJ markers in ZO-2 -/- EBs were analyzed by Western blot. Protein was extracted from ES cells differentiated into EBs for either 5 or 10 days. All three ZO proteins were expressed in EBs (Figure 46). ZO-2 was absent in ZO-2-/- and downregulated in ZO-2-/+ EBs. The expression of ZO-1 and ZO-3 was not significantly changed on either day 5 or 10 in ZO-2+/+, -/+ or -/- EBs. Also the expression of other junction proteins such as occludin and cingulin was not changed in ZO-2 -/- EBs (Figure 46). These data suggest that ZO-2 deficiency does not affect the expression levels of the TJ and AJ markers analyzed.

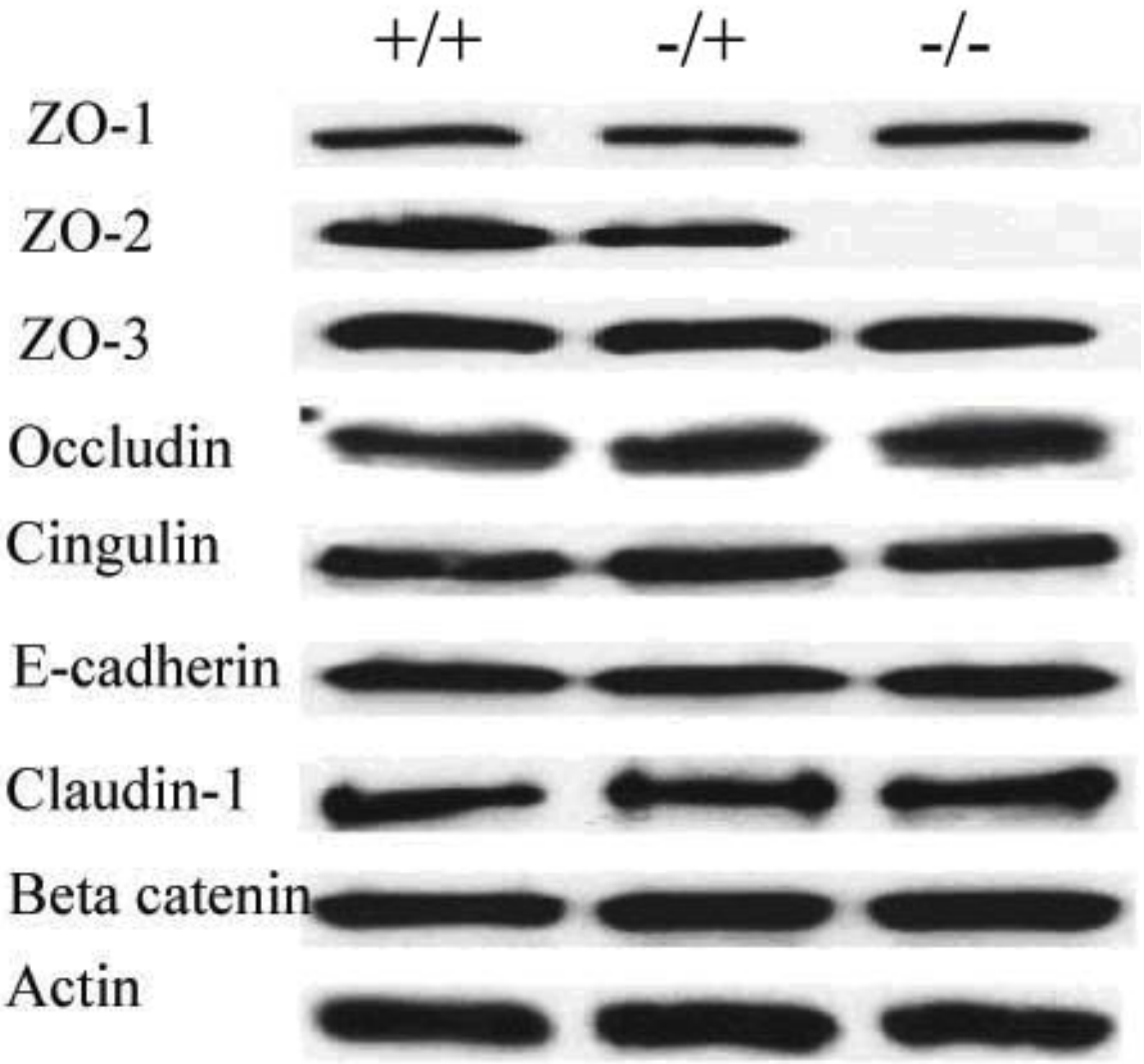

Figure 46 Protein expressions in ZO-2-/- EBs. *Western blot analysis was done on lysates of day 10 EBs to access the expression of ZO proteins and TJ and AJ markers. ZO-2 was not expressed in ZO-2 -/- EBs and downregulated in ZO-2 -/+ EBs. The expression of ZO-1, ZO-3 and the other TJ and AJ markers indicated was not altered in either ZO-2 -/- or ZO-2 -/+ EBs. The expression of occludin, cingulin, E-cadherin, claudin-1 and β-catenin was also not altered in ZO-2-/- EBs.*

9.3 Normal localization of selected TJ and AJ markers in epithelia of ZO-2-/- EBs

Given the role of ZO proteins as scaffolds that tether TJ proteins to the cytoskeleton, we analyzed by immunostaining if the subcellular distribution of selected junction markers was affected. As shown in Figure 47A, ZO-2 was strongly expressed in the epithelia of ZO-2+/+ EBs and particularly enriched at sites of cell-cell contact. As expected, no specific ZO-2 staining was found in ZO-2-/- EBs. ZO-1, ZO-3 and the other TJ and AJ markers analyzed, including occludin and E-cadherin, were also expressed in the epithelia of EBs (Figure 47B, C, D, F, and G). None of these proteins was mislocalized in ZO-2 -/- EBs. Furthermore, the prominent apical localization of moesin was maintained in ZO-2-/- EBs (Figure 48). This, together with the lateral localization of E-cadherin, indicated that the ability of TJs to maintain the asymmetric distribution of membrane proteins between the apical and basolateral domains remained intact.

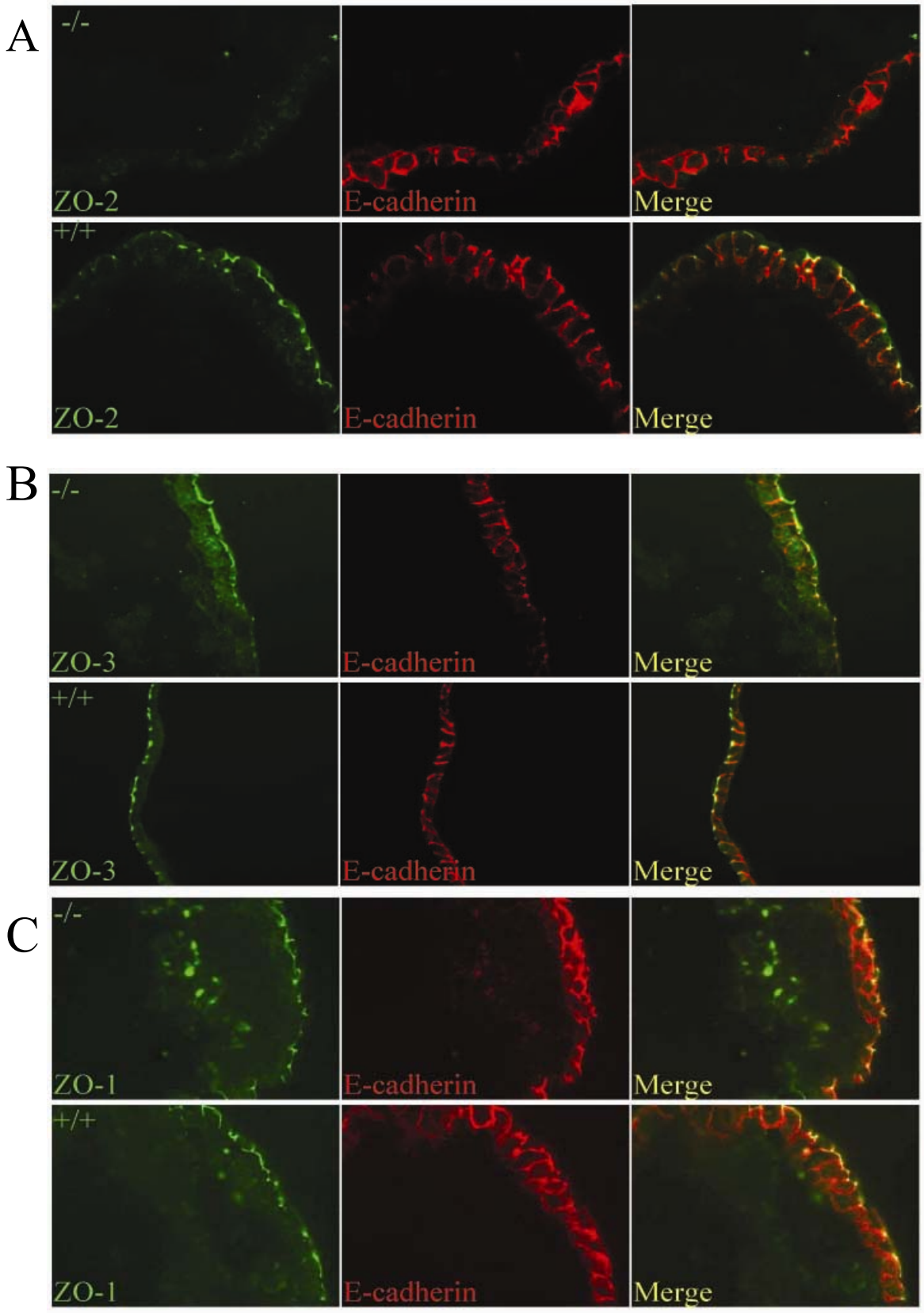
A
-/-
ZO-2
E-cadherin
Merge
+/+
ZO-2
E-cadherin
Merge
B
-/-
ZO-3
E-cadherin
Merge
+/+
ZO-3
E-cadherin
Merge
C
-/-
ZO-1
E-cadherin
Merge
+/+
ZO-1
E-cadherin
Merge

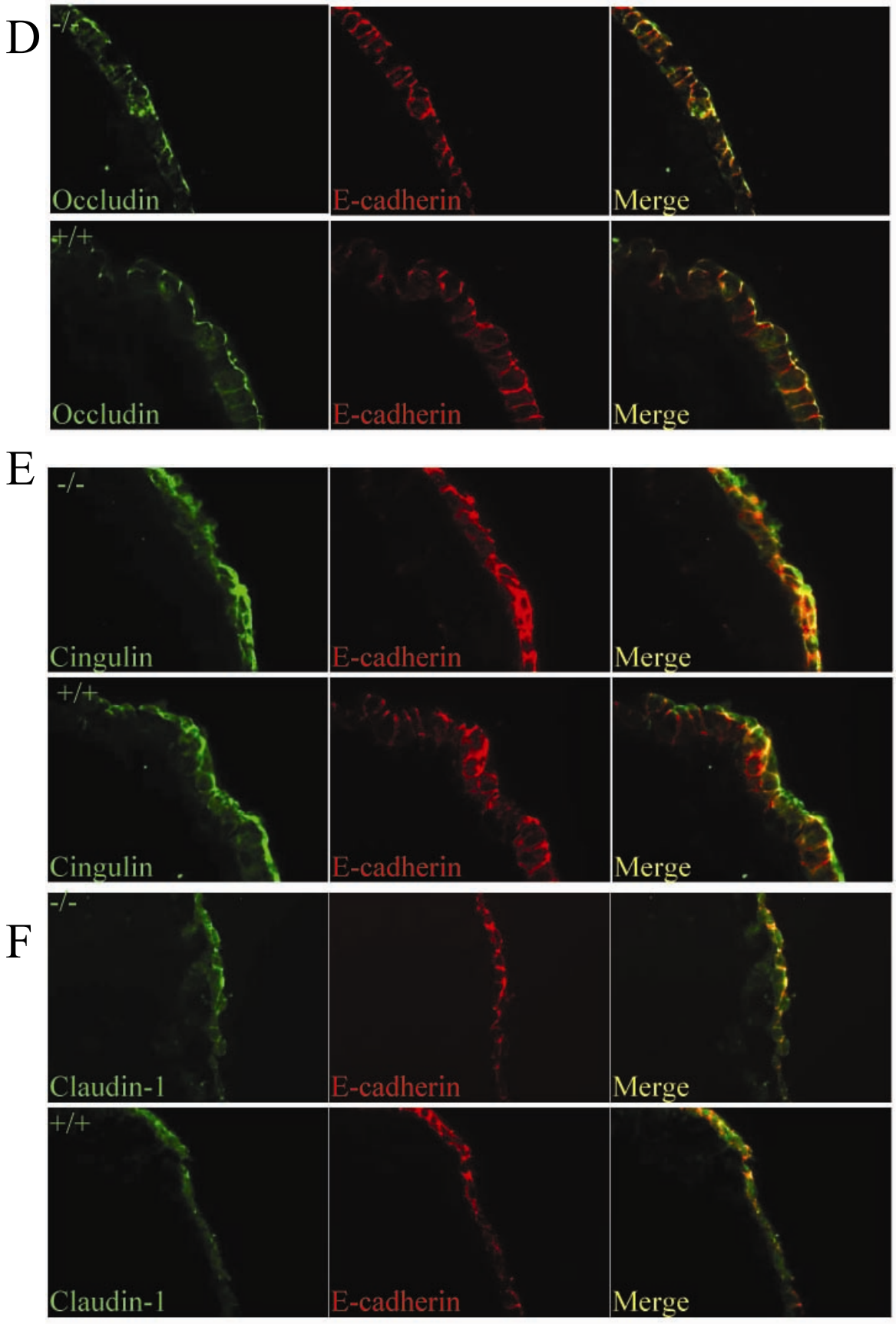
D
-/-
Occludin
E-cadherin
Merge
+/+
Occludin
E-cadherin
Merge
E
-/-
Cingulin
E-cadherin
Merge
+/+
Cingulin
E-cadherin
Merge
F
-/-
Claudin-1
E-cadherin
Merge
+/+
Claudin-1
E-cadherin
Merge

G

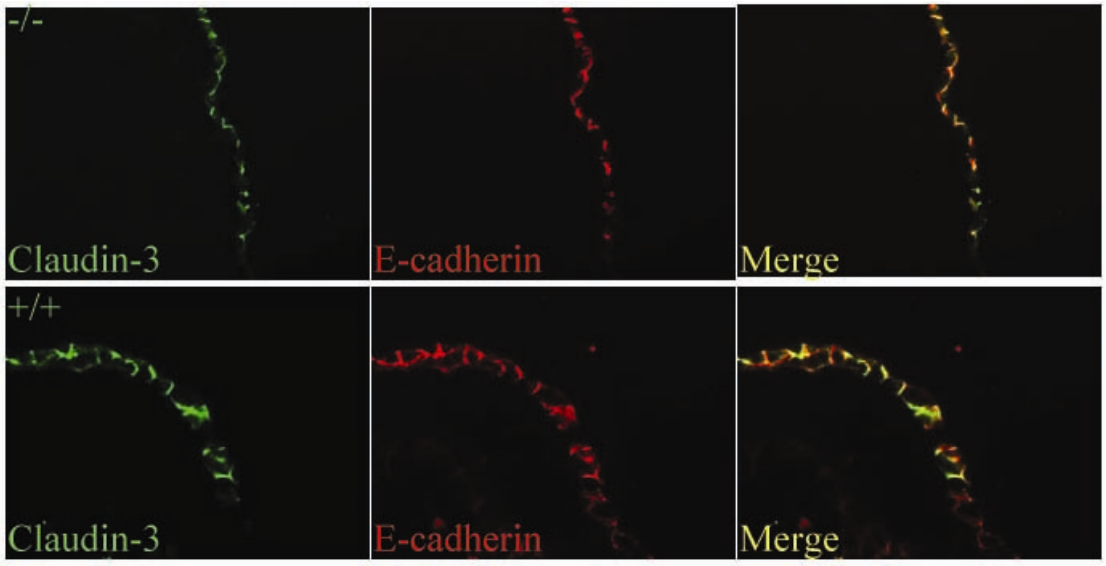

Figure 47 Distribution of ZO proteins and selected TJ and AJ markers in ZO-2-/- EBs. *(A) ZO-2 is not expressed in ZO-2-/- EBs and the distribution of E-cadherin is not altered. (B, C, D, E, F, G) The distribution of ZO-1, ZO-3, occludin, cingulin, claudin-1 and claudin-3 is not affected in ZO-2-/-*

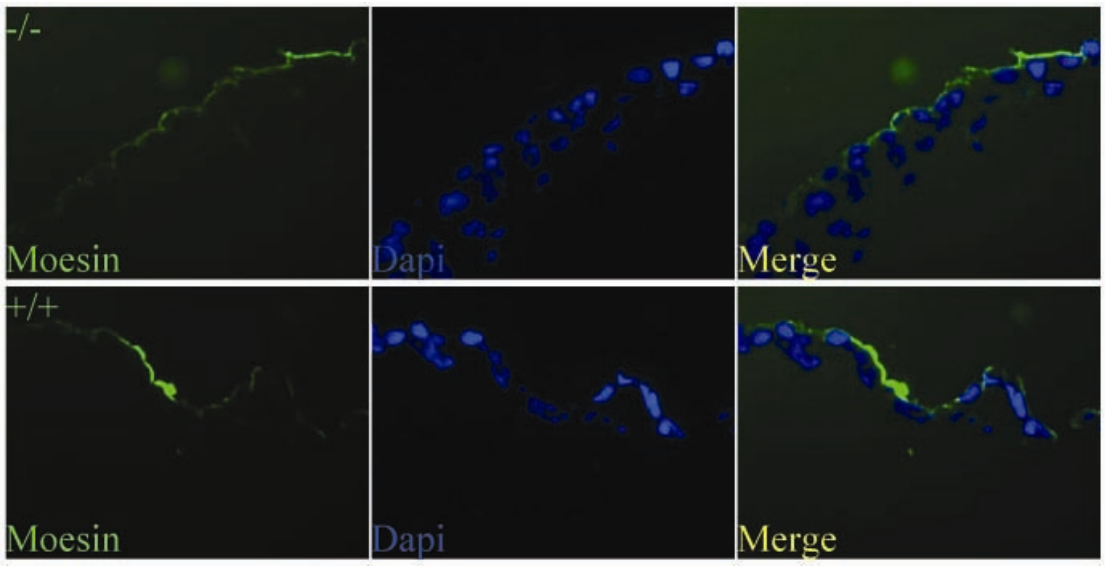

Figure 48 The apico-basolateral polarity is not affected in ZO-2-/- EBs. *Sections across day 15 ZO-2-/- and ZO-2+/+ EBs labeled with antibodies to the apical marker moesin.*

9.4 The TJ structure and function are unaffected in ZO-2-/- EBs

To assess the structural integrity of TJs, we analyzed day 5 and day 10 EBs sections by EM. As shown in Figure 49A, apical junctional complexes were readily detected as electron dense plaques, where the intercellular space between adjacent epithelial cells was obliterated. In both ZO-2+/+ and ZO-2 -/- EBs, the TJ plaques were well developed.

Permeability analysis was done to assess the TJ integrity by monitoring lanthanum nitrate leakage in ZO-2+/+ and ZO-2-/- EBs (Figure 49B). Lanthanum did not penetrate into ZO-2+/+ or ZO-2-/- EBs, indicating an intact paracellular barrier. As a control, WT EBs were pretreated with EDTA, which is known to disrupt TJs. In this case, lanthanum leaked into the EBs and could be readily detected in the intercellular space of adjoining cells. In summary, these data indicate that ZO-2 deficiency does no affect the structural or functional integrity of TJs in EBs cultured in vitro.

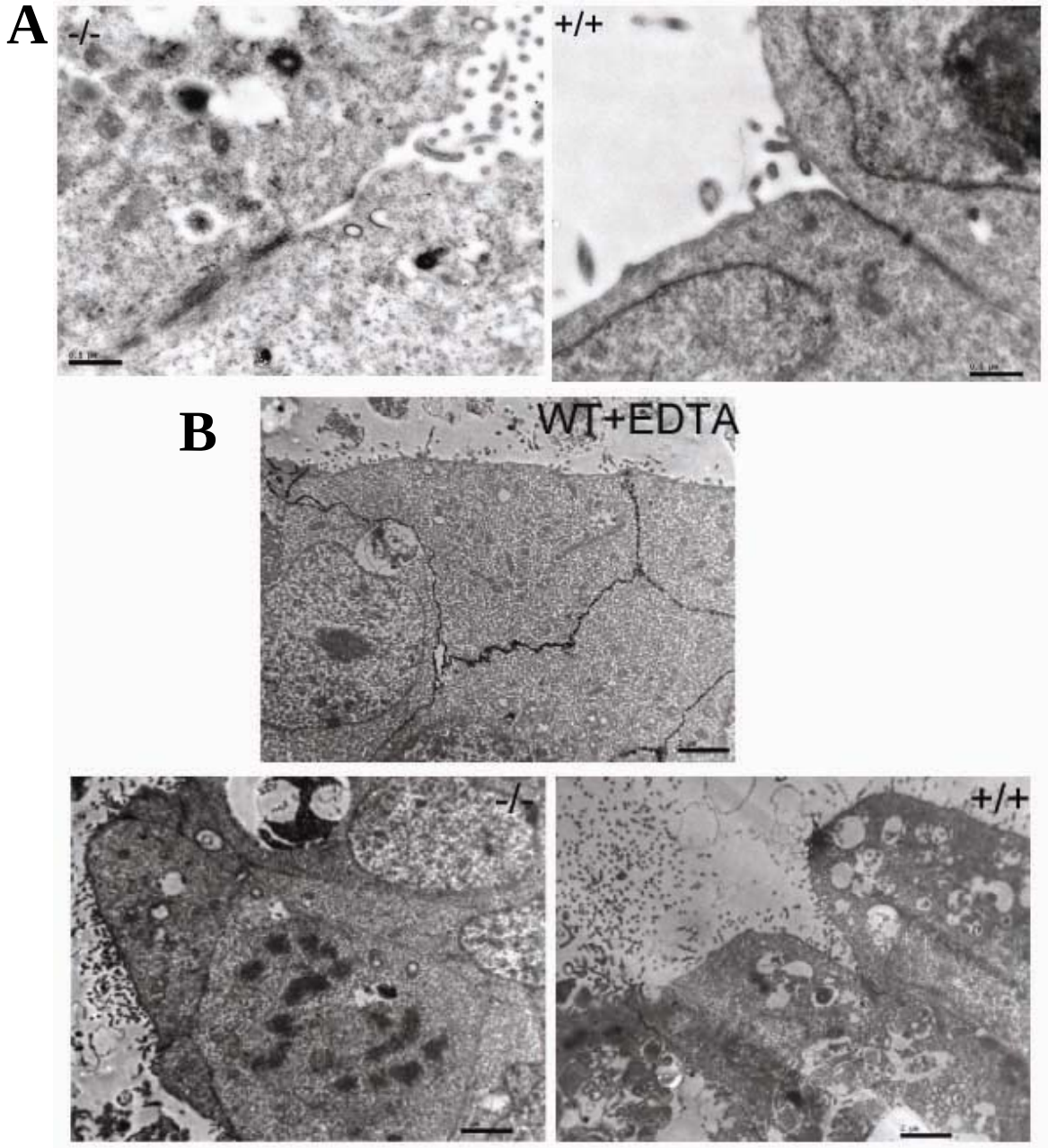

Figure 49 The architecture and permeability barrier of the apical junctional complex are not altered in cells of ZO-2 -/- EBs*. (A) Day 10 EBs were sectioned and analyzed by TEM to visualize the apical junctional complex. Typical electron dense plaques were readily detected at the apical pole of the lateral membrane of adjacent cells in both ZO-2-/- and ZO-2+/+ EBs (B) Day 10 EBs were postfixed in lanthanum nitrate and processed for transmission electron microscopy. Note the presence of lanthanum in intercellular spaces of EDTA treated ZO-2+/+ EBs, but not in ZO-2-/- and ZO-2+/+ EBs.*

9.5 ZO-2-/- EBs are of a larger size as compared to that of ZO-2+/+ EBs.

ZO-2 -/- EBs were found to be larger than ZO-2+/+ EBs (Figure 50A). To assess the cause for formation of larger EBs, cell numbers were monitored in cultures transferred from a 2 day hanging drop in differentiation media into suspension. From day 1 in suspension culture onwards, 10 EBs were randomly picked, trypsinized and the cell numbers determined by counting (Figure 50B). While the cell number in ZO-2+/+ and ZO-2 -/- EBs was initially similar, it then increased faster in ZO-2 -/- EBs during the following days in culture. By day 8, ZO-2-/- EBs were much larger than ZO-2+/+ EBs and the cell number was about twice that of controls. This analysis indicates that either increased cell proliferation or reduced cell death contribute to the formation of larger sized ZO-2-/- EBs. This will be analyzed in detail in a future study.

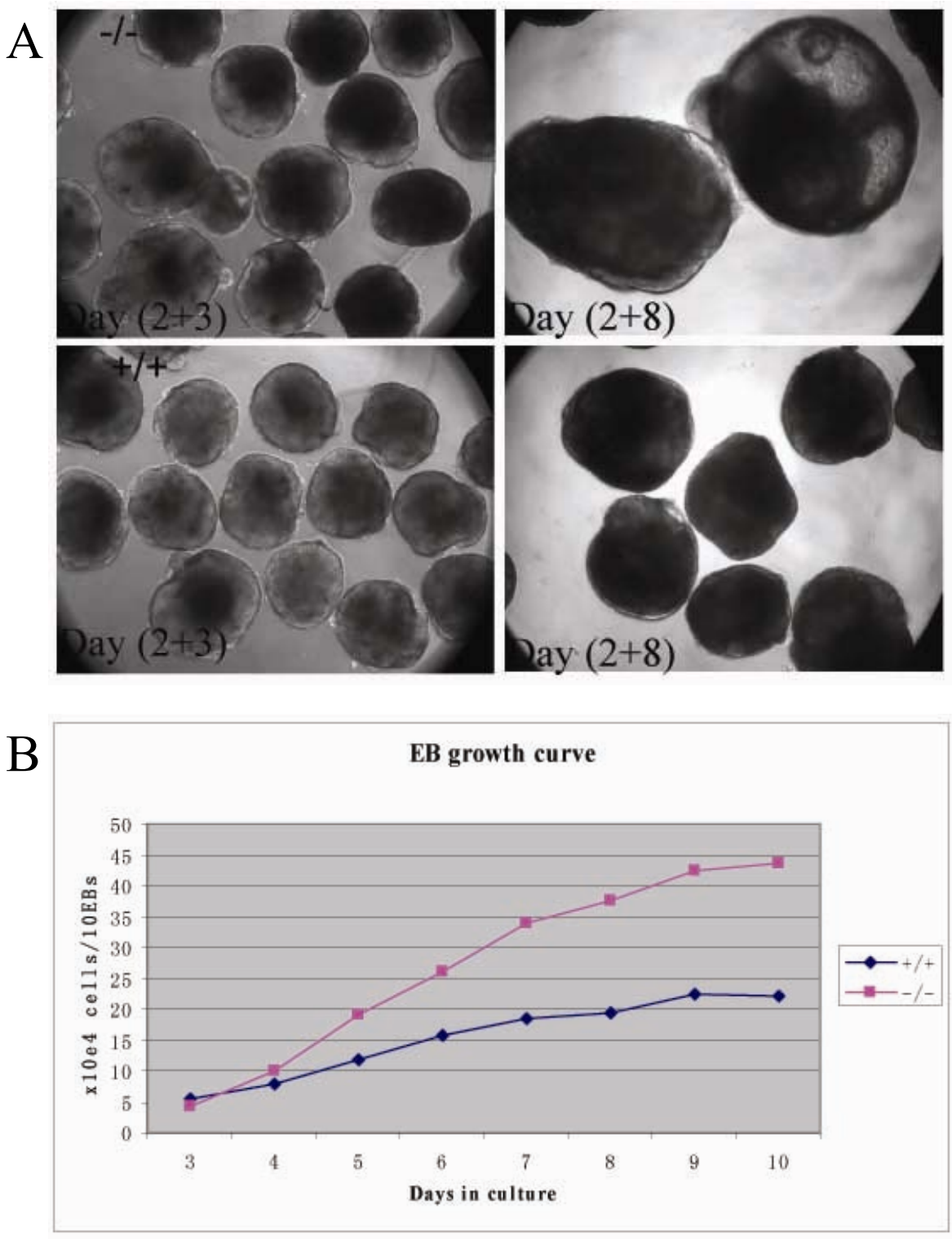

Figure 50 Volume of ZO-2-/- EBs. *(A) ZO-2-/- EBs are larger than ZO-2+/+ EBs. (B) Cell number of EBs. ZO-2-/- EBs contain more cells than ZO-2+/+ EBs.*

9.6 Discussion

ZO-2-/- ES cells were generated to analyze the role of ZO-2 in TJ function in EBs. The protein expression levels and membrane localization of several selected TJ and AJ markers were not affected. The electron dense plaque of the apical junctional complex observed by TEM was intact in ZO-2-/- EBs. Furthermore, apical-basolateral polarity and the barrier to lanthanum diffusion were not altered in ZO-2-/- EBs. Since ZO-1 and ZO-3 are highly expressed in the epithelia of EBs, they might compensate for the function of ZO-2. Consistently, visceral endoderm epithelial-like ZO-3-/- cells derived from F9 teratocarcinoma retain a normal molecular TJ architecture in the absence of ZO-2 expression (Adachi et al. 2006). Therefore, at least in EBs cultured in vitro, ZO-2 is dispensable for the establishment of functional TJs. Interestingly, however, both the structure and barrier function of TJs was compromised in ZO-2-/- E7.5 embryos (see Chapter 4). As discussed above, this may reflect the fact that embryos are exposed to "physiological stress", which could affect the robustness of TJs in the absence of ZO-2. Alternatively, the obaserved strucutal and functional defects of TJs observed in embryos may be a consequence of the observed deterioration of ZO-2-/- embryos around E6.5-7.5 as evidenced by a decreased proliferation and an enhanced apoptosis.

Cultured ZO-2-/- EBs were larger than WT EBs. Preliminary data indicates an upregulation of cyclin D1 expression in ZO-2-/- EBs (data not shown), consistent with a recent report that ZO-2 transcriptionally downregulates cyclin D1 (Huerta et al., 2007). ZO-2 has also been shown to associate with several transcription factors in epithelial cells, including Jun and Fos (Betanzos et al. 2004). In sparse cultures, Jun and Fos colocalize with ZO-2 both in the nucleus and at the plasma membrane of MDCK cells. Once cells

reach confluence, Jun and Fos proteins are exclusively present at the plasma membrane. Since Jun and Fos are regulators of cellular proliferation, transformation and death (Shaulian et al. 2002), the lack of ZO-2 might affect the regulation of Jun and Fos activity and thus deregulate cell growth in both EBs and teratomas.

Chapter 10 Generation and phenotypic analysis of ZO-1-/-ZO-2-/- ES cells

10.1 Generation of ZO-1-/-ZO-2-/- ES cells

To generate ES cells carring both inactivated ZO-1 and ZO-2 genes, the previously described ZO-1-/- ES cells (see Chapter 3) were transfected with cre-recombinase expression vector (Taniguchi et al. 1998) to delete the floxed Neo gene present in the mutant ZO-1 allele. Cells were selected in puromycin for the presence of the cre-plasmid and surviving clones screened for the deletion of the Neo gene based on their sensitivity to G418. G418 sensitive clones were expanded and those that had lost the cre-plasmid were identified by their sensitivity to puromycin. These ES cell clones were then used to inactivate the ZO-2 gene using the targeting vector described in Chapter 9. Inactivation of both the ZO-1 and ZO-2 genes was confirmed by Western blot analysis (Figure 51A), leading to the identification of six independent ZO-1-/-ZO-2-/- ES cell clones. These ZO-1-/-ZO-2-/- ES cells showed the same morphology as WT ES cells (Figure 51B).

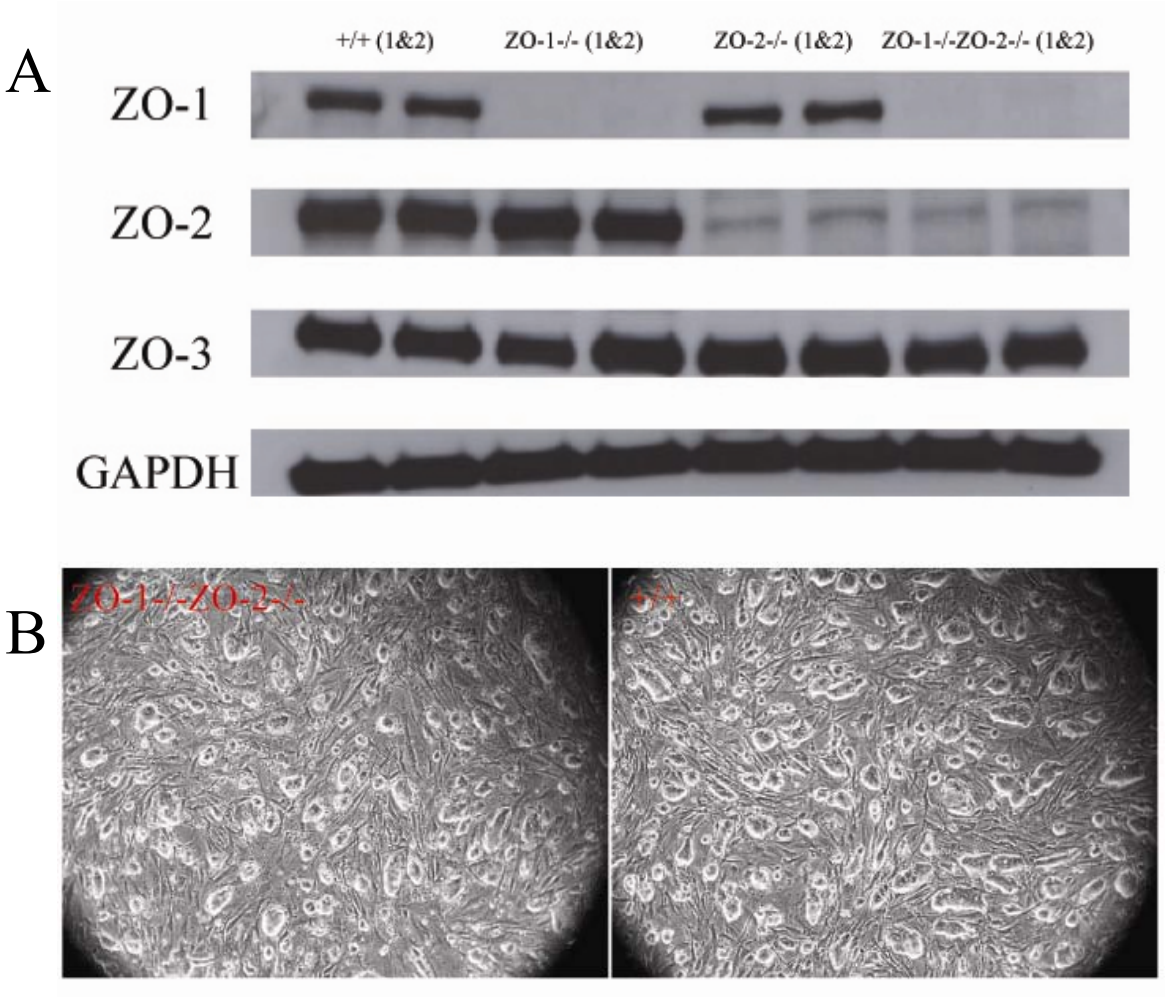

Figure 51 Characterization of ZO-1-/-ZO-2-/- ES cells. *(A) ZO-1 and ZO-2 are not expressed in ZO-1-/-ZO-2-/- ES cell. The expression of ZO-3 is not altered. (B) ZO-1-/-ZO-2-/- ES cells have similar morphology as WT ES cells.*

10.2 Protein expression in ZO-1-/-ZO-2-/- EBs

Given the strong expression of ZO-1 and ZO-2 proteins in wild-type EBs, expression levels of different TJ and AJ markers was analyzed by Western blot in ZO-1-/-ZO-2-/- EBs. As expected, neither ZO-1 nor ZO-2 was expressed in ZO-1-/-ZO-2-/- EBs (Figure 52). As observed for ZO-1-/- EBs, ZO-3 was also downregulated in ZO-1-/-ZO-2-/- EBs. The expression levels for occludin, cingulin, E-cadherin and claudin-3 did not differ significantly between WT, ZO-1-/-, ZO-2-/- and ZO-1-/-ZO-2-/- EBs (Figure 52).

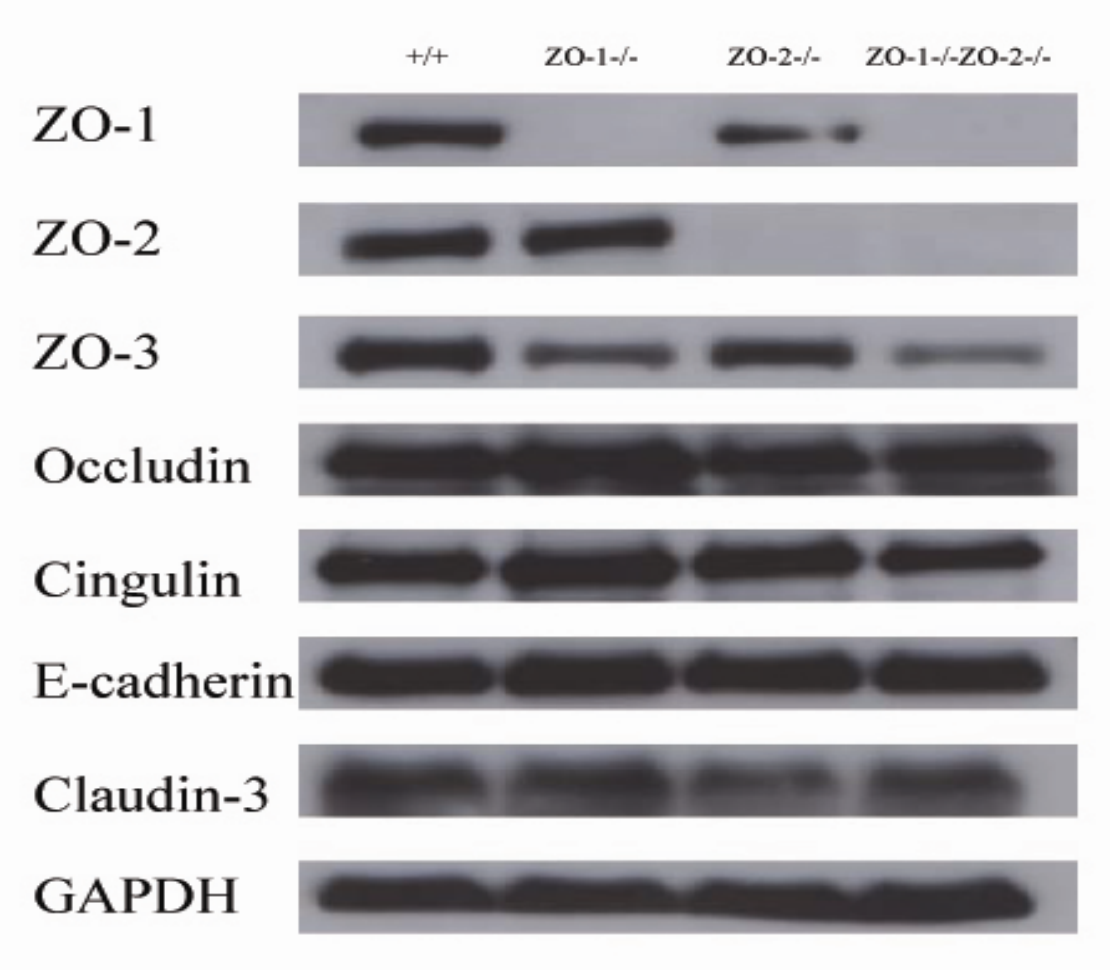

Figure 52 Protein expressions in ZO-1-/-ZO-2-/- EBs. *ZO-1 and ZO-2 are not expressed in ZO-1-/-ZO-2-/- EBs. The expression of ZO-3 is downregulated in ZO-1-/- and ZO-1-/-ZO-2-/- EBs. The expression of occludin, cingulin, E-cadherein and claudin-3 is not altered in ZO-1-/-ZO-2 EBs.*

10.3 The volume of ZO-1-/-ZO-2-/- EBs is larger as compared to that of WT EBs.

The volume of ZO-1-/-ZO-2-/- EBs was larger when compared to their WT counterparts (Figure 53A) and their surface had a smoother appearance. I therefore assessed cell growth in the EBs using hanging drop cultures. At different times (3-10 days) in hanging drop culture, 10 EBs were picked, trypsinized and the number of cells counted. As shown in Figure 53, the cell number in ZO-1-/-ZO-2-/- EBs increased faster over time as compared to WT EBs. On day 10, 10 pooled ZO-1-/-ZO-2-/- EBs contained almost twice the number of cell than a pool of 10 WT EBs.

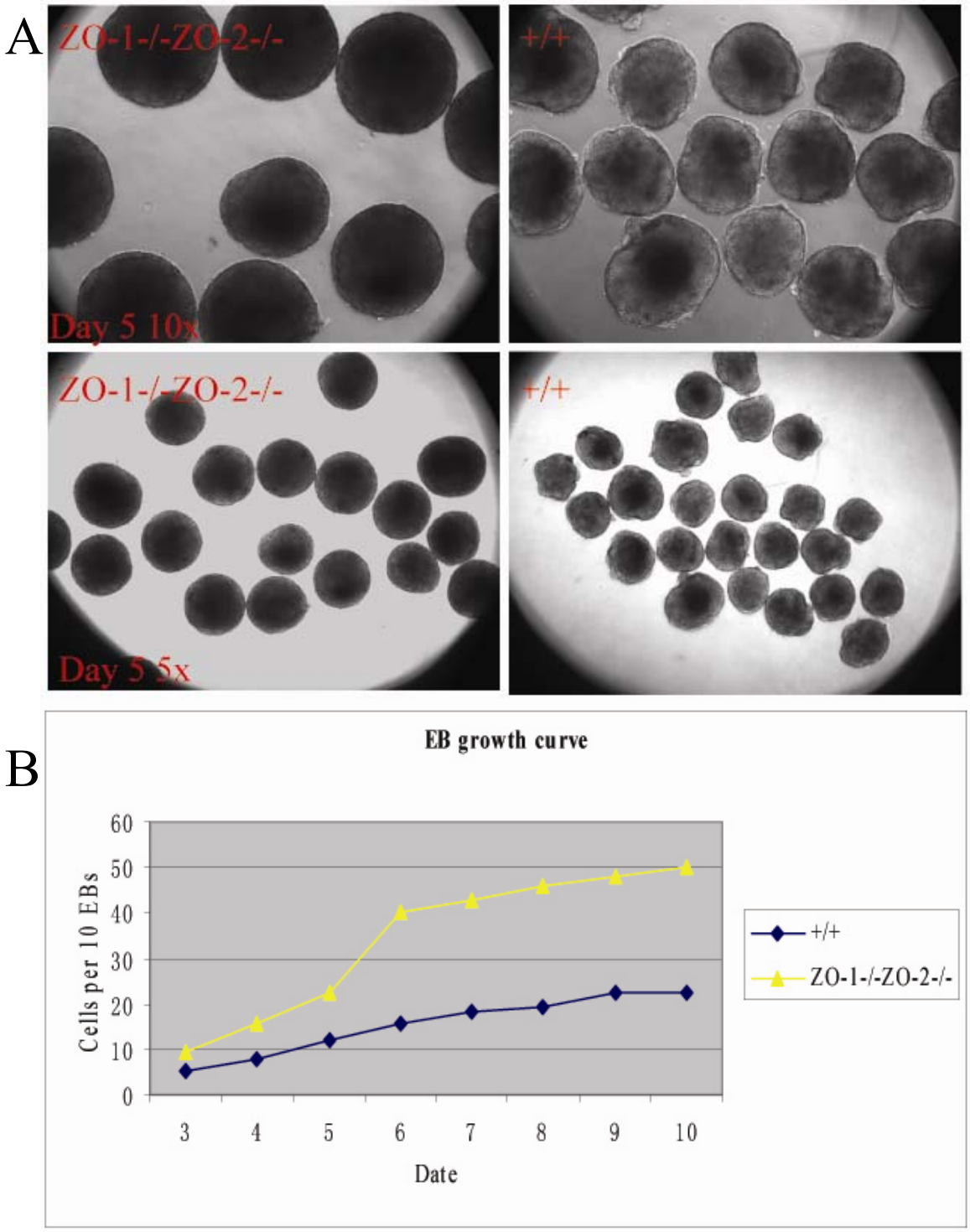

Figure 53 Morphology and cell growth curve of ZO-1-/-ZO-2-/- EBs. *(A) Day 5 ZO-1-/-ZO-2-/- EBs have a larger volume than WT EBs. ZO-1-/-ZO-2-/- EBs have a smooth surface and are regular in shape. (B) ZO-1-/-ZO-2-/- EBs consist of more cells at any given time than WT EBs.*

10.4 ZO-1/ZO-2 double knockout affects cell attachment and migration.

The smoother appearance of the surface observed in ZO-1-/-ZO-2-/- EBs (Figure 53) may reflect differences in structure and/or composition of the plasma membrane and affect the attachment and migration of the cells. To monitor cell attachment and migration, cells were transferred from a 2 day drop culture into suspension culture in bacterial dishes for 5 days and then seeded into 24-well tissue culture plates. After two days, +/+, ZO-1-/- and ZO-2-/- EBs attached to the bottom of the tissue culture plate and the cells spread out from the EBs. In contrast, both attachment and speading of cells from ZO-1-/-ZO-2-/- EBs were significantly delayed (Figure 54A). The cells of ZO-1-/-ZO-2-/- EBs showed extended spreading only around day 5 and they formed smaller colonies (Figure 54B). These data strongly suggest that cell attachment, cell migration and cell proliferation are affected in EBs lacking both ZO-1-/- and ZO-2-/-.

In order to analyze in more detail the surface of ZO-1-/-ZO-2-/- EBs, EBs transferred from 2 day hanging drop culture into 5 day suspension culture were subjected to scanning electronic microscopy. ZO-1-/-ZO-2-/- EBs had apparent discontinuities in the surface cell layer and the cells had a more fibroblastic appearance, obviously different from WT, ZO-1-/- or ZO-2-/- EBs (Figure 55). These changes in the surface and the cell morphology observed for ZO-1-/-ZO-2-/- EBs may thus explain their compromised attachment and migration.

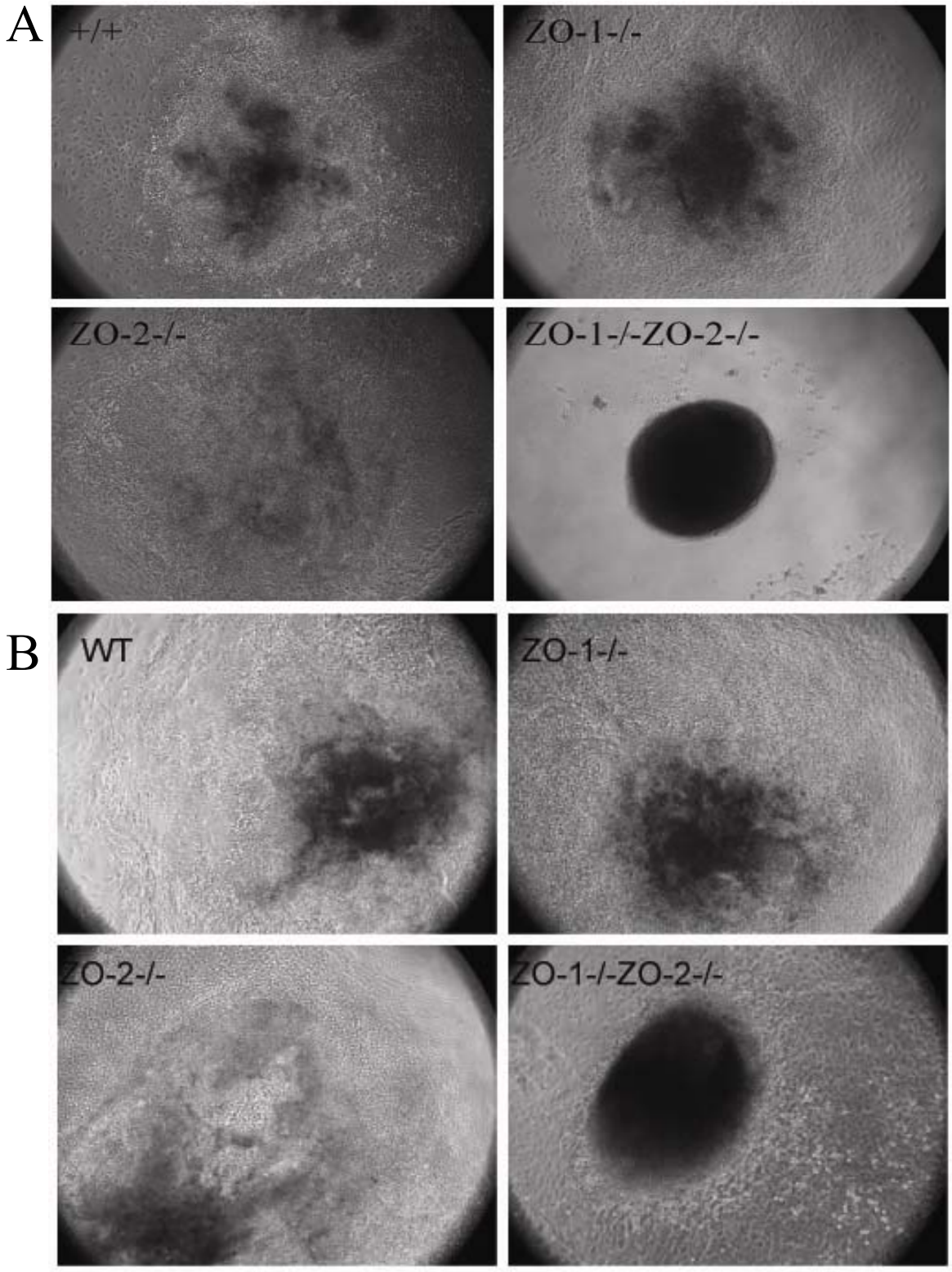

Figure 54 Morphology of EBs after 2 days and 5 days culture on normal cell culture plates*. The cells of +/+, ZO-1-/- and ZO-2-/- EBs attached to the bottom and spread out, while both attachment and spreading of cells from ZO-1-/-ZO-2-/- EBs were delayed (A) 2 days culture; (B) 5 days culture.*

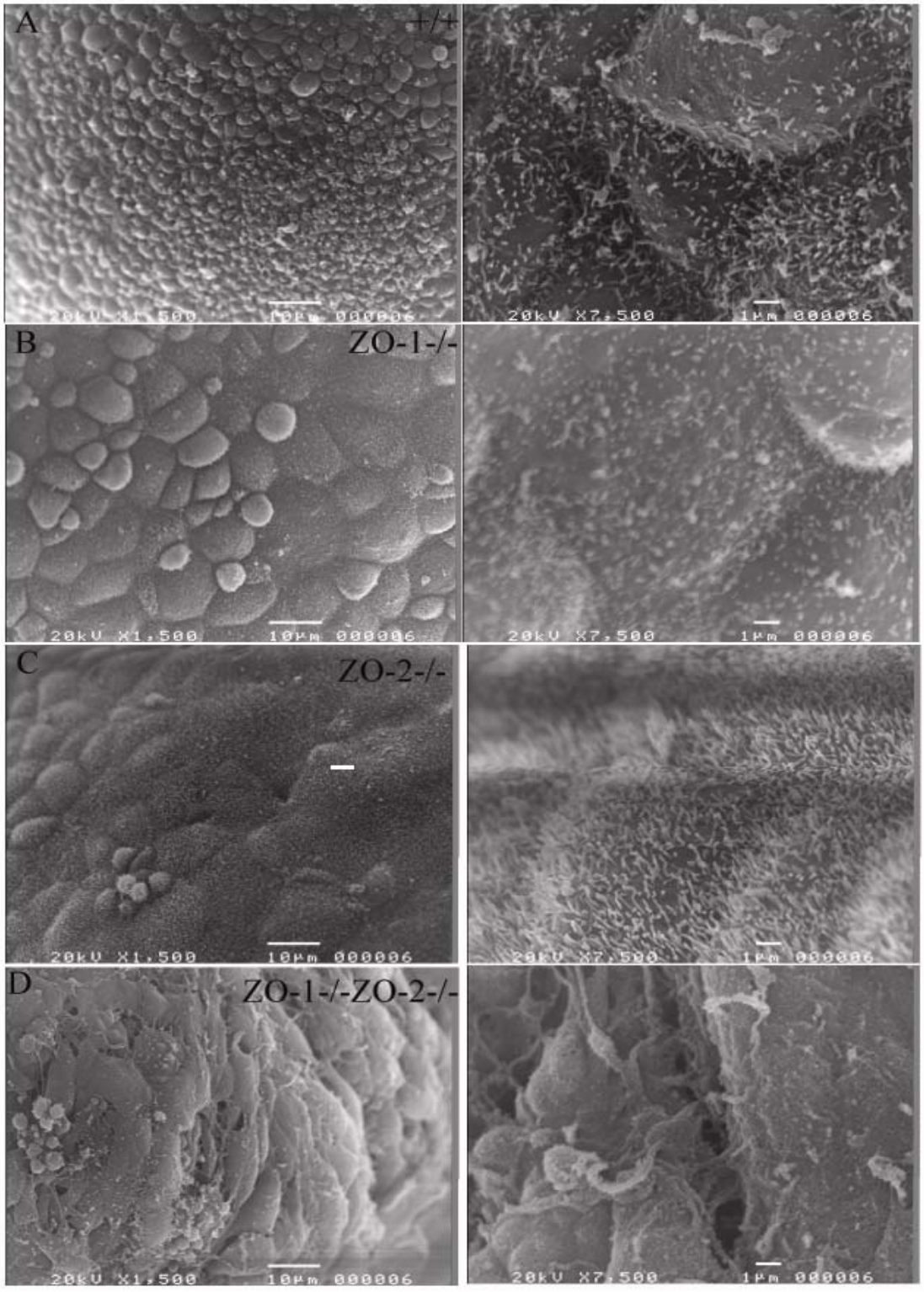

Figure 55 Scanning electron microscopy of day (2+5) EBs. *The surface of ZO-1-/-ZO-2 -/- EBs showed discontinuities in the cell layer and the cells had a more fibroblastic morphology.*

10.5 Discussion

As discussed above, both ZO-1-/- and ZO2-/- deficiency lead to larger EBs. As expected, also ZO-1-/-ZO-2-/- EBs were larger than WT EBs, but their volume was not increased as compared to that of single knock-out EBs, consistent with the two proteins playing a role in a common pathway. When ZO-1-/-ZO-2-/- EBs were transferred to normal cell culture plates for 2 days, WT EBs were flat and their cells spread, whereas ZO-1-/-ZO-2-/- EBs remained spherical in shape and the cells did not spread. Given the well established role of actin in cell migration (Suetsugu et al. 2003) and the known interaction of ZO-1 and ZO-2 with filamentous actin (Fanning et al., 1998; Wittchen et al., 1999), a role for ZO-1 and/or ZO-2 in organizing the actin cytoskeleton may not only be critical for the formation of TJs, but also for cell migration. ZO-1 interacts thorugh its C-terminus with actin directly and indirectly via the actin binding protein 4.1 (Itoh et al. 1997; Fanning et al. 1998; Mattagajasingh et al., 2000). Futhermore, the N-terminus of ZO-1 can mediate associations with the E-cadherin/alpha, β-catenin complex (Itoh et al. 1997), which plays a critical role in cell migration (refs). ZO-2 can also interact with F-actin directly (Wittchen et al. 1999) or indirectly via protein 4.1 (Mattagajasingh et al. 2000). Furthermore, given the severe effect of the lack of ZO-1 on TJs, the proper distribution of membrane proteins important for adhesion such as integrins and cadherins may be affected in ZO-1-/-ZO-2-/- EBs.

Chapter 11 Generation and phenotypic analysis of ZO-2-/-ZO-3-/- embryonic stem cells

11.1 Isolation of ZO-3-/- ES cells

To obtain ZO3-/- ES cells, 129Sv ZO-3-/- male and female mice were mated, E3.5 blastocysts collected from uteri of the pregnant mice and cultured for 4 days. Individual colonies were dissociated and inner mass cells with ES cell morphology derived as described in Materials and Methods (Chapter 2). Using this approach, two independent ZO-3 null ES cell clones were isolated from the inner cell mass. ZO-3-/- ES cells were differentiated into EBs and the expression level and localization of TJ and AJ markers analyzed and found to be unaffected in ZO-3-/- EBs (Figure 56, 57)

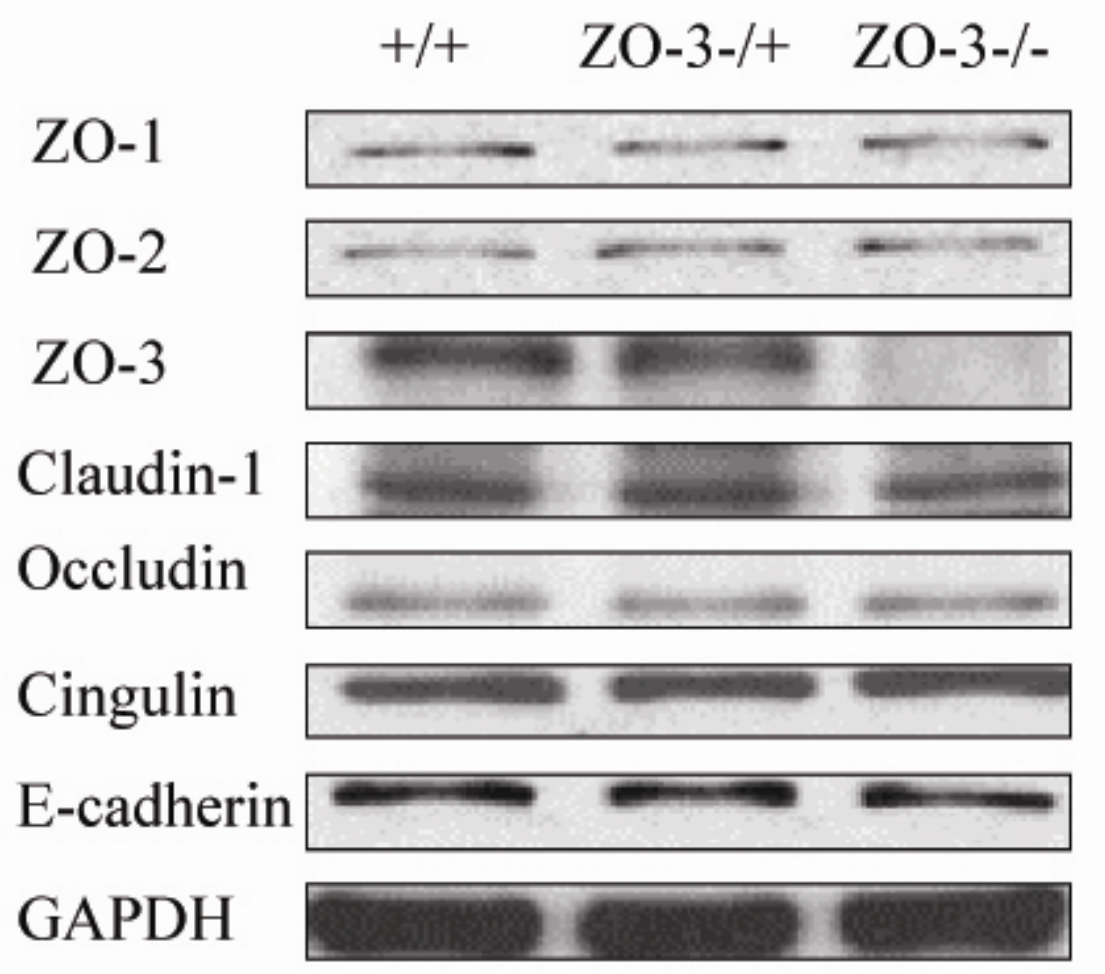

Figure 56 Expression levels of ZO proteins and TJ and AJ markers in ZO-3-/- EBs. *As expected, ZO-3 is not expressed in ZO-3-/- EBs. The expression levels of ZO-1, ZO-2, and other TJ and AJ markers are not altered in ZO-3-/- EBs.*

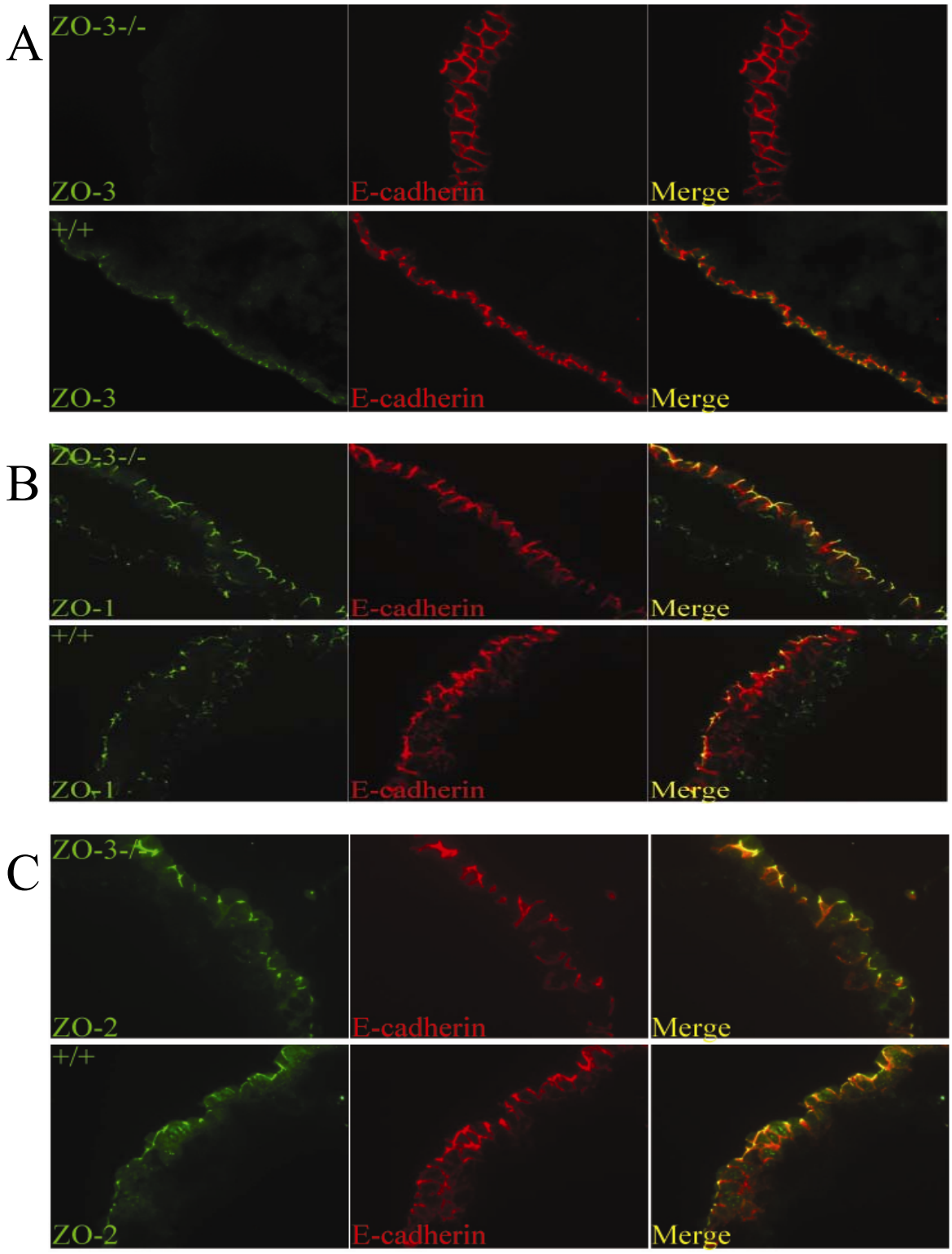

Figure 57 ZO protein expressions in ZO-3-/- EBs. *(A) ZO-3 is not expressed in ZO-3-/- EBs. (B, C) The distribution of ZO-1 and ZO-2 is not altered in either ZO-3-/+ and ZO-3 -/- EBs.*

11.2 Generation of ZO-2-/-ZO-3-/- ES cells

The floxed Neo gene in the ZO-3 mutant allele was removed by transfecting individual ZO-3-/- ES cells with a plasmid encoding cre recombinase (Taniguchi et al. 1998). Cells carrying the plasmid were selected with puromycin and surviving clones tested for sensitivity to G418, indicating excision of the Neo gene. Clones sensitive to G418 were amplified, tested for their sensitivity to puromycin to identify clones that had lost the cre plasmid, and transfected with the ZO-2 targeting vector. ZO-2 knockout was then achieved in the ZO-3-/- ES cell line as described in Chapter 9 for the inactivation of ZO-2. Inactivation of the ZO-2 and ZO-3 gene was confirmed by Western blot (Figure 58A) and five independent ZO-2-/-ZO-3-/- ES cell clones were identified from the screening. All these double knockout ES cells did not show any morphological differences as compared to WT ES cells (Figure 58B).

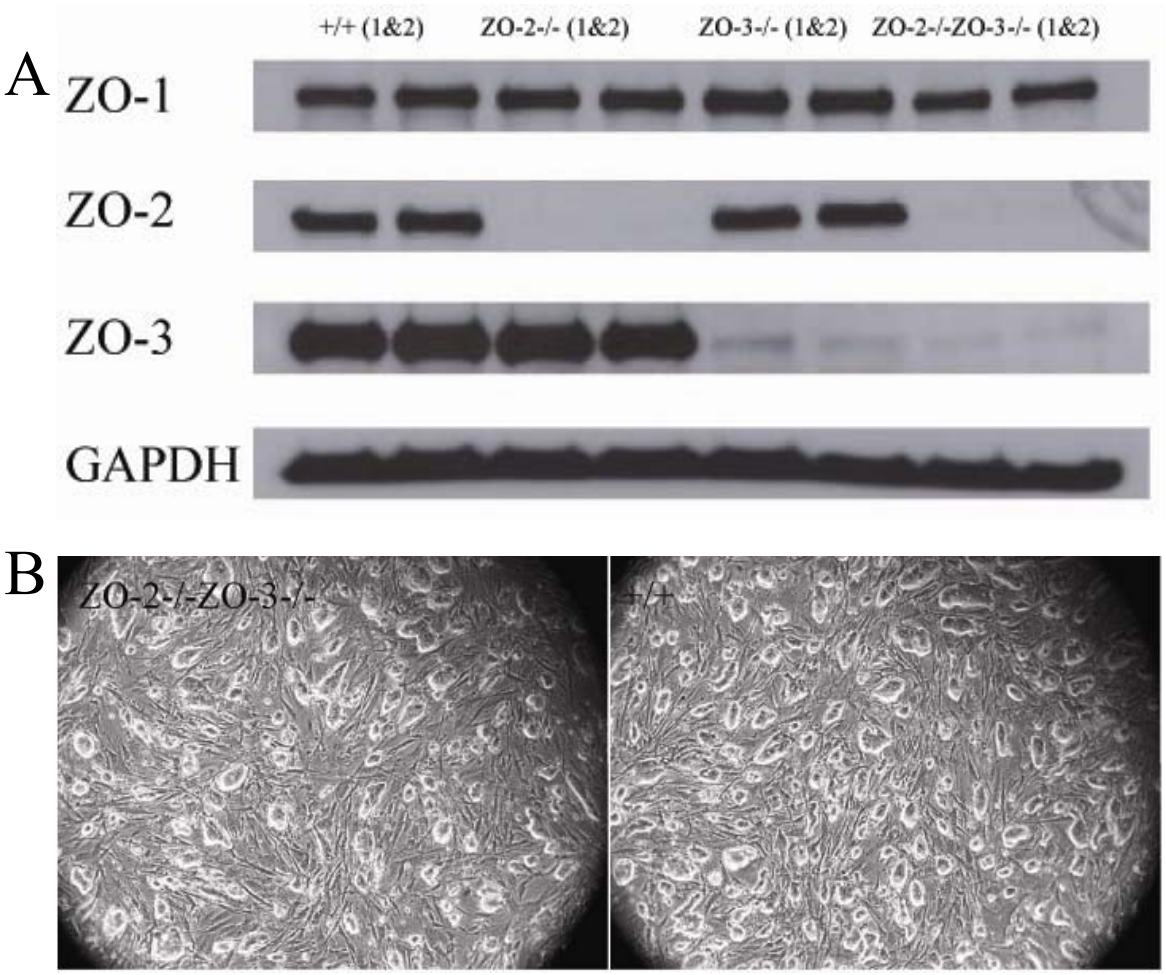

Figure 58 Characterization of ZO-2-/-ZO-3-/- ES cells. *(A) ZO protein expression in ZO-2-/-ZO-3-/- ES cells. ZO-2 and ZO-3 are not expressed in the double knockout ES cells. The expression of ZO-1 is not obviously altered. (B) ZO-2-/-ZO-3-/- ES cells have a similar morphology as WT ES cells.*

11.3 The expression levels of TJ and AJ markers are not altered in ZO-2-/-ZO-3-/- EBs.

Given the strong expression of ZO-2 and ZO-3 proteins in EBs, the expression levels of different tight junction and adherens junction markers in ZO-2-/-ZO3-/- EBs were analyzed by Western blot. As expected, no ZO-2 and ZO-3 was detected in ZO-2-/-ZO-3 -/- EBs (Figure 59). The expression levels of ZO-1, occludin, cingulin, E-cadherin and claudin-3 were not significantly differenent between WT, ZO-2-/-, ZO-3-/- and ZO-2-/-ZO-3-/- EBs (Figure 59).

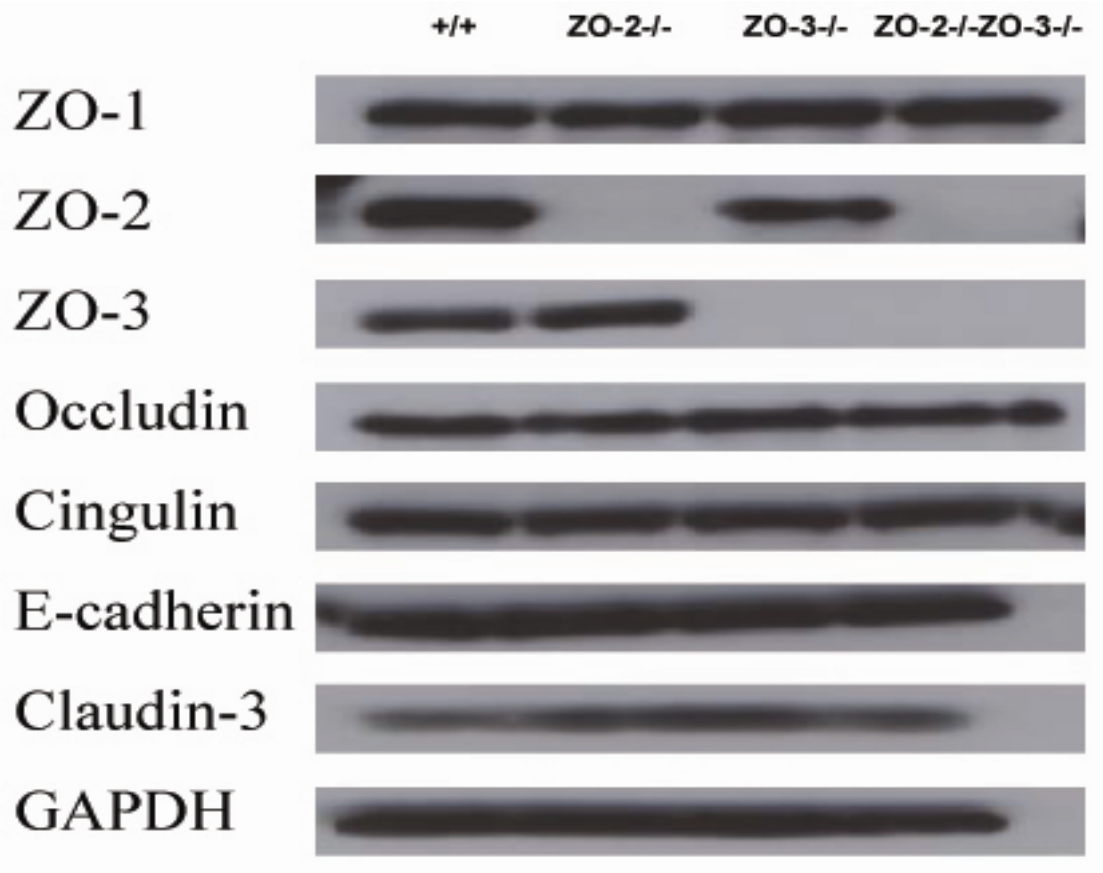

Figure 59 Expression levels of ZO proteins and TJ and AJ markers ZO-2-/-ZO-3-/- EBs. *ZO-2 and ZO-3 are not expressed in ZO-2-/-ZO-3-/- EBs. The expression levels of ZO-1, TJ and AJ markers are not altered in ZO-2-/-ZO-3-/- EBs.*

11.4 The localization of TJ and AJ markers is not altered in ZO-2-/-ZO-3-/- EBs.

Given the role of ZO-2 and ZO-3 as scaffold proteins that localize proteins to TJs we analyzed by immunostaining if the subcellular distribution of selected TJ markers was affected. As expected, no specific ZO-2 and ZO-3 staining was found in ZO-2-/-ZO-3-/- EBs (Figure 60A, B). ZO-1, occludin, cingulin and claudin-6 were all well localized to TJs in ZO-2-/-ZO-3-/- EBs (Figure 60C, D, E, F). Furthermore, the localization of the apical marker moesin and the lateral marker E-cadherin was unchanged in ZO-2-/-ZO-3 -/- EBs (Figure 61), indicating that the ability of TJs to maintain the asymmetric distribution of membrane proteins to the apical and basolateral domains was unaffected when both ZO-2 and ZO-3 were knocked out.

The structural integrity and permeability barrier function of TJs in ZO-2-/-ZO-3-/- EBs will be analyzed in future experiments.

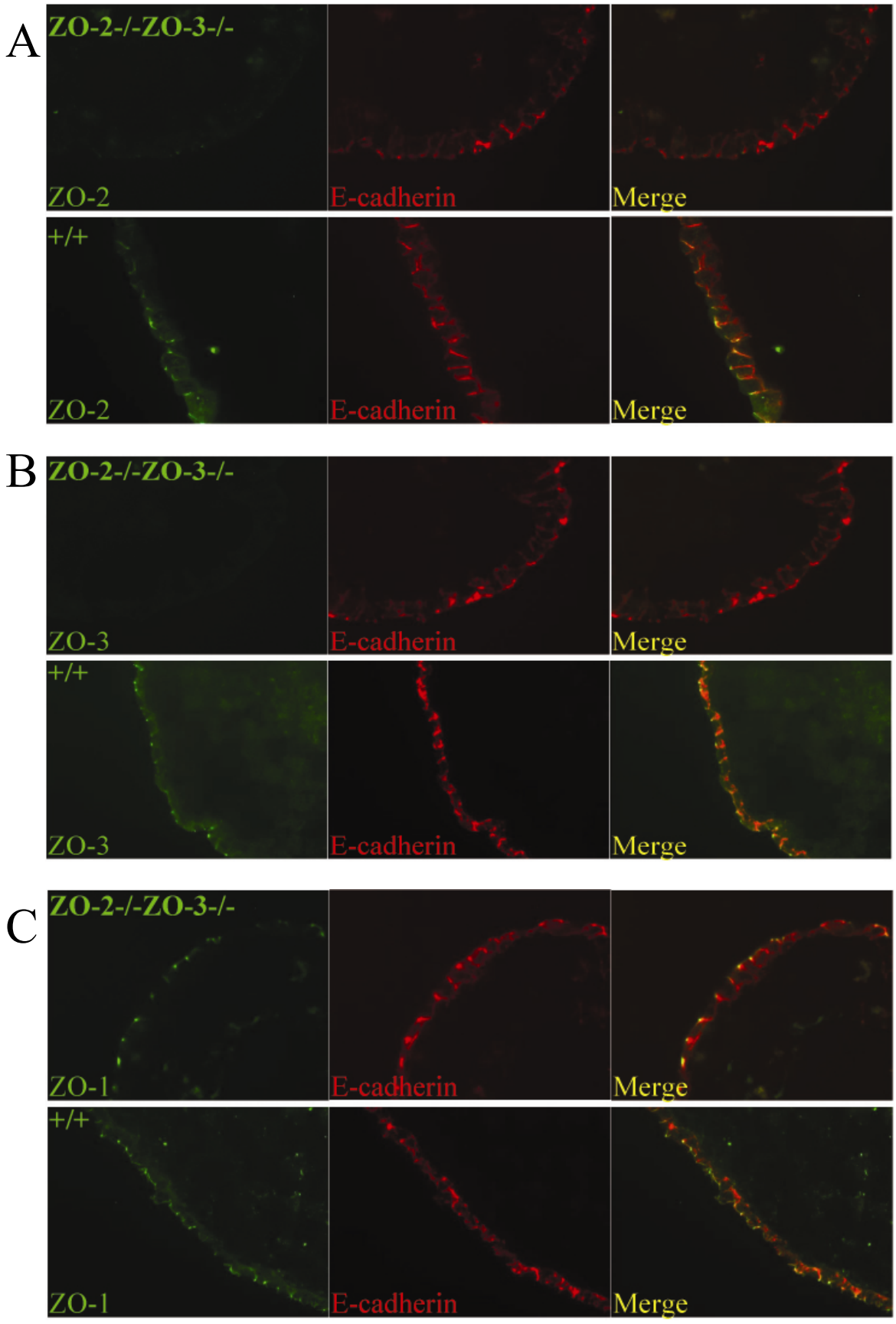
A
ZO-2-/-ZO-3-/-
ZO-2
E-cadherin
Merge
+/+
ZO-2
E-cadherin
Merge
B
ZO-2-/-ZO-3-/-
ZO-3
E-cadherin
Merge
+/+
ZO-3
E-cadherin
Merge
C
ZO-2-/-ZO-3-/-
ZO-1
E-cadherin
Merge
+/+
ZO-1
E-cadherin
Merge

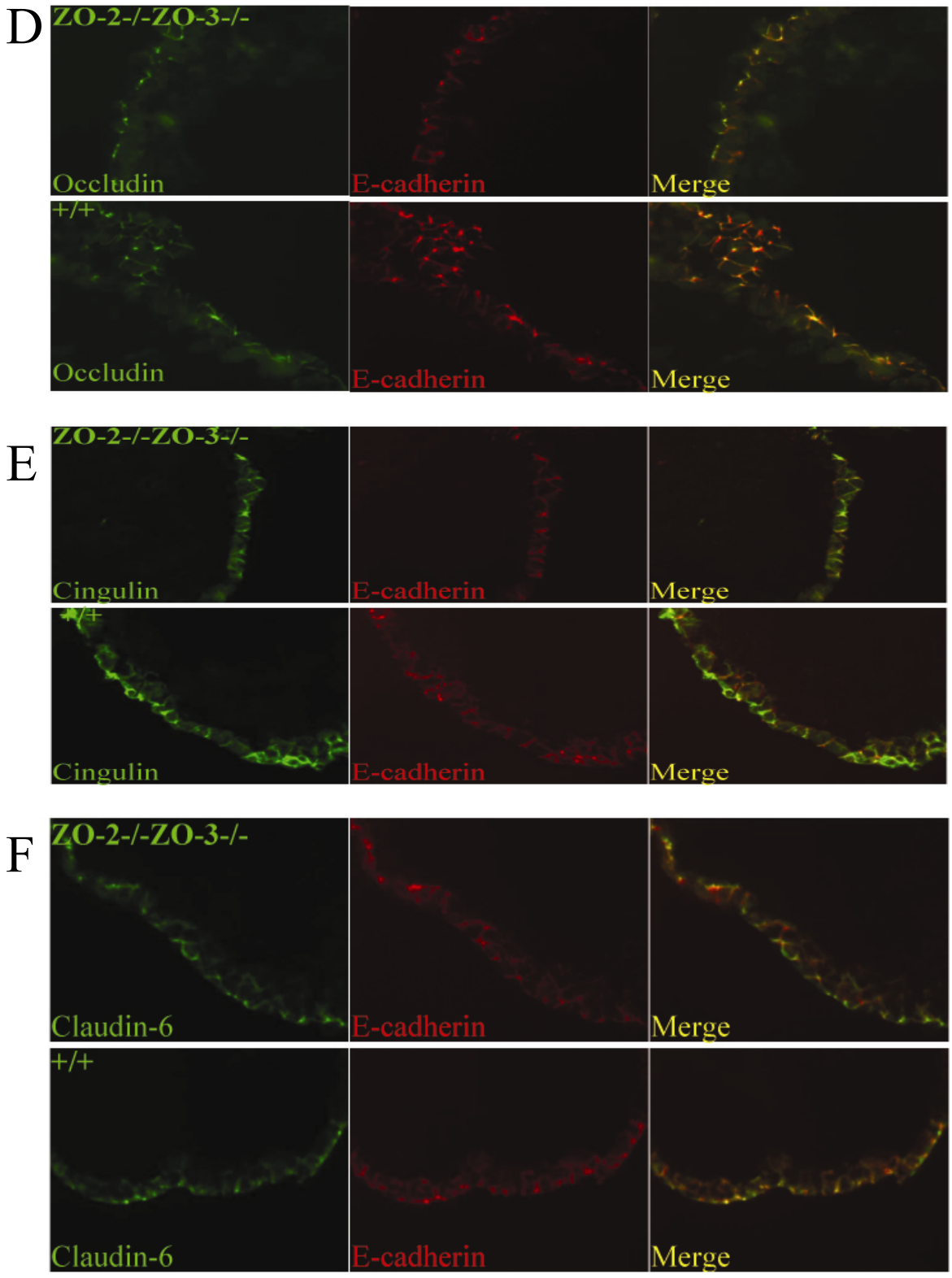

Figure 60 Distribution of ZO proteins, TJ and AJ markers in ZO-2-/-ZO-3 EBs. *(A, B) ZO-2 and ZO-3 are not expressed in ZO-2-/-ZO-3-/- EBs. (C, D, E, F) The localization of ZO-1, occludin, cingulin and claudin-6 is not altered in ZO-2-/-ZO-3-/- EBs.*

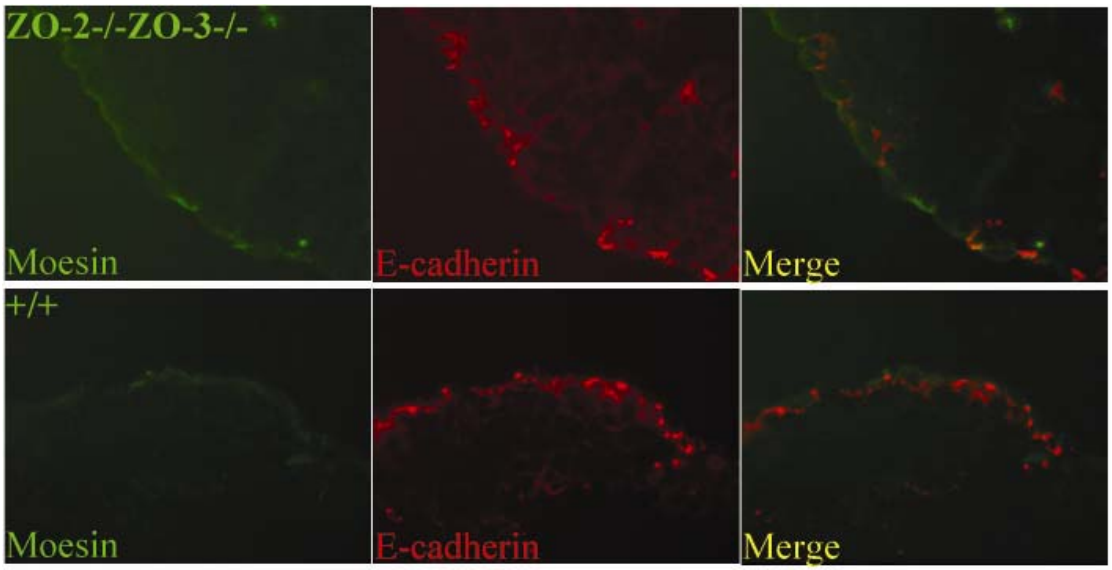

Figure 61 Apical-basolateral polarity is not affected in ZO-2-/-ZO-3-/- EBs. *The apical marker moesin and lateral marker E-cadherin are correctly localized in ZO-2-/-ZO-3-/- EBs.*

11.5 Disscussion

ZO-2-/-ZO-3-/- ES cells were generated to determine if the absence of both ZO proteins had an effect on the formation of functional TJs in EBs. In ZO-2-/-ZO-3-/- EBs, the protein expression levels and localization of various TJ and AJ markers analyzed were not affected. The apical-basal polarity of the epithelial cells was maintained. Our findings are thus consistent with a recent report that visceral endoderm epithelial-like ZO-3-/- cells retain a normal molecular TJ architecture even when ZO-2 expression is suppressed (Adachi et al. 2006). Therefore, at least in EBs cultured in vitro, ZO-2 and ZO-3 are dispensable for the formation of functional TJs. However, similar to ZO-2-/- embryos, embryos lacking both ZO proteins apparently died after implantation (see Chapter 7). As discussed above, a similar difference was observed between ZO-2-/- EBs and embryos and may be attributed to physiological stress during embryo growth in the in vivo environment.

Chapter 12 Summary and perspectives

TJs are critical components of epithelia and endothelia, where they are involved in maintaining apical basal cell polarity, the formation of protective barriers and the selective exchange of solutes between different tissue compartments. Deregulation of TJ function has been associated with many pathological conditions and several components of TJ act as receptors for pathogens (Sawada et al., 2003). Members of the ZO protein family were among the first TJ proteins to be identified and have been extensively characterized (González-Mariscal et al. 2000, 2003; Köhler et al., 2005; Matter et al., 2003, 2007). As scaffolding proteins, ZO proteins engage in multiple protein-protein interactions. ZO not only link transmembrane TJ proteins to the actin cytoskeleton, but recent evidence points to a central role for ZO proteins in organizing signaling networks that regulate, possibly in response to the cell-cell contact, vesicle trafficking, gene expression, and cell proliferation and differentiation (González-Mariscal et al. 2000, 2003; Köhler et al., 2005; Matter et al., 2003, 2007). Interestingly, ZO proteins are not restricted to TJs in epithelia or endothelia, but are also found in TJs or TJ-like structures formed by other cell types such as Schwann cells (Poliak et al., 2002) and cadiomyocytes (Borrmann et al., 2006), as well as in AJs (Ikenouchi et al., 2007) and gap junctions (Segretain et al., 2004; Hunter et al., 2005; Laing et al., 2005).

One intriguing question is the relevance for three closely related ZO genes in mammals. At the beginning of this work, it was thought that ZO proteins show a high degree of redundancy, a notion based on the silencing of ZO protein expression, either individually or in combination, in different cell lines (Medina et al., 2000; Umeda et al.,

2004, 2006; Adachi et al. 2006; McNeil et al., 2006; Hernandez et al., 2007). Although sometimes conflicting, these results strongly suggested that individual ZO proteins may be largely dispensable for TJ structure and/or function. In the course of my studies, this idea was reinforced by the lack of a phenotype for a mouse carrying an inactivated ZO-3 gene.

To address the role of different ZO-proteins in a more physiological context, I generated mice in which ZO protein genes were inactivated by homologous recombination, either individually or in combination. The finding that mice lacking ZO-1 or ZO-2, but not ZO-3, shows early embryonic lethality have clearly established non-redundant roles for these proteins. Furthermore, this is to my knowledge the first time that ZO proteins have been shown to be critical for mammalian development. Furthermore, I was able to rescue the embryonic lethality of ZO-2 null mice by generating ZO-chimera, which revealed interesting phenotypes in the testis, kidney and the inner ear, establishing unique functions for ZO-2 in different tissues of adult mice.

As an alternative to the characterization of ZO proteins in transgenic mice, I generated ES cells lacking one or several ZO proteins. This approach has allowed me to compare different properties and functions of TJs lacking ZO proteins in an in vivo and an in vitro system. Among the 3 ZO proteins, the loss of ZO-1 showed the most severe effect on TJ structure. Surprisingly, ZO-2 was important for TJ structure and possibly barrier function in vivo, but not in EBs in vtiro. This finding indicates that under physiological stress or perhaps depending on cell type, the absence of a particular protein may have a more profound effect on TJ structure/function. This could, to some extent,

also explain the conflicting results reported in the literature for the silencing of ZO protein expression in different tissue culture cell types.

My work has also opened several interesting venues for future work. First, it will be of interest to analyze in further detail the embryonic lethality associated with the lack of ZO-1. Second, characterization of the phenotypes observed for the ZO-2 chimera and the generation of conditional ZO-2 (and ZO-1) knock-out mice will establish distinct functions for these proteins in different tissues of the adult animal. Third, it will be important to determine where for extraembryonic development ZO-2 is important. Forth, the lack of either ZO-1 or ZO-2 results in enlarged EBs, suggesting that either proliferation and/or apoptosis are affected. Fifth, the observation that the absence of ZO-1 promotes mesoderm formation indicates that individual ZO proteins may be involved in cell lineage determination during development. The availability of ES cells lacking ZO proteins will allow researchers to address the requirement of individual ZO proteins for the differentiation of ES cells into specific cell lineages. Finally, the fundamental question if a phenotype associated with the lack of a ZO protein is due to the loss of transmembrane TJ protein and cytoskeleton tethering, or the disruption of signaling networks organized by these scaffolding proteins, will need to be addressed.

In conclusion, my work has established critical and non-redundant roles for individual ZO proteins in early development of mammals. Furthrmore, it has unraveled new cellular and physiological processes where ZO proteins may play a role.

REFERENCES

Adachi M, Inoko A, Hata M, Furuse K, Umeda K, Itoh M, Tsukita S. (2006) Normal establishment of epithelial tight junctions in mice and cultured cells lacking expression of ZO-3, a tight-junction MAGUK protein Mol. Cell Biol. 26: 9003-9015

Anderson JM, Stevenson BR, Jesaitis LA, Goodenough DA, Mooseker MS. (1988) Characterization of ZO-1, a protein component of the tight junction from mouse liver and Madin-Darby canine kidney cells J. Cell Biol. 106: 1141-1149

Ando-Akatsuka Y, Yonemura S, Itoh M, Furuse M, Tsukita S. (1999) Differential behavior of E-cadherin and occludin in their colocalization with ZO-1 during the establishment of epithelial cell polarity J. Cell Physiol. 179: 115-125

Akoyev V, Takemoto DJ. (2007) ZO-1 is required for protein kinase C gamma-driven disassembly of connexin 43. Cell Signal. 19: 958-67

Assémat E, Bazellières E, Pallesi-Pocachard E, Le Bivic A, Massey-Harroche D. (2007) Polarity complex proteins. Biochim. Biophys. Acta. [Epub ahead of print]

Balda MS, Anderson JM. (1993) Two classes of tight junctions are revealed by ZO-1 isoforms. Am. J. Physiol. 264: C918-C924

Balda MS, Matter K. (2000) The tight junction protein ZO-1 and an interacting transcription factor regulate ErbB-2 expression. EMBO. J. 19: 2024-2033

Balda MS, Garrett MD, Matter K. (2003) The ZO-1-associated Y-box factor ZONAB regulates epithelial cell proliferation and cell density. J. Cell Biol. 160:423-432

Barker RJ, Price RL, Gourdie RG. (2002) Increased association of ZO-1 with connexin43 during remodeling of cardiac gap junctions. Circ. Res. 90: 317-324

Bazzoni G, Martinez-Estrada OM, Orsenigo F, Cordenonsi M, Citi S, Dejana E. 9(2000) Interaction of junctional adhesion molecule with the tight junction components ZO-1, cingulin, and occludin. J. Biol. Chem. 275: 20520-20526

Beatch M, Jesaitis LA, Gallin WJ, Goodenough DA, Stevenson BR. (1996) The tight junction protein ZO-2 contains three PDZ (PSD-95/Discs-Large/ZO-1) domains and an alternatively spliced region. J. Biol. Chem. 271: 25723-25726.

Betanzos A, Huerta M, Lopez-Bayghen E, Azuara E, Amerena J, González-Mariscal L. (2004) The tight junction protein ZO-2 associates with Jun, Fos and C/EBP transcription factors in epithelial cells. Exp. Cell Res. 292: 51-66

Bevilacqua A, Loch-Caruso R, Erickson RP. (1989) Abnormal development and dye coupling produced by antisense RNA to gap junction protein in mouse preimplantation embryos Proc. Natl. Acad. Sci. U. S. A. 86: 5444-5448

Billings SD, Walsh SV, Fisher C, Nusrat A, Weiss SW, Folpe AL. (2004) Aberrant expression of tight junction-related proteins ZO-1, claudin-1 and occludin in synovial sarcoma: an immunohistochemical study with ultrastructural correlation. Mod. Pathol. 17: 141-149

Borrmann CM, Grund C, Kuhn C, Hofmann I, Pieperhoff S, Franke WW. (2006) The area composita of adhering junctions connecting heart muscle cells of vertebrates. II. Colocalizations of desmosomal and fascia adhaerens molecules in the intercalated disk. Eur J. Cell Biol. 85:469-485.

Byers S, Graham R, Dai HN, Hoxter B. (1991) Development of Sertoli cell junctional specializations and the distribution of the tight-junction-associated protein ZO-1 in the mouse testis Am. J. Anat. 191: 35-47

Carlton VE, Harris BZ, Puffenberger EG, Batta AK, Knisely AS, Robinson DL, Strauss KA, Shneider BL, Lim WA, Salen G, Morton DH, Bull LN. (2003) Complex inheritance of familial hypercholanemia with associated mutations in TJP2 and BAAT. Nat. Genet. 34: 91-96

Caruana G. (2002) Genetic studies define MAGUK proteins as regulators of epithelial cell polarity. Int. J. Dev. Biol. 46: 511-518

Chen HJ, Lin CM, Lin CS, Perez-Olle R, Leung CL, Liem RK. (2006) The role of microtubule actin cross-linking factor 1 (MACF1) in the Wnt signaling pathway. Genes Dev. 2006 20: 1933-1945

Chen VC, Li X, Perreault H, Nagy JI. (2006) Interaction of zonula occludens-1 (ZO-1) with alpha-actinin-4: application of functional proteomics for identification of PDZ domain-associated proteins. J. Proteome Res. 5: 2123-2134

Chen, Y.-H., C. Merzdorf, D.L. Paul, and D.A. Goodenough. 1997. COOH terminus of occludin is required for tight junction barrier function in early Xenopus embryos. J. Cell Biol. 138: 891-899

Chlenski A, Ketels KV, Tsao MS, Talamonti MS, Anderson MR, Oyasu R, Scarpelli DG. (1999a) Tight junction protein ZO-2 is differentially expressed in normal pancreatic ducts compared to human pancreatic adenocarcinoma. Int. J. Cancer. 82: 137-144

Chlenski A, Ketels KV, Engeriser JL, Talamonti MS, Tsao MS, Koutnikova H, Oyasu R, Scarpelli DG. (1999b) zo-2 gene alternative promoters in normal and neoplastic human pancreatic duct cells. Int. J. Cancer. 83: 349-358

Chlenski A, Ketels KV, Korovaitseva GI, Talamonti MS, Oyasu R, Scarpelli DG. (2000) Organization and expression of the human zo-2 gene (tjp-2) in normal and neoplastic tissues Biochim. Biophys. Acta. 1493: 319-324

Cordenonsi M, D'Atri F, Hammar E, Parry DA, Kendrick-Jones J, Shore D, Citi S. (1999) Cingulin contains globular and coiled-coil domains and interacts with ZO-1, ZO-2, ZO-3, and myosin. J. Cell Biol. 147: 1569-1582

Davies TC, Barr KJ, Jones DH, Zhu D, Kidder GM. (1996) Multiple members of the connexin gene family participate in preimplantation development of the mouse. Dev. Genet. 18: 234-243

D'Atri F, Nadalutti F, Citi S. (2002) Evidence for a functional interaction between cingulin and ZO-1 in cultured cells. J. Biol. Chem. 277: 27757-27764

Doetschman TC, Eistetter H, Katz M, Schmidt W, Kemler R. (1985) The in vitro development of blastocyst-derived embryonic stem cell lines: formation of visceral yolk sac, blood islands and myocardium. J. Embryol. Exp. Morphol. 87:27-45

Dym M, Fawcett DW. (1970) The blood-testis barrier in the rat and the physiological compartmentation of the seminiferous epithelium. Biol. Reprod. 3:308-326.

Ebnet K, Schulz CU, Meyer Zu Brickwedde MK, Pendl GG, Vestweber D. (2000) Junctional adhesion molecule interacts with the PDZ domain-containing proteins AF-6 and ZO-1. J. Biol. Chem. 275: 27979-27988

Eckert JJ, McCallum A, Mears A, Rumsby MG, Cameron IT, Fleming TP. (2004) Specific PKC isoforms regulate blastocoel formation during mouse preimplantation development. Dev. Biol. 274:384-401

Fanning AS, Jameson BJ, Jesaitis LA, Anderson JM. (1998) The tight junction protein ZO-1 establishes a link between the transmembrane protein occludin and the actin cytoskeleton. J. Biol. Chem. 273: 29745-29653

Fanning AS, Anderson JM. (1999) PDZ domains: fundamental building blocks in the organization of protein complexes at the plasma membrane. J. Clin. Invest. 103: 767-772

Fanning AS, Little BP, Rahner C, Utepbergenov D, Walther Z, Anderson JM. (2007) The unique-5 and -6 motifs of ZO-1 regulate tight junction strand localization and scaffolding properties. Mol. Biol. Cell. 18: 721-731

Fink C, Weigel R, Hembes T, Lauke-Wettwer H, Kliesch S, Bergmann M, Brehm RH. (2006) Altered expression of ZO-1 and ZO-2 in Sertoli cells and loss of blood-testis barrier integrity in testicular carcinoma in situ. Neoplasia. 8: 1019-1027.

Fleming TP, McConnell J, Johnson MH, Stevenson BR. (1989) Development of tight junctions de novo in the mouse early embryo: control of assembly of the tight junction-specific protein, ZO-1. J. Cell Biol. 108: 1407-1418

Fleming TP, Hay MJ. (1991) Tissue-specific control of expression of the tight junction polypeptide ZO-1 in the mouse early embryo Development 113: 295-304

Furuse M, Itoh M, Hirase T, Nagafuchi A, Yonemura S, Tsukita S, Tsukita S. (1994) Direct association of occludin with ZO-1 and its possible involvement in the localization of occludin at tight junctions J. Cell Biol. 127: 1617-1626

Giepmans BN, Verlaan I, Moolenaar WH. (2001) Connexin-43 interactions with ZO-1 and alpha- and beta-tubulin Cell Commun. Adhes. 8: 219-223

Giepmans BN. (2004) Gap junctions and connexin-interacting proteins. Cardiovasc. Res. 62: 233-245

Glaunsinger BA, Weiss RS, Lee SS, Javier R. (2001) Link of the unique oncogenic properties of adenovirus type 9 E4-ORF1 to a select interaction with the candidate tumor suppressor protein ZO-2. EMBO. J. 20: 5578-5586.

González-Mariscal L, Islas S, Contreras RG, García-Villegas MR, Betanzos A, Vega J, Diaz-Quiñónez A, Martín-Orozco N, Ortiz-Navarrete V, Cereijido M, Valdés J. (1999) Molecular characterization of the tight junction protein ZO-1 in MDCK cells. Exp. Cell Res. 248: 97-109.

González-Mariscal L, Betanzos A, Avila-Flores A. (2000) MAGUK proteins: structure and role in the tight junction. Semin Cell Dev. Biol. 11: 315-324

González-Mariscal L, Betanzos A, Nava P, Jaramillo BE. (2003) Tight junction proteins. Prog Biophys Mol. Biol. 81:1-44

González-Mariscal L, Ponce A, Alarcón L, Jaramillo BE. (2006) The tight junction protein ZO-2 has several functional nuclear export signals. Exp. Cell Res. 312: 3323-3335

Gottardi CJ, Arpin M, Fanning AS, Louvard D. (1996) The junction-associated protein, zonula occludens-1, localizes to the nucleus before the maturation and during the remodeling of cell-cell contacts. Proc. Natl. Acad. Sci. U. S. A. 93: 10779-10784

Guillemot L, Paschoud S, Pulimeno P, Foglia A, Citi S. (2008) The cytoplasmic plaque of tight junctions: A scaffolding and signalling center. Biochim. Biophys. Acta. 1778: 601-613

Gumbiner B, Lowenkopf T, Apatira D. (1991) Identification of a 160-kDa polypeptide that binds to the tight junction protein ZO-1 Proc. Natl. Acad. Sci. U. S. A. 88: 3460-3464

Hachiro T, Kawahara K, Sato R, Yamauchi Y, Matsuyama D. (2007) Changes in the fluctuation of the contraction rhythm of spontaneously beating cardiac myocytes in cultures with and without cardiac fibroblasts. Biosystems. 90:707-715.

Haskins J, Gu L, Wittchen ES, Hibbard J, Stevenson BR. (1998) ZO-3, a novel member of the MAGUK protein family found at the tight junction, interacts with ZO-1 and occludin. J. Cell Biol. 141: 199-208

Hernandez S, Chavez Munguia B, Gonzalez-Mariscal L. (2007) ZO-2 silencing in epithelial cells perturbs the gate and fence function of tight junctions and leads to an atypical monolayer architecture. Exp. Cell Res. 313:1533-1547

Hiroi Y, Kudoh S, Monzen K, Ikeda Y, Yazaki Y, Nagai R, Komuro I. (2001) Tbx5 associates with Nkx2-5 and synergistically promotes cardiomyocyte differentiation. Nat. Genet. 28:276-280

Hoover KB, Liao SY, Bryant PJ. (1998) Loss of the tight junction MAGUK ZO-1 in breast cancer: relationship to glandular differentiation and loss of heterozygosity. Am. J. Pathol. 153: 1767-1773

Hopkins AM, Li D, Mrsny RJ, Walsh SV, Nusrat A. (2000) Modulation of tight junction function by G protein-coupled events. Adv. Drug. Deliv. Rev. 41: 329-340

Howarth AG, Hughes MR, Stevenson BR. (1992) Detection of the tight junction-associated protein ZO-1 in astrocytes and other nonepithelial cell types Am. J. Physiol. 262: C461-469

Huerta M, Muñoz R, Tapia R, Soto-Reyes E, Ramírez L, Recillas-Targa F, González-Mariscal L, López-Bayghen E. (2007) Cyclin D1 Is Transcriptionally Down-Regulated by ZO-2 via an E Box and the Transcription Factor c-Myc. Mol. Biol Cell. 18: 4826-4836

Hulander M, Wurst W, Carlsson P, Enerbäck S. (1998) The winged helix transcription factor Fkh10 is required for normal development of the inner ear. Nat. Genet. 20:374-376

Hunter AW, Barker RJ, Zhu C, Gourdie RG. (2005) Zonula occludens-1 alters connexin43 gap junction size and organization by influencing channel accretion. Mol. Biol. Cell. 16: 5686-5698

Ikari A, Hirai N, Shiroma M, Harada H, Sakai H, Hayashi H, Suzuki Y, Degawa M, Takagi K. (2004) Association of paracellin-1 with ZO-1 augments the reabsorption of divalent cations in renal epithelial cells. J. Biol Chem. 279: 54826-54832

Ikenouchi J, Umeda K, Tsukita S, Furuse M, Tsukita S. (2007) Requirement of ZO-1 for the formation of belt-like adherens junctions during epithelial cell polarization. J. Cell Biol. 176: 779-786

Inoko A, Itoh M, Tamura A, Matsuda M, Furuse M, Tsukita S. (2003) Expression and distribution of ZO-3, a tight junction MAGUK protein, in mouse tissues Genes Cells. 8: 837-845

Islas S, Vega J, Ponce L, González-Mariscal L. (2002) Nuclear localization of the tight junction protein ZO-2 in epithelial cells. Exp. Cell Res. 274: 138-148

Itoh M, Nagafuchi A, Moroi S, Tsukita S. (1997) Involvement of ZO-1 in cadherin-based cell adhesion through its direct binding to alpha catenin and actin filaments. J. Cell Biol. 138: 181-192

Itoh M, Morita K, Tsukita S. (1999a) Characterization of ZO-2 as a MAGUK family member associated with tight as well as adherens junctions with a binding affinity to occludin and alpha catenin. J. Biol. Chem. 274: 5981-5986

Itoh M, Furuse M, Morita K, Kubota K, Saitou M, Tsukita S. (1999b) Direct binding of three tight junction-associated MAGUKs, ZO-1, ZO-2, and ZO-3, with the COOH termini of claudins. J. Cell Biol. 147: 1351-1363

Jaramillo BE, Ponce A, Moreno J, Betanzos A, Huerta M, Lopez-Bayghen E, Gonzalez-Mariscal L. (2004) Characterization of the tight junction protein ZO-2 localized at the nucleus of epithelial cells. Exp. Cell Res. 297: 247-258

Johnson LG. (2005) Applications of imaging techniques to studies of epithelial tight junctions. Adv. Drug Deliv. Rev. 57:111-21

Kaihara T, Kawamata H, Imura J, Fujii S, Kitajima K, Omotehara F, Maeda N, Nakamura T, Fujimori T. (2003) Redifferentiation and ZO-1 reexpression in liver-metastasized colorectal cancer: possible association with epidermal growth factor receptor-induced tyrosine phosphorylation of ZO-1. Cancer Sci. 94: 166-172

Kausalya PJ, Reichert M, Hunziker W. (2001) Connexin45 directly binds to ZO-1 and localizes to the tight junction region in epithelial MDCK cells. FEBS. Lett. 505: 92-96

Kausalya PJ, Phua DC, Hunziker W. (2004) Association of ARVCF with zonula occludens (ZO)-1 and ZO-2: binding to PDZ-domain proteins and cell-cell adhesion regulate plasma membrane and nuclear localization of ARVCF. Mol. Biol. Cell. 15: 5503-5515

Kemler R, Hierholzer A, Kanzler B, Kuppig S, Hansen K, Taketo MM, de Vries WN, Knowles BB, Solter D. (2004) Stabilization of beta-catenin in the mouse zygote leads to premature epithelial-mesenchymal transition in the epiblast. Development. 31: 5817-5824

Kleeff J, Shi X, Bode HP, Hoover K, Shrikhande S, Bryant PJ, Korc M, Büchler MW, Friess H. (2001) Altered expression and localization of the tight junction protein ZO-1 in primary and metastatic pancreatic cancer Pancreas. 23: 259-265

Köhler K, Zahraoui A. (2005) Tight junction: a co-ordinator of cell signalling and membrane trafficking. Biol. Cell. 97: 659-665

Kojima T, Kokai Y, Chiba H, Yamamoto M, Mochizuki Y, Sawada N. (2001) Cx32 but not Cx26 is associated with tight junctions in primary cultures of rat hepatocytes. Exp. Cell Res. 263:193-201

Kurihara H, Anderson JM, Farquhar MG. (1992) Diversity among tight junctions in rat kidney: glomerular slit diaphragms and endothelial junctions express only one isoform of the tight junction protein ZO-1. Proc. Natl. Acad. Sci. U. S. A. 89: 7075-7079.

Kurihara H, Anderson JM, Farquhar MG. (1995) Increased Tyr phosphorylation of ZO-1 during modification of tight junctions between glomerular foot processes Am. J. Physiol. 1268: F514-524

Laing JG, Chou BC, Steinberg TH. (2005) ZO-1 alters the plasma membrane localization and function of Cx43 in osteoblastic cells. J. Cell Sci. 118: 2167-2176

Lee S, Gilula NB, Warner AE. (1987) Gap junctional communication and compaction during preimplantation stages of mouse development Cell. 51: 851-860

Li CX, Poznansky MJ. (1990) Characterization of the ZO-1 protein in endothelial and other cell lines J. Cell Sci. 97: 231-237

Li X, Olson C, Lu S, Kamasawa N, Yasumura T, Rash JE, Nagy JI. (2004a) Neuronal connexin36 association with zonula occludens-1 protein (ZO-1) in mouse brain and interaction with the first PDZ domain of ZO-1 Eur. J. Neurosci. 19: 2132-2146

Li X, Ionescu AV, Lynn BD, Lu S, Kamasawa N, Morita M, Davidson KG, Yasumura T, Rash JE, Nagy JI. (2004b) Connexin47, connexin29 and connexin32 co-expression in oligodendrocytes and Cx47 association with zonula occludens-1 (ZO-1) in mouse brain Neuroscience. 126: 611-630

Martínez-Contreras R, Galindo JM, Aguilar-Rojas A, Valdés J. (2003) Two exonic elements in the flanking constitutive exons control the alternative splicing of the alpha exon of the ZO-1 pre-mRNA. Biochim. Biophys. Acta. 1630: 71-83

Mattagajasingh SN, Huang SC, Hartenstein JS, Benz EJ Jr. (2000) Characterization of the interaction between protein 4.1R and ZO-2. A possible link between the tight junction and the actin cytoskeleton J. Biol. Chem. 275: 30573-30585

Matter K, Balda MS. (2003) Signalling to and from tight junctions. Nat. Rev. Mol. Cell Biol. 4:225-236

Matter K, Balda MS. (2007) Epithelial tight junctions, gene expression and nucleo-junctional interplay. J. Cell Sci. 120: 1505-1511

McNeil E, Capaldo CT, Macara IG. (2006) Zonula occludens-1 function in the assembly of tight junctions in Madin-Darby canine kidney epithelial cells. Mol. Biol. Cell. 17:1922-1932.

McGee AW, Dakoji SR, Olsen O, Bredt DS, Lim WA, Prehoda KE. (2001) Structure of the SH3-guanylate kinase module from PSD-95 suggests a mechanism for regulated assembly of MAGUK scaffolding proteins Mol. Cell. 8: 1291-1301

Medina R, Rahner C, Mitic LL, Anderson JM, Van Itallie CM. (2000) Occludin localization at the tight junction requires the second extracellular loop. J. Membr. Biol. 178: 235-247

Métais JY, Navarro C, Santoni MJ, Audebert S, Borg JP. (2005) hScrib interacts with ZO-2 at the cell-cell junctions of epithelial cells. FEBS. Lett. 579: 3725-3730

Montalto M, Cuoco L, Ricci R, Maggiano N, Vecchio FM, Gasbarrini G. (2002) Immunohistochemical analysis of ZO-1 in the duodenal mucosa of patients with untreated and treated celiac disease. Digestion. 65: 227-233

Morita K, Tsukita S, Miyachi Y. (2004) Tight junction-associated proteins (occludin, ZO-1, claudin-1, claudin-4) in squamous cell carcinoma and Bowen's disease Br. J. Dermatol. 151: 328-334

Müller D, Kausalya PJ, Claverie-Martin F, Meij IC, Eggert P, Garcia-Nieto V, Hunziker W. (2003) A novel claudin 16 mutation associated with childhood hypercalciuria abolishes binding to ZO-1 and results in lysosomal mistargeting. Am. J. Hum. Genet. 73: 1293-1301

Müller SL, Portwich M, Schmidt A, Utepbergenov DI, Huber O, Blasig IE, Krause G. (2005) The tight junction protein occludin and the adherens junction protein alpha-catenin share a common interaction mechanism with ZO-1. J. Biol. Chem. 280: 3747-3756

Mullin JM, Laughlin KV, Ginanni N, Marano CW, Clarke HM, Peralta Soler A. (2000) Increased tight junction permeability can result from protein kinase C activation/translocation and act as a tumor promotional event in epithelial cancers. Ann. N. Y. Acad. Sci. 915: 231-236

Naito AT, Shiojima I, Akazawa H, Hidaka K, Morisaki T, Kikuchi A, Komuro I. (2006) Developmental stage-specific biphasic roles of Wnt/beta-catenin signaling in cardiomyogenesis and hematopoiesis Proc. Natl. Acad. Sci. U. S. A. 103: 19812-19817

Nielsen PA, Baruch A, Shestopalov VI, Giepmans BN, Dunia I, Benedetti EL, Kumar NM. (2003) Lens connexins alpha3Cx46 and alpha8Cx50 interact with zonula occludens protein-1 (ZO-1). Mol. Biol. Cell. 14: 2470-2481

Pelletier RM, Okawara Y, Vitale ML, Anderson JM. (1997) Differential distribution of the tight-junction-associated protein ZO-1 isoforms alpha+ and alpha- in guinea pig Sertoli cells: a possible association with F-actin and G-actin. Biol. Reprod. 57: 367-376

Penes MC, Li X, Nagy JI. (2005) Expression of zonula occludens-1 (ZO-1) and the transcription factor ZO-1-associated nucleic acid-binding protein (ZONAB)-MsY3 in glial cells and colocalization at oligodendrocyte and astrocyte gap junctions in mouse brain. Eur. J. Neurosci. 22: 404-418

Polette M, Gilles C, Nawrocki-Raby B, Lohi J, Hunziker W, Foidart JM, Birembaut P. (2005) Membrane-type 1 matrix metalloproteinase expression is regulated by zonula occludens-1 in human breast cancer cells. Cancer Res. 65:7691-7698.

Poliak S, Matlis S, Ullmer C, Scherer SS, Peles E. (2002) Distinct claudins and associated PDZ proteins form different autotypic tight junctions in myelinating Schwann cells. J. Cell Biol. 159:361-372

Poritz LS, Garver KI, Green C, Fitzpatrick L, Ruggiero F, Koltun WA. (2007) Loss of the tight junction protein ZO-1 in dextran sulfate sodium induced colitis. J. Surg. Res. 140: 12-19

Rash JE, Pereda A, Kamasawa N, Furman CS, Yasumura T, Davidson KG, Dudek FE, Olson C, Li X, Nagy JI. (2004) High-resolution proteomic mapping in the vertebrate central nervous system: close proximity of connexin35 to NMDA glutamate receptor clusters and co-localization of connexin36 with immunoreactivity for zonula occludens protein-1 (ZO-1). J. Neurocytol. 33: 131-151

Rashbass P, Cooke LA, Herrmann BG, Beddington RS. (1991) A cell autonomous function of Brachyury in T/T embryonic stem cell chimaeras. Nature. 353:348-351

Reichert M, Müller T, Hunziker W. (2000) The PDZ domains of zonula occludens-1 induce an epithelial to mesenchymal transition of Madin-Darby canine kidney I cells. Evidence for a role of beta-catenin/Tcf/Lef signaling. J. Biol. Chem. 275:9492-500

Rincon-Choles H, Vasylyeva TL, Pergola PE, Bhandari B, Bhandari K, Zhang JH, Wang W, Gorin Y, Barnes JL, Abboud HE. (2006) ZO-1 expression and phosphorylation in diabetic nephropathy Diabetes. 55: 894-900

Roh MH, Liu CJ, Laurinec S, Margolis B. (2002) The carboxyl terminus of zona occludens-3 binds and recruits a mammalian homologue of discs lost to tight junctions. J. Biol. Chem. 277: 27501-9

Rudnicki MA, Schnegelsberg PN, Stead RH, Braun T, Arnold HH, Jaenisch R. (1993) MyoD or Myf-5 is required for the formation of skeletal muscle. Cell. 75: 1351-1359

Ryeom SW, Paul D, Goodenough DA. (2000) Truncation mutants of the tight junction protein ZO-1 disrupt corneal epithelial cell morphology. Mol. Biol. Cell. 11: 1687-1696

Saitou M, Fujimoto K, Doi Y, Itoh M, Fujimoto T, Furuse M, Takano H, Noda T, Tsukita S. (1998) Occludin-deficient embryonic stem cells can differentiate into polarized epithelial cells bearing tight junctions. J. Cell Biol. 141: 397-408

Salama NN, Eddington ND, Fasano A. (2006) Tight junction modulation and its relationship to drug delivery Adv. Drug Deliv. Rev. 58: 15-28

Sasaki H, Matsui C, Furuse K, Mimori-Kiyosue Y, Furuse M, Tsukita S. (2003) Dynamic behavior of paired claudin strands within apposing plasma membranes. Proc. Natl. Acad. Sci. U. S. A. 100: 3971-3976.

Sawada N, Murata M, Kikuchi K, Osanai M, Tobioka H, Kojima T, Chiba H. (2003) Tight junctions and human diseases. Med. Electron Microsc. 36:147-156.

Sato N, Fukushima N, Maitra A, Matsubayashi H, Yeo CJ, Cameron JL, Hruban RH, Goggins M. (2003) Discovery of novel targets for aberrant methylation in pancreatic carcinoma using high-throughput microarrays Cancer Res. 63: 3735-3742

Schnabel E, Anderson JM, Farquhar MG. (1990) The tight junction protein ZO-1 is concentrated along slit diaphragms of the glomerular epithelium. J. Cell Biol. 111: 1255-1263

Segretain D, Fiorini C, Decrouy X, Defamie N, Prat JR, Pointis G. (2004) A proposed role for ZO-1 in targeting connexin 43 gap junctions to the endocytic pathway Biochimie. 86: 241-244

Shaulian E, Karin M. (2002) AP-1 as a regulator of cell life and death Nat. Cell Biol. 4: E131-136

Sheth B, Fesenko I, Collins JE, Moran B, Wild AE, Anderson JM, Fleming TP. (1997) Tight junction assembly during mouse blastocyst formation is regulated by late expression of ZO-1 alpha+ isoform. Development. 124: 2027-2037

Sheth B, Fontaine JJ, Ponza E, McCallum A, Page A, Citi S, Louvard D, Zahraoui A, Fleming TP. (2000) Differentiation of the epithelial apical junctional complex during

mouse preimplantation development: a role for rab13 in the early maturation of the tight junction. Mech. Dev. 97: 93-104

Sidhu SS, Bader GD, Boone C. (2003) Functional genomics of intracellular peptide recognition domains with combinatorial biology methods Curr. Opin. Chem. Biol. 7: 97-102

Sinha D, Wang Z, Ruchalski KL, Levine JS, Krishnan S, Lieberthal W, Schwartz JH, Borkan SC. (2004) Lithium activates the Wnt and phosphatidylinositol 3-kinase Akt signaling pathways to promote cell survival in the absence of soluble survival factors. Am. J. Physiol. Renal Physiol. 288: F703-F713

Singh D, Solan JL, Taffet SM, Javier R, Lampe PD. (2005) Connexin 43 interacts with zona occludens-1 and -2 proteins in a cell cycle stage-specific manner. J. Biol. Chem. 280: 30416-30421

Song X, Zhao Y, Narcisse L, Duffy H, Kress Y, Lee S, Brosnan CF. (2005) Canonical transient receptor potential channel 4 (TRPC4) co-localizes with the scaffolding protein ZO-1 in human fetal astrocytes in culture. Glia. 49: 418-429

Stevenson BR, Siliciano JD, Mooseker MS, Goodenough DA. (1986) Identification of ZO-1: a high molecular weight polypeptide associated with the tight junction (zonula occludens) in a variety of epithelia. J. Cell Biol. 103: 755-766

Suetsugu S, Takenawa T. (2003) Regulation of cortical actin networks in cell migration. Int. Rev. Cytol. 229:245-286.

Sunshine C, Francis S, Kirk KL. (2000) Rab3B regulates ZO-1 targeting and actin organization in PC12 neuroendocrine cells. Exp. Cell Res. 257: 1-10

Taniguchi M, Sanbo M, Watanabe S, Naruse I, Mishina M, Yagi T. (1998) Efficient production of Cre-mediated site-directed recombinants through the utilization of the puromycin resistance gene, pac: a transient gene-integration marker for ES cells. Nucleic Acids Res. 26: 679-680

Tam PP, Loebel DA. (2007) Gene function in mouse embryogenesis: get set for gastrulation. Nat. Rev. Genet. 8: 368-381

Tan X, Egami H, Ishikawa S, Kurizaki T, Hirota M, Ogawa M. (2005) Zonula occludens-1 (ZO-1) redistribution is involved in the regulation of cell dissociation in pancreatic cancer cells. Dig. Dis. Sci. 50: 1402-1409

Torres M, Giráldez F. (1998). The development of the vertebrate inner ear. Mech. Dev. 71:5-21

Toyofuku T, Yabuki M, Otsu K, Kuzuya T, Hori M, Tada M. (1998) Direct association of the gap junction protein connexin-43 with ZO-1 in cardiac myocytes J. Biol. Chem. 273: 12725-12731

Toyofuku T, Akamatsu Y, Zhang H, Kuzuya T, Tada M, Hori M. (2001) c-Src regulates the interaction between connexin-43 and ZO-1 in cardiac myocytes. J. Biol. Chem. 276: 1780-1788

Traweger A, Fuchs R, Krizbai IA, Weiger TM, Bauer HC, Bauer H. (2003) The tight junction protein ZO-2 localizes to the nucleus and interacts with the heterogeneous nuclear ribonucleoprotein scaffold attachment factor-B. J. Biol. Chem. 278: 2692-700

Tsapara A, Matter K, Balda MS. (2006) The heat-shock protein Apg-2 binds to the tight junction protein ZO-1 and regulates transcriptional activity of ZONAB. Mol. Biol. Cell. 17: 1322-1330

Tsukita S, Furuse M, Itoh M. (2001) Multifunctional strands in tight junctions. Nat Rev Mol. Cell Biol. 2:285-293.

Walsh SV, Hopkins AM, Nusrat A. (2000) Modulation of tight junction structure and function by cytokines Adv. Drug Deliv. Rev. 41: 303-313

Umeda K, Matsui T, Nakayama M, Furuse K, Sasaki H, Furuse M, Tsukita S. (2004) Establishment and characterization of cultured epithelial cells lacking expression of ZO-1 J. Biol. Chem. 279: 44785-44794

Umeda K, Ikenouchi J, Katahira-Tayama S, Furuse K, Sasaki H, Nakayama M, Matsui T, Tsukita S, Furuse M, Tsukita S. (2006) ZO-1 and ZO-2 independently determine where claudins are polymerized in tight-junction strand formation. Cell. 126: 741-754

Utepbergenov DI, Fanning AS, Anderson JM. (2006) Dimerization of the scaffolding protein ZO-1 through the second PDZ domain. J. Biol. Chem. 281: 24671-24677

Van Itallie CM, Balda MS, Anderson JM. (1995) Epidermal growth factor induces tyrosine phosphorylation and reorganization of the tight junction protein ZO-1 in A431 cells. J. Cell Sci. 108: 1735-1742

Weiler F, Marbe T, Scheppach W, Schauber J. (2005) Influence of protein kinase C on transcription of the tight junction elements ZO-1 and occludin. J. Cell Physiol. 204: 83-86.

Watson PM, Anderson JM, Vanltallie CM, Doctrow SR. (1991) The tight-junction-specific protein ZO-1 is a component of the human and rat blood-brain barriers. Neurosci Lett. 129: 6-10

Willott E, Balda MS, Heintzelman M, Jameson B, Anderson JM. (1992) Localization and differential expression of two isoforms of the tight junction protein ZO-1 Am. J. Physiol. 262: C1119-C1124

Willott E, Balda MS, Fanning AS, Jameson B, Van Itallie C, Anderson JM. (1993) The tight junction protein ZO-1 is homologous to the Drosophila discs-large tumor suppressor protein of septate junctions. Proc. Natl. Acad. Sci. U. S. A. 90: 7834-7838

Wittchen ES, Haskins J, Stevenson BR. (1999) Protein interactions at the tight junction Actin has multiple binding partners, and ZO-1 forms independent complexes with ZO-2 and ZO-3. J. Biol. Chem. 274: 35179-35185.

Wittchen ES, Haskins J, Stevenson BR. (2000) Exogenous expression of the amino-terminal half of the tight junction protein ZO-3 perturbs junctional complex assembly. J. Cell Biol. 151: 825-836

Wittchen ES, Haskins J, Stevenson BR. (2003) NZO-3 expression causes global changes to actin cytoskeleton in Madin-Darby canine kidney cells: linking a tight junction protein to Rho GTPases. Mol. Biol. Cell. 14: 1757-1768

Xu J, Kausalya PJ, Phua DC, Ali SM, Hossain Z, Hunziker W. (2008) Early embryonic lethality of mice lacking ZO-2, but Not ZO-3, reveals critical and nonredundant roles for individual zonula occludens proteins in mammalian development. Mol. Cell Biol. 28:1669-1678

Yamaguchi TP, Takada S, Yoshikawa Y, Wu N, McMahon AP. (1999) T (Brachyury) is a direct target of Wnt3a during paraxial mesoderm specification. Genes Dev. 13: 3185-3190

Yamamoto T, Harada N, Kano K, Taya S, Canaani E, Matsuura Y, Mizoguchi A, Ide C, Kaibuchi K. (1997) The Ras target AF-6 interacts with ZO-1 and serves as a peripheral component of tight junctions in epithelial cells. J. Cell Biol. 139: 785-795

Yamamoto T, Harada N, Kawano Y, Taya S, Kaibuchi K. (1999) In vivo interaction of AF-6 with activated Ras and ZO-1. Biochem. Biophys. Res. Commun.259: 103-107